Summer 7-28-2018

The effects of prenatal alcohol exposure on the resting state functional brain connectivity in a sample of individuals with fetal alcohol spectrum disorder

Carlos I. Rodriguez
University of New Mexico

Carlos I. Rodriguez

Candidate

Psychology

Department

This dissertation is approved, and it is acceptable in quality and form for publication:

Approved by the Dissertation Committee:

Derek Hamilton, Ph.D., Chairperson

Dan Savage, Ph.D.

Vince Calhoun, Ph.D.

Julia Stephen, Ph.D.

The effects of prenatal alcohol exposure on the resting state functional brain connectivity in a sample of individuals with fetal alcohol spectrum disorder

Carlos I. Rodriguez

B.A., Psychology, Western State College of Colorado

M.S., Psychology, The University of New Mexico

DISSERTATION

Submitted in partial fulfillment of the requirements for the degree of

Doctor of Philosophy

Psychology

Department of Psychology

University of New Mexico

Albuquerque, NM 87131

July 2018

Dedication

For my dear daughter, Chloe.

Acknowledgements

I would like to thank my advisor and dissertation committee chair, Dr. Derek Hamilton. I am grateful for the opportunities train in his laboratory and for his assistance in implementing parts of this project. In addition, I would like to thank the rest of my committee members, Drs. Vince Calhoun, Dan Savage III, and Julia Stephen. I am grateful for their knowledge, guidance and feedback. I would also like to thank Dr. Victor Vergara, for his invaluable mentorship, patience, and encouragement to grow and develop as a scientist. Also among those who deserve mention here are Dr. Flor Espinoza for her generosity and assistance in developing crucial aspects of this project.

The effects of prenatal alcohol exposure on the resting state functional brain connectivity in a sample of individuals with fetal alcohol spectrum disorder

BY

Carlos I. Rodriguez

B.A., Psychology, Western State College of Colorado

M.S., Psychology, The University of New Mexico

Abstract

It is well established that alcohol exposure during prenatal development can lead to a heterogeneous and wide ranging set of morphological and neurobehavioral deficits that are collectively known as Fetal Alcohol Spectrum Disorders (FASDs). Previous neuroimaging research conducted on individuals with FASD has primarily employed graph-theoretical based analysis methods on functional imaging data to elucidate the impact of prenatal alcohol on brain connectivity. This study applied a widely used computational algorithm, group

independent components analysis (gICA), to extract coherent sets of voxels that were correlated with one another as a measure of functional network connectivity (FNC) in a sample of adolescents and young adults with prenatal alcohol exposure. Connectivity measures were then compared to those of healthy controls and related to measures of intelligence. Increases in connectivity magnitude were observed in the Alcohol Related Neurodevelopmental Disorder (ARND) group.

Changes in connectivity were frequently observed in midline frontal and posterior components implicated in default mode and visual networks. Measures of connectivity were also associated with intelligence scores in related regions. The results presented here add to the small, but growing, literature on the consequences of prenatal alcohol exposure on resting state functional connectivity and their relationship to neuropsychological assessment.

Table of Contents

List of Figures

List of Tables

Appendices

Introduction

Fetal Alcohol Spectrum Disorder (FASD) describes a broad range of physical, cognitive, and behavioral effects caused by exposure to alcohol during prenatal development (Bertrand et al., 2005; Sokol, Delaney-Black, & Nordstrom, 2003). The term FASD encompasses several categorical labels that, since the first published report of the teratogenic effects of alcohol in the 1970's, have included Fetal Alcohol Syndrome (FAS), partial fetal alcohol syndrome (pFAS), alcohol related birth defects (ARBD), alcohol related neurodevelopmental disorder (ARND), and neurodevelopmental disorder associated with prenatal alcohol exposure (ND-PAE) (Kable et al., 2015; Williams, Smith, & Committee On Substance, 2015).

Of all the categorical labels for the wide range of adverse effects related to prenatal alcohol exposure, FAS was the first to be described in the research literature, is considered the most severe, and is linked to heavy prenatal alcohol exposure (PAE) (Jones & Smith, 1973, 1975). In children, FAS is characterized by growth deficiencies, often falling below the 10^{th} percentile for height and weight, and facial dysmorphologies such as elongated palpebral fissures, a smooth philtrum, and a thin upper vermillion border (Jones & Smith, 1973, 1975). Furthermore, FAS is associated with nervous system abnormalities that included changes in gray and white matter volumes (Lebel et al., 2012), cortical area (Autti-Ramo et al., 2002), total brain volume (Astley et al., 2009b), and white matter structural integrity (Wozniak et al., 2006; Wozniak et al., 2009) among

others. To complicate matters further, children and adults with FAS can exhibit profound alterations in measures of intelligence (Kodituwakku, 2007), executive functioning (Connor, Sampson, Bookstein, Barr, & Streissguth, 2000; Green et al., 2009), various forms of working memory (Astley et al., 2009a; Malisza et al., 2005), response inhibition (Fryer et al., 2007; O'Brien et al., 2013), verbal learning (Sowell et al., 2007), and number processing (Santhanam et al., 2011).

While the terms of pFAS, ARBD, and ARND may not be as strongly associated with the severe physical dysmorphologic characteristics of FAS, they are nonetheless associated with subtle and persistent deficits in the neuropsychological features related to full blown FAS (Connor et al., 2000; Mattson & Riley, 1998; Santhanam et al., 2011). Collectively, all categorical labels within the FASD umbrella are marked by common and long-lasting cognitive and behavioral abnormalities that range in severity and that can contribute negatively to adaptive functioning and poor life outcomes (Connor et al., 2000; Santhanam et al., 2011).

Early epidemiological studies of FASD estimated the nationwide prevalence of FAS alone at 0.1% in the United States (May & Gossage, 2001). However, May & Gossage (2001) also suggested that for every child with FAS, there are five others that while exposed to prenatal alcohol, may not meet the diagnostic criteria for diagnosis of FAS. Moreover, this study relied passive surveillance methods consisting of convenience samples from community health clinics (May et al., 2014; May & Gossage, 2001). As a result, true prevalence

rates for FAS and FASD may have been underestimated in the United States. To remedy these concerns, May and colleagues (2014) utilized an active sampling method whereby facial dysmorphology measures were gathered from a sample of elementary school children. The authors reported prevalence rates between 2.4% and 4.8% for the entire FASD continuum. Despite utilizing novel sample sources, May and others (2014) still cautioned that FASD prevalence rates may be underestimated as the authors relied on facial dysmorphology scores that may not capture the entire spectrum of consequences related to alcohol exposure during prenatal development. Regardless of sampling sources, the acquisition of accurate prevalence rates may be influenced by other factors. One possibility is that women may choose to withhold information regarding alcohol consumption during pregnancy for fear of stigmatization. Another factor is related to the misdiagnosis of FASD as Attention Deficit Hyperactivity Disorder (ADHD) due to similar behavioral features between the two diagnoses (Kodituwakku, 2007; Williams et al., 2015).

Current prevalence rates are also suspect due to research conducted on alcohol use behaviors in women. One study reported that 10.2% of pregnant women, aged 18-44, engaged in alcohol consumption during the 30 days prior to survey data collection (Tan, Denny, Cheal, Sniezek, & Kanny, 2015). The same report demonstrated that in general, prior 30-day drinking rates—whether binge or any use—among women, pregnant or not, vary tremendously by state and range from 27.6% (Utah) on the low end to 62.8% (Oregon) on the high end. This

study shed light on the potential risk for FASD in the U.S. Moreover, a recent study demonstrated that heavy drinking rates—a well-established risk factor for FASD—among women increased substantially from 2002 to 2012 indicating a potential increase in risk for increasing future prevalence rates for FASD in the U.S. (Dwyer-Lindgren et al., 2015). Given the current estimates of FASD prevalence, reports of maternal drinking during pregnancy, and the increases of heavy drinking rates among women, it is perhaps unsurprising that FASD stands as the leading preventable cause of birth defects and neurodevelopmental disabilities in the U.S. (Williams et al., 2015) highlighting the designation of FASD as a serious public health concern.

When considering the wide range of deficits in cognition and social functioning resulting from prenatal alcohol exposure, it is not difficult to imagine how FASD is associated to academic impairments (Mattson & Riley, 1998) and adaptive functioning difficulties (Kodituwakku, Handmaker, Cutler, Weathersby, & Handmaker, 1995) that contribute to challenges in finding and maintaining meaningful employment or increase the risk of incarceration (Popova, Stade, Bekmuradov, Lange, & Rehm, 2011).

The adverse outcomes associated with FASD contribute to an estimated economic impact that ranges from $1.937 billion to $9.687 billion per year (Popova et al., 2011). These costs include estimates associated with, educational interventions, residential services, and lost productivity. True annual cost expenditures may also be higher due to underestimated prevalence rates,

under-diagnosis of FASD, and because the costs of FASD in the criminal justice system in the United States are often not adequately considered.

Currently, FASD has no cure and adults affected by PAE may face a lifetime of difficulty in leading independent lives. Children with FASD represent a challenge for parents, caregivers, and educators yet the current interventions for FASD are limited. Existing interventions are aimed at developing parenting strategies, developing social interaction skills in children with FASD, and support groups (Paley & O'Connor, 2011). Pharmacological treatments have included neuroleptic and stimulant administration with the former showing better results (Frankel, Paley, Marquardt, & O'Connor, 2006). Recent reports of diet supplementation with exogenous choline have shown promising preliminary results on specific measures of learning (Wozniak et al., 2015). Regardless of treatment approach, researchers have noted that early interventions are integral for producing more positive outcomes in individuals with FASD (Peadon, Rhys-Jones, Bower, & Elliott, 2009; Streissguth et al., 2004).

However, to maximize the effectiveness of interventions, screening and diagnostic efforts must take place earlier in the lifespan. FASD diagnosis, especially in non-dysmorphic varieties, represents a significant challenge due to the limited approaches available which typically rely on facial dysmorphology measures. As a result, the National Institutes of Health has designated the development of novel FASD diagnostic approaches as a critical research goal. Improved diagnostic strategies may benefit from an increased understanding and

incorporation of the neurofunctional correlates of FASD to compliment maternal reports of drinking during pregnancy, and the tools based on facial dysmorphologies.

An extensive body of literature utilizing magnetic resonance imaging (MRI)-based methods has demonstrated several structural deficits associated with PAE. Among these deficits, the most frequently observed are reductions in brain volume (microcephaly), agenesis of the corpus callosum, abnormalities in white matter organization, enlarged ventricles (ventriculomegaly), and a small cerebellum (Donald et al., 2015; Moore, Migliorini, Infante, & Riley, 2014; Wozniak & Muetzel, 2011).

A supporting body of literature has also employed functional MRI-based approaches to measure fluctuations in blood-oxygen-level-dependent (BOLD) signals that are thought to reflect synchronized patterns of neural activity due to neurovascular mechanisms regulating blood flow (Logothetis, Pauls, Augath, Trinath, & Oeltermann, 2001). Many of these studies have acquired BOLD signals during cognitive and behavioral tasks that asses working memory (Astley et al., 2009a), spatial working memory (Malisza et al., 2005), response inhibition (Fryer et al., 2007; O'Brien et al., 2013), and number processing (Meintjes et al., 2010; Santhanam et al., 2011).

Much less represented in the functional MRI of FASD literature are investigations in the resting-state—a methodological approach in which participants are not asked to respond to stimuli or perform behavioral tasks

during image acquisition. Functional neuroimaging data gathered at rest state can be subjected to several analyses to measure functional connectivity—an investigative framework that aims to capture the statistical and temporal patterns of endogenously generated brain activity across multiple brain areas. This framework operates under the assumption that complex behavioral and cognitive processes rely on highly sophisticated, distributed, and coordinated activation patterns (Bullmore & Sporns, 2009; Snyder & Raichle, 2012). Functional connectivity can also be utilized to explore the relationships between intrinsic patterns of brain activity and future performance on tasks (Tavor et al., 2016) and in psychiatric (Etkin, Prater, Schatzberg, Menon, & Greicius, 2009; Greicius et al., 2007) and neurological conditions (Greicius, Srivastava, Reiss, & Menon, 2004; He et al., 2007). These approaches may prove useful for clinicians working with FASD populations as it provides an additional perspective that aims to build a more complete understanding of the condition.

To date, only a handful of studies have investigated resting state fMRI-based functional connectivity in individuals with FASD. Santhanam and colleagues (2011) investigated resting state activation of the default mode network (DMN) —a set of brain structures that include the medial prefrontal cortex, precuneus, bilateral temporal lobes, and the posterior cingulate cortex that exhibit a high degree of coherence at rest—in a sample of young adults (ages 20-26) with FASD. The authors reported reduced functional connectivity between the medial prefrontal cortex and the posterior cingulate cortex at rest in

the alcohol exposed group. Furthermore, the authors reported the most significant changes occurred in a group of FASD participants who exhibited facial dysmorphologies indicating a relationship between abnormal functional connectivity and the facial characteristics associated with FAS. It is hypothesized that dysfunction in resting state network activation may be related to the cognitive and behavioral deficits associated with PAE.

An additional report of resting state connectivity stemmed from a study that showed microstructural deficits in the white matter fibers of the posterior regions of the corpus callosum in children with FASD as measured by diffusion MRI. As a follow up study, the same research group conducted a seed based functional connectivity analysis using cortical regions known to communicate through the posterior regions of the corpus callosum. First, diffusion weighted images were used to perform white matter tractography along seven anatomical sub-regions of the corpus callosum. The bilateral cortical end-terminal regions of the tractography results were utilized as seed regions to gather voxel timecourse activations from function MRI scans. Bilateral timecourse activations were then correlated to ascertain a measure of functional connectivity. While healthy controls showed coherent activation between bilateral regions of interests (ROIs), PAE children did not display the same degree of interhemispheric connectivity. This investigation was key in demonstrating a relationship between structural and functional connectivity of regions that communicate through the corpus callosum.

A report by the same research group later employed a graph theoretical approach to explore global, as opposed to regional, functional connectivity to include brain structures beyond the previously targeted cortical para-central regions in a sample of children (ages 10-17) (Wozniak et al., 2013). The researchers utilized structural MRI data to identify 34 unilateral (68 bilateral) ROIs that were then mapped onto functional MRI data to extract voxel-wise time courses. Average time course activations for each region were then correlated to ascertain a measure of connectivity strength. Spatial ROIs and connectivity measures were then then fed into a computational algorithm to determine graph theoretical measures of network connectivity such as global efficiency and path length. Higher path lengths, an index of how many brain regions are utilized to transmit information, was observed in the FASD group, suggesting abnormal information processing. Compared to controls, a small reduction of approximately 3% in path efficiency was also observed for PAE children, further indicating aberrant connectivity as a result of PAE. Finally, an overall measure of global efficiency was reduced by approximately 2% in FASD children. The authors suggested that while the differences were small, the effect sizes were strong and concluded that PAE may contribute to less efficient information processing and may underlie some of the cognitive deficits observed in FASD.

While the previous studies relied on participants from a Midwest region of the United States, a subsequent study examined resting-state FNC assessed by graph theory measures derived from fMRI data collected from a large multi-site

sample of FASD children and controls. Abnormal FNC was observed in a relatively large portion of participants where documented alcohol exposure did not lead to definitive evidence of facial dysmorphology. The authors noted that FNC measures may in fact be informative for discriminating alcohol exposed individuals from non-exposed individuals with high specificity and points to the potential utility of functional connectivity analyses to aid in the FASD diagnostic process.

The extant literature of fMRI based studies of children with FASD has primarily relied on seed based approaches. Seed based analyses require the *a priori* selection of an initial voxel or region that is hypothesized to be involved in a network of interest. In contrast to seed based approaches, independent component analysis does not require the selection of an *a priori* region of interest. ICA is a data exploration technique based on computational algorithms that were developed to extract the functional relationships between multiple signals from various sources (Bell & Sejnowski, 1995). When applied to fMRI data, ICA can identify distinct features that represent coherent brain activity (van den Heuvel & Hulshoff Pol, 2010). In the case of fMRI, components represent stationary sets of voxels whose activations vary together in time and are maximally distinguishable from other sets (Hyvärinen, Karhunen, Oja, & NetLibrary Inc., 2001; Stone, 2004). Importantly, ICA may also be applied at the group level to extract common features in patterns of brain activation gathered at

rest from large samples of participants (Allen et al., 2011) and reveal relationships that may be overlooked by seed based approaches.

The following study characterized and compared measures of resting state fMRI functional connectivity in a sample of adolescents and young adults with FASD and healthy controls recruited from urban and rural areas of New Mexico. Measures of functional connectivity were derived from pairwise correlations from average independent component time-courses. Furthermore, measures of whole, gray, and white matter volumes were obtained and compared across groups to investigate the contribution of various tissues to connectivity. Finally, FNC measures were related to the results of neuropsychological assessments that consisted of overall intelligence and sub-test scores from Wechsler's Abbreviated Scale of Intelligence (WASI-II).

Methods

Participants

Sixty-three male and female adolescent participants (aged 12-22) were previously recruited from urban and rural New Mexico for primary data collection as part of two separate studies. Informed consent by participants or parents (if subject was under the age of 18) was provided in accordance with institutional guidelines. Data collection protocols were approved by the Research Review Committee of the University of New Mexico Health Sciences Center.

FASD Diagnostic Procedures

Diagnostic procedures were previously reported elsewhere (Coffman et al., 2013; Stephen, Coffman, Stone, & Kodituwakku, 2013). Briefly, an interdisciplinary team consisting of a pediatrician, neuropsychologist, and child psychologist at the University of New Mexico Fetal Alcohol Diagnostic and Evaluation clinic diagnosed PAE participants for Fetal Alcohol Syndrome (FAS), partial fetal alcohol syndrome (pFAS), or alcohol related neurodevelopmental disorder (ARND) based on modified criteria from the National Academy of Medicine (previously known as Institute of Medicine) guidelines (Hoyme et al., 2005; Stratton et al., 1996). All FASD participants had confirmed PAE gathered from sources such as maternal interviews, eyewitness reports, legal (e.g. driving while impaired) or from medical records. Healthy control participants had no evidence of previous neurodevelopmental disorders or known exposure to prenatal alcohol nor other controlled substances. For comparisons of FNC and behavior, FASD participants were disaggregated into separate ARND and FAS groups due to null results observed with a combined FASD group.

Neuropsychological Assessments

Participants were also assessed for general cognitive ability through the two-subtest form of the Wechsler Abbreviated Scale of Intelligence (WASI) (Wechsler, 1999). The two-subtest WASI was chosen for its shortened duration and its correlation to more in depth tests of intelligence (Wechsler, 1999). However, it should be noted that several participants were recruited from rural

New Mexico and were not native English speakers. Subtest scores were utilized to correlate with measures of functional network connectivity. Behavioral measures were analyzed with Matlab's anova1 and multcompare functions and measures of effect size were calculated with the Measures of Effect Size toolbox.

MRI Data Acquisition

All MRI data was gathered at the Mind Research Network (MRN) using a Siemens Trio 3-Tesla scanner with a 12-channel radio frequency coil. Structural T1-weighted MR images were obtained with a multiecho 3D MPRAGE sequence [FOV = 256mm x 256mm, matrix = 256 x 256, TE = 1.64, 3.5, 5.36, 7.22, 9.08 ms, TR = 2530ms, TI = 1200 ms, flip angle = 7 $^{\circ}$, number of excitations = 1, slice thickness = 1mm, and 192 slices]. Depending on the sample, Functional T2*-weighted MRI images were obtained during a 5 or 5.5 minute resting state scan with a gradient-echo EPI sequence [FOV = 240mm x 240mm, matrix = 64 x 64, voxel size = 3.75mm x 3.75mm x 4.55mm, TR = 2000ms, TE = 29ms, flip angle = 75°, slice thickness = 3.55 mm, slice gap = 1.05 mm]. Only the first 5 minutes of each functional scan were used for data processing and analyses.

MRI Data Preprocessing

All images were partly pre-processed using an automated pipeline procedure developed at the MRN previously described elsewhere (Bockholt et al., 2010). Automated preprocessing consisted of realignment and slice timing correction in Statistical Parametric Mapping 5 (SPM5) (Friston et al., 1994). Realigned and slice-time corrected volumes were then normalized to the

Montreal Neurological Institute (MNI) Space in SPM5. Normalized and realigned volumes were then despiked utilizing the AFNI 3dDespike program (Cox, 1996) to mitigate the impact of large sudden movements during image acquisition. A combination of 12 motion related regressors (x, y, z, roll, pitch, yaw and their derivatives) were utilized in a multiple regression using the icatb_regress function implemented in Matlab R2012b (Mathworks; Nattick, MA) to model the impact of in-scanner head motion on signal. The resulting timecourses were detrended with the icatb_detrend function running in Matlab R2012b (Mathworks; Nattick, MA) to guard against the effects of small movements during image acquisition. Following motion parameter regression and detrending, image volumes were smoothed with a 10mm full-width half-maximum (FWHM) Gaussian kernel with SPM5 (Friston et al., 1994).

Brain Volume Estimates

Intracranial, whole brain, gray matter, and white matter volume estimates were calculated using data from an automated voxel based morphometry (VBM) analysis pipeline. Briefly, the SPM-5 based pipeline consisted of converting T1 DICOM images to NIfTI format, tissue segmentation into gray matter, white matter, and cerebrospinal fluid, normalization, and smoothing with a 10mm FWHM Gaussian kernel (Segall et al., 2009). Intracranial volume estimates were gathered by summing gray matter, white matter, and cerebrospinal fluid tissue-segmented images for each subject and multiplying by the volume of each voxel and converted to cubic centimeters. Whole brain volume estimates were

gathered in a similar fashion with the exception that cerebrospinal fluid images were excluded from the calculations to render an estimate of gray and white matter tissue volume only. Gray and white matter volume estimates were gathered by converting the corresponding tissue segmented images to cubic centimeters.

Independent Component Feature Extraction

Following image pre-processing, fMRI data were processed using the Group ICA of fMRI Toolbox (GIFT) running in Matlab. The INFOMAX algorithm was selected for feature identification at the group level. As described in Allen and colleagues (2011), a total of 75 independent components were selected in GIFT to extract networks with known anatomical origin and functional relevance (Allen et al., 2011) while 113 principal components were selected for data reduction. Additionally, component timecourses were temporally filtered using a low pass filter with a 0.15Hz frequency cut-off. All independent components were visually inspected for artifactual features including motion-related and susceptibility artifacts, spectral power characteristics, and anatomical location. Components that exhibited artifactual features and were localized to CSF or white matter were excluded from further analyses. The remaining components were then sorted and grouped based on the location of the corresponding peak intensity value according to MNI space.

Functional Network Connectivity Analyses

Data output from the gICA toolbox included pairwise Pearson correlation values calculated between the average timecourses of voxels contained in each component. Because r-values are limited to the upper and lower bounds of 1 and -1 respectively, the sampling distribution is susceptible to skew and thus z-transformed correlation values were utilized for subsequent analyses. Additionally, to account for the wide age range, all z-transformed values were regressed for age utilizing the Matlab regress function. Statistical analyses on all possible pairwise correlations were then conducted utilizing the ttest1, ttest2, and the anovan (2x2 design with prenatal condition and sex as factors) functions in Matlab. All ANOVAs were subjected to Bonferroni and a false discovery rate (FDR) multiple comparison procedure based on the Storrey (1995) method. A follow up group information guided ICA (GIGICA), was conducted to further explore FNC relationships, however, this analysis did not yield any statistical differences among groups that passed multiple correction procedures.

Brain-Behavior Correlations

To explore the relationship between behavior and functional network connectivity, measures from the WASI-II were correlated to measures of functional network connectivity. Due to logistical reasons, not all participants completed neuropsychological assessments and thus brain-behavior correlations excluded participants with missing values. The results of these relationships were calculated using the Pearson corrcoef Matlab function and show the degree of

correlation between each possible pairwise coupling of components and full scale IQ estimate, Vocabulary subtest score, and Matrix Reasoning subtest score.

Results

Subject Elimination and Motion

One male control subject was eliminated from analyses due to severe signal drop-out in the acquired functional images. A total of 4 additional participants (1 female ARND, 1 female control, and 2 male controls) were eliminated from further analyses due to excessive motion utilizing a 3mm threshold of maximum movement derived from the realignment parameters and by exhibiting three standard deviations beyond the mean in the frame-wise displacement measure described by (Power, Barnes, Snyder, Schlaggar, & Petersen, 2012). After subject elimination, no statistically significant differences, were found in measures of motion in the 3 translation and 3 rotation parameters between alcohol exposed and control groups [X translation: t= -0.9590, df=56, p=0.3417 g=-0.2560; Y translation: t=1.4451, df=56, p=0.1540, g=.3858; z translation: t=0.2372, df=56, p=0.8134; roll rotation: t=0.8325, df=56, p=0.4087, g=0.2222 ; pitch rotation: t=-0.2931, df=56, p=0.7719, g=-0.0778 ; yaw rotation: t= -0.9990, df=56, p=0.3221, g=-0.2667] when comparing controls with alcohol exposed groups.

Demographic Information

Available demographic information for participants, including age at scan and the composition of the sample with respect to sex and FASD diagnosis, is shown in Table 1. Only one participant met the diagnostic criteria for pFAS and was placed in the ARND group for subsequent statistical analyses based on an average IQ score more similar to that of ARND rather than the FAS participants. Results of summary statistics (mean and standard deviation) after excluding participants with excessive motion or significant signal drop-out are also shown in Table 1. The results of comparisons of age and sex are also displayed. The mean age for both FASD and control groups was approximately 16.3 years. A two-sample t-test conducted on the age data revealed no statistically significant difference in age across the FASD and Control participants. However, it should be noted that the age of participants ranged from 12 to 22.8 years. In fact, three FASD participants (2 FAS and 1 ARND) were above 21 years of age at the time of MRI data acquisition. A chi-squared test conducted on the numbers of male and female participants in each of the FASD and Control groups revealed no statistically significant difference in the representation of each gender within each prenatal condition. Because analyses conducted with two groups yielded null results on measures of FNC and the reported results disaggrated the FASD group into separate ARND and FAS groups.

Table 1 – Demographic Characteristics and Summary Statistics of Participants Retained for Analyses.

Shown here are the 58 participants retained for gICA. FASD, fetal alcohol spectrum disorder; FAS, fetal alcohol syndrome; pFAS, partial FAS; ARND, alcohol-related neurodevelopmental disorder.

N (%) or Mean +/- SD	**FASD (n=22)**		**Control (n=36)**		**Statistical Test**
Age at MRI scan	16.3636	+/- 3.0075	16.3278	+/- 2.4911	t= -0.0491, df: 56, sd: 2.6964, p =0.9610
Gender					
Male	14	(24%)	20	(34%)	
Female	8	(14%)	16	(28%)	χ^2 =0.3676, p=0.5443
FASD Category					
FAS	13	(59%)	-		-
pFAS	1	(5%)	-		-
ARND	8	(36%)	-		-
IQ	77.74	+/- 12.22	105.09	+/- 12.95	
Vocab	30.3529	+/- 8.13	53.66	+/- 8.53	
Matrix	31.53	+/- 10.52	37.16	+/- 12.60	

Intracranial Volume Estimates in cm^3					
Male	1330.20	+/- 188.14	1436.30	+/- 103.86	
Female	1181.90	+/- 101.10	1363.90	+/- 147.00	Group: F(1,57) =12.54, p=0.0008 Sex: F(1,57)=7.2, df=1,57, p=0.0097 Interaction: F(1,57)=0.71, p=0.4038
Whole Brain Volume Estimates in cm^3					
Male	1114.34	+/- 170.51	1211.80	+/-118.94	
Female	1000.41	+/- 69.66	1122.56	+/-127.64	Group: F(1,57)=9.1, p=0.0039 Sex: F(1,57)=7.8, p=0.0072 Interaction: F(1,57)=0.11, p=0.7361
Gray Matter Volume Estimates in cm^3					
Male	669.59	+/- 68.26	746.05	+/-65.10	
Female	620.42	+/- 39.78	688.11	+/-71.44	Group: F(1,57)=15.63, p=0.0002 Sex: F(1,57)=8.63, p=0.0049 Interaction: F(1,57)=0.06, p=0.8107

White Matter Volume **Estimates in cm^3**					
Male	419.52	+/- 62.12	465.72	+/-58.80.	
Female	379.99	+/- 34.80	434.38	+/-63.52	Group: F(1,57)=9.57, p=0.0031 Sex: F(1,57)=4.75, p=0.0337 Interaction: F(1,57)=0.06, p=0.8021

Neuropsychological Measurements

Because not all participants returned for a post-scan neuropsychological assessment, the following results here were derived from available data and measures for missing participants were not estimated or interpolated as the primary aim of this research was to examine functional network connectivity. Available measures of overall IQ, Vocabulary subscores, and Matrix Reasoning subscores from the WASI-II were compared using separate one-way ANOVAs utilizing sub-diagnosis (control, FAS, or pFAS/ARND) as separate levels.

The results of the one-way ANOVA conducted on the available measures for IQ revealed a significant effect in the omnibus test [$F(2,50) = 27.99$, $p<0.01$, $\eta^2_p=0.5385$]. Marginal means and results from the a post-hoc Bonferroni multiple comparison procedure are displayed in Figure 1 and indicated controls ($\bar{x}=105.09$, $s=12.95$) are significantly higher in IQ measures when compared to the ARND($\bar{x}=81.14$, $s=14.80$, $p<0.0001$, $g=1.77$) groups and FAS ($\bar{x}=75.75$, $s=10.64$, $p<0.0001$, $g=2.33$). However, comparison of the FAS and ARND groups did not yield a statistically significant difference after multiple comparisons correction ($p=1.0$, $g=0.42$). An additional 2-way ANOVA was conducted with the inclusion of sex as a factor that did not result in any statistically significant differences for the main effect of sex [$F(1,50)=0.0579$, $p=0.8109$, $\eta^2_p=0.0013$] (see Appendix 1).

Figure 1 – Mean WASI-II IQ.

Mean WASI-II IQ estimates for control, FAS, and ARND groups. *** indicates a p< (0.05/3).

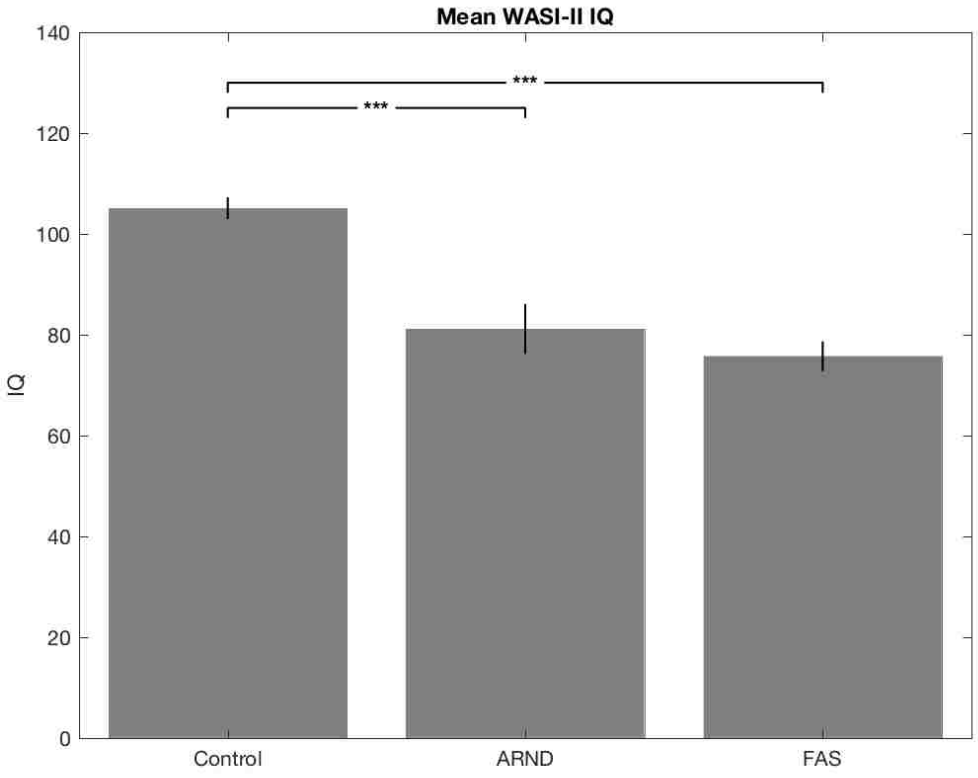

A one-way ANOVA conducted on measures of Vocabulary revealed a statistically significant effect in the omnibus test [$F(2,50) = 42.87$, $p<0.01$, $\eta^2_p=0.6508$]. After a post-hoc Bonferroni multiple comparison correction, it was determined that controls ($\bar{x}=53.66$, $s=8.53$) demonstrated statistically significantly higher measures on vocabulary when compared to ARND ($\bar{x}=32.43$, $s=10.66$, $p<0.0001$, $g=2.34$) and FAS ($\bar{x}=28.90$, $s=6.01$, $p =0.0001$, $g=3.02$) groups. Similar to the measures of IQ, no statistically significant differences in vocabulary measures were found between the FAS and ARND groups ($p=1.0$, $g=0.41$). An additional 2-way ANOVA including sex as a factor did not reveal any statistically significant differences for sex [$F(1,50) = 3.5305$, $p=0.0667$, $\eta^2_p =0.0727$] (see Appendix 1).

Figure 2 – Mean WASI-II Vocabulary Subtest Scores.

Mean WASI-II vocab scores for control, FAS, and ARND groups. *** indicates a p< (0.05/3).

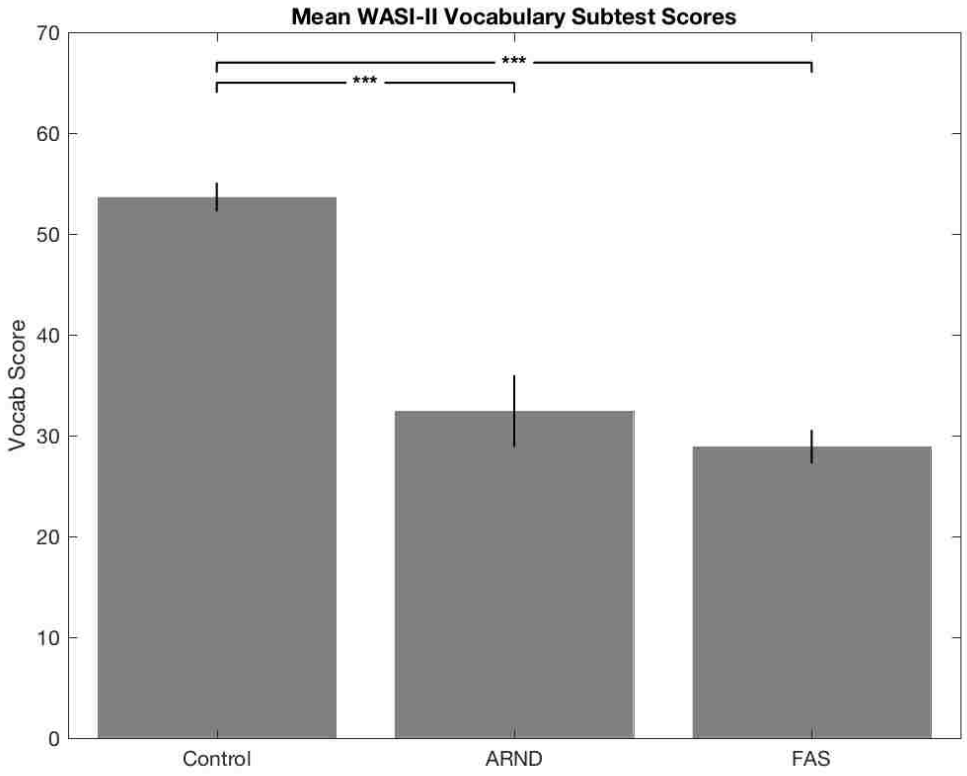

Results from a one-way ANOVA on Matrix Reasoning measures revealed no statistical significant effects in the omnibus test [$F(2,48)=1.3$, $p=0.2821$, $\eta^2_p=.0535$]. An additional 2-way ANOVA with sex added as a variable displayed no statistical significant difference for sex [$F(1,48) = 2.88$, $p=0.0967$, $\eta^2_p =0.0605$] (see Appendix 1).

Figure 3 – Mean WASI-II Matrix Reasoning Subtest Scores.

Mean WASI-II matrix reasoning scores for control, FAS, and ARND groups.

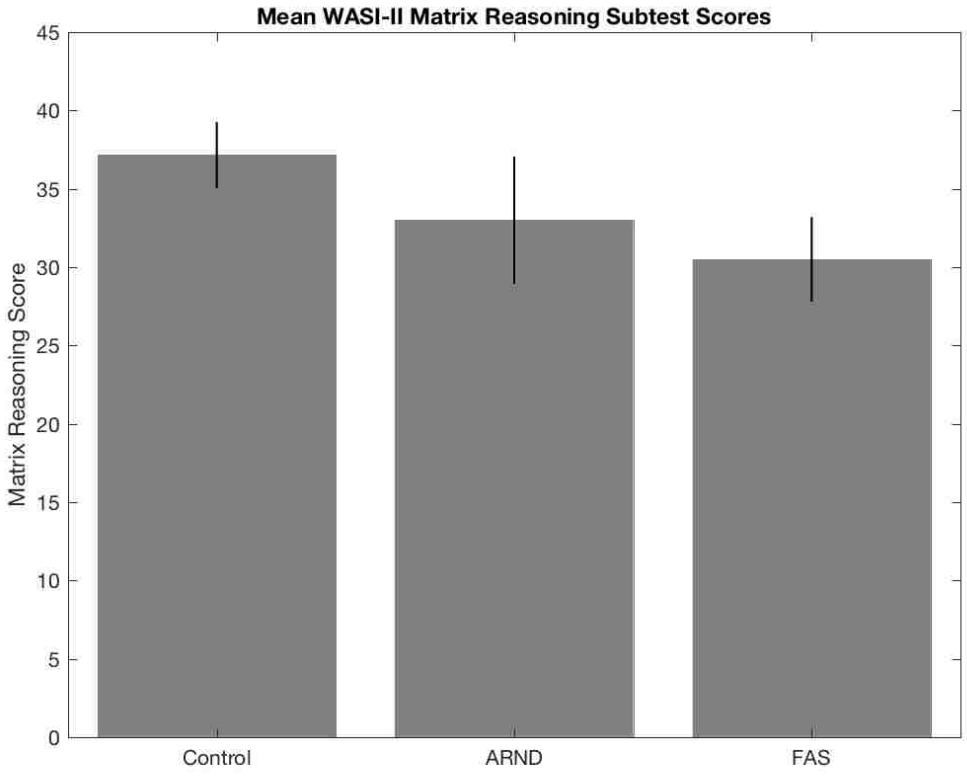

The results of the separate ANOVAs on neuropsychological measurements collectively indicate that the reductions in overall measures of IQ in alcohol exposed participants are driven by reductions in Vocabulary subtest scores, as statistically significant differences between control, FAS, and ARND groups are not observed in comparisons of Matrix Reasoning.

Brain Volume Estimates

Brain volume estimates were compared by examining differences in intracranial volume (includes CSF, gray, and white matter), whole brain volume (gray matter and white matter only), and separate estimates of gray and white matter with separate two-way ANOVAs.

For comparisons of intracranial volume, one control participant exhibited intracranial volume greater than three standard deviations from the mean of all participants and was excluded from further statistical analyses. Summary statistics for intracranial volume are shown in Table 1. A two-way analysis of variance with group (FASD or Control) and sex as factors revealed statistically significant effects for prenatal group [$F(1,56)=12.54$, $p=0.0008$, $\eta^2_p=0.1913$] and sex [$F(1,56) = 7.2$, $p=0.0097$, $\eta^2_p=0.1196$], but not for the interaction [$F(1,56)=0.71$, $p=0.4038$, $\eta^2_p=0.0132$] suggesting total intracranial volume was higher in controls and in males.

For brain volume estimates, all participants were retained for calculations. Summary statistics for brain volume are also shown in Table 1. A two-way analysis of variance with prenatal group and sex as main factors revealed statistically significant effects for group [$F(1,57) = 9.1$, $p=0.0039$, $\eta^2_p=0.1443$] and sex [$F(1,57) = 7.8$, $p=0.0072$, $\eta^2_p= 0.1262$] suggesting brain volume was higher in control and male participants. As observed for the intracranial volume estimates, no statistically significant interaction [$F(1,57) = 0.11$, $p=0.7361$, $\eta^2_p=0.0021$] was observed for brain volume estimates.

Gray matter estimates are also shown in Table 1 and were compared using a two-way analysis of variance. One control subject was removed from the analysis as the subject exhibited gray matter volume greater than 3 standard deviations beyond the mean. A statistically significant effect of group [$F(1,56) = 15.63$, $p=0.0002$, $\eta^2_p=0.227$] and sex [$F(1,56) = 8.63$, $p=0.0049$, $\eta^2_p=0.1400$] were observed further supporting the observation of greater volume in controls and males. The group by sex interaction was not statistically significant [$F(1,56) = 0.06$, $p=0.8107$, $\eta^2_p=0.0011$].

Estimates of white matter volume were subjected a two-way analysis of variance (shown in Table 1) and revealed statistically significant effects for prenatal group [$F(1,57) = 9.57$, $p=0.0031$, $\eta^2_p=0.1505$] and sex [$F(1,57) = 4.75$, $p=0.0337$, $\eta^2_p=0.0808$] suggesting reductions in white matter among FASD and females. The group by sex interaction was not statistically significant [$F(1,57) = 0.06$, $p=0.8$, $\eta^2_p=0.0012$].

Collectively, these results demonstrate that female and alcohol exposed participants exhibit reductions in intracranial, whole brain, gray, and white matter volumes. However, it is important to note that reductions in various volume estimates observed in females should be interpreted with caution as it is a typically observed sexually dimorphic characteristic.

Components

In total, 75 components were selected for extraction from the gICA. Of the 75, 32 were excluded from further analyses based on the peak value located in white matter structures or cerebrospinal fluid, spectral power characteristics (such as strong representation of high frequency timecourses), or due to the presence of artifactual features upon visual inspection. A total of forty-three components for subsequent analyses were retained. Figure 4 displays all retained components in the sagittal, coronal, and axial views of the peak value for each component overlaid on a T1 structural image. Components were distributed across the entire brain and were organized into auditory, visual, sensory-motor, fronto-parietal, default mode, subcortical, and cerebellar networks based on the anatomical location of the peak component value and on correlations with other networks (e.g. DMN components typically exhibited negative correlations with non DMN components). In all, 1 auditory (AUD), 11 sensory-motor (SEN), 8 visual (VIS), 4 cerebellar (CBLM), 11 default mode (DMN), 6 fronto-parietal (FR-PR), and 2 subcortical (SBCRT) components were retained. Components in each grouping are ordered numerically within their grouping according to the component number out of the initial 75 components. Table 2 shows grouping labels, component number, corresponding anatomical location, and coordinates of the component peak value.

Figure 4 – Component images in sagittal, coronal, and axial sections.

Component images are shown along the anatomical planes corresponding to the peak component value. Components were grouped into sensory-motor (A), default mode (B), fronto-parietal (C), visual (D), cerebellar (E), and subcortical and auditory (F) networks.

A) Sensory-Motor

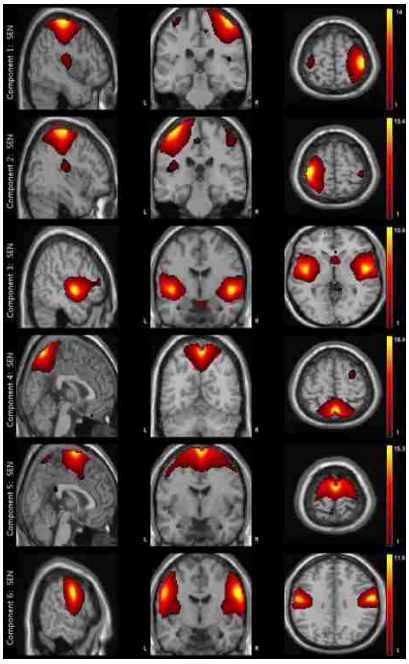

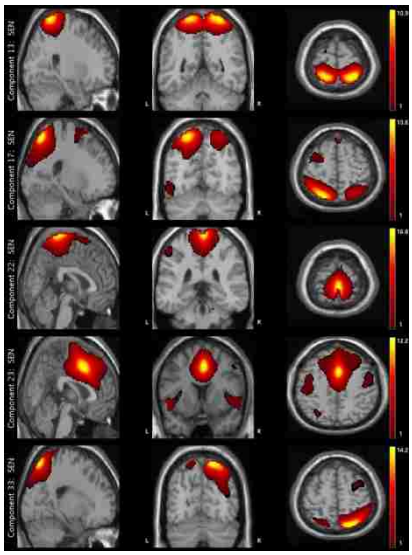

B) Default Mode

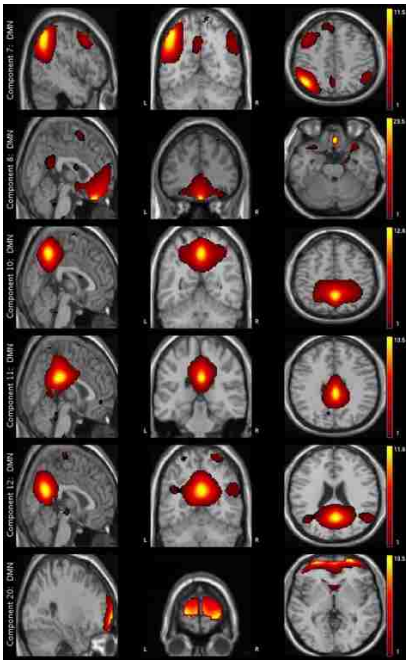

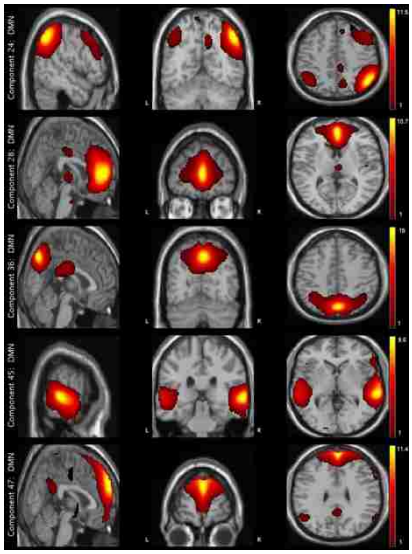

C) Fronto-Parietal

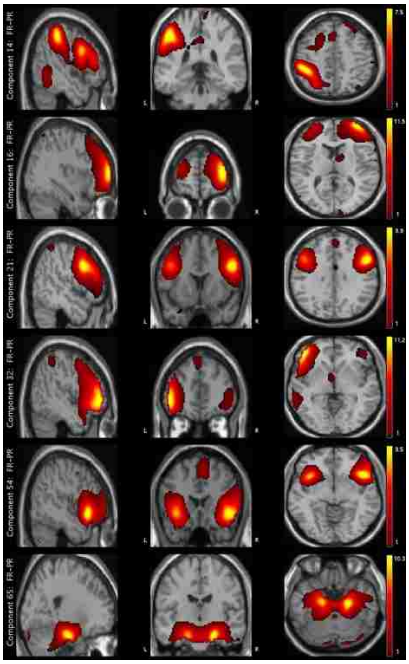

D) Visual

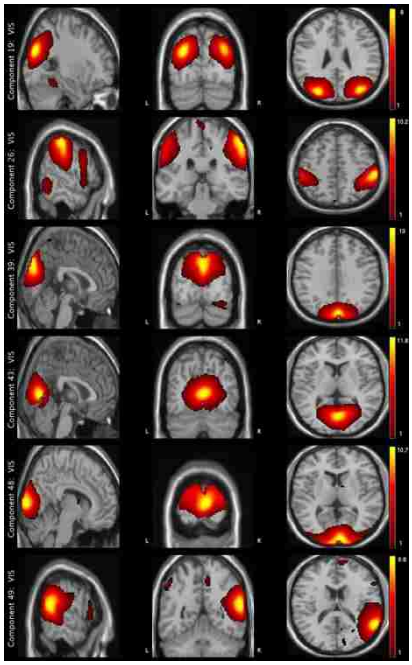

E) Cerebellar

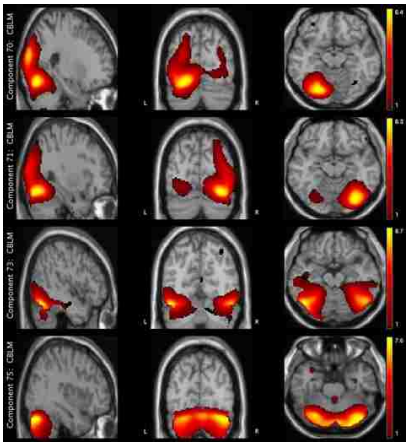

F) Subcortical and Auditory

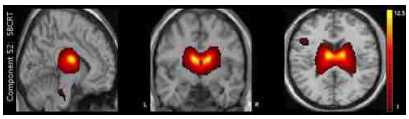

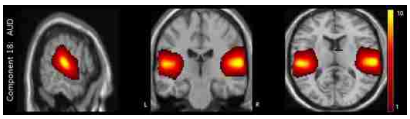

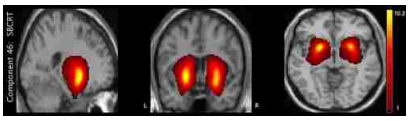

Table 2 – Component Number, Coordinates, Anatomical Location, and Network Label.

AUD, auditory component; SEN, sensory motor components, VIS, visual components; DMN, default mode network components; SBCRT, subcortical components; FR-PR, fronto-parietal components, CBLM, cerebellar components.

Component Number	**Anatomical Coordinates**	**Anatomical Location**	**Grouping Network**
1	42,-28,66	Right Postcentral Gyrus	SEN
2	-40,-26,66	Left Postcentral Gyrus	SEN
3	48,-4,0	Bilateral Insular Cortex	SEN
4	0,-62,62	Bilateral Precuneus, Midline	SEN
5	0,-4,74	Bilateral Supplementary Motor Area, Midline	SEN
6	58,-6,32	Bilateral Post Central Gyrus	SEN
7	-48,-60,46	Left Angular Gyrus, Precuneus, Right Angular Gyrus	DMN
8	0,34,-24	Bilateral Rectal Gyrus, Anterior Cingulate Cortex	DMN
10	0, -54,48	Bilateral Precuneus	DMN
11	0, -30,30	Bilateral Posterior Cingulate Cortex	DMN
12	0,-58,24	Bilateral Precuneus	DMN
13	24,-50,72	Bilateral Superior Parietal Lobule	SEN
14	-50,36,48	Left Inferior Parietal Lobule, Inferior Frontal Gyrus	FR-PR

16	34,60,12	Right Superior Frontal Gyrus	FR-PR
17	-24,-66,60	Left Superior Parietal Lobule	SEN
18	58,-22,12	Bilateral Superior Temporal Gyrus	AUD
19	-30,-80,28	Bilateral Occipital Gyrus	VIS
20	26,66,0	Bilateral Superior Frontal Gyrus, Anterior Cingulate Cortex	DMN
21	48,12,32	Bilateral Superior Frontal Gyrus	FR-PR
22	0,-36,74	Bilateral Paracentral Lobule	SEN
23	0,10,44	Bilateral Supplementary Motor Area	SEN
24	48,-60,46	Right Angular Gyrus	DMN
26	56,-30,50	Right Inferior Parietal Lobule, Supra Marginal Gyrus	VIS
28	0,50,10	Bilateral Anterior Cingulate Cortex	DMN
32	-48,42,-2	Left Inferior Frontal Gyrus	FR-PR
33	18,-72, 60	Right Superior Parietal Lobule	SEN
36	0,-72,44	Bilateral Precuneus, Posterior Cingulate Cortex	DMN
39	0,-84,34	Bilateral Cuneus	VIS
43	0,-72,8	Bilateral Lingual Gyrus	VIS
45	62,-30,2	Bilateral Middle and Superior Temporal Gyrus	DMN
46	-24,6,-4	Bilateral Basal Ganglia	SBCRT

47	0,60,30	Superior Medial Gyrus	DMN
48	6,-96,8	Bilateral Calcarine Gyrus	VIS
49	58,-52,18	Right Middle Temporal Gyrus	VIS
52	-10,-8,18	Bilateral Thalamus	SBCRT
54	44,20,-6	Bilateral Insular Cortex	FR-PR
57	54,-66,4	Bilateral Middle and Inferior Temporal Gyrus	VIS
60	20,-48,-2	Bilateral Lingual Gyrus	VIS
65	20,-16,-24	Bilateral Parahippocampal Gyrus	FR-PR
70	-26,-76,-14	Left Cerebellum	CBLM
71	30,-76,-14	Right Cerebellum	CBLM
73	-48,-66,-18,	Bilateral Cerebellum	CBLM
75	36,-78,-26	Bilateral Cerebellum	CBLM

Connectivity Magnitude Scores

For each subject, each overall average pairwise connectivity measure was squared and summed to attain a measure of connectivity magnitude. The following represents the results of statistical comparisons conducted with the anova1 function in Matlab on mean connectivity magnitude scores between control, FAS, and a combined pFAS/ARND group. The omnibus test of a one-way ANOVA revealed a statistically significant effect of connectivity magnitude score $F(2,57)=9.75$, $p=0.0002$, $\eta^2_p = 0.2617$]. A follow up Bonferroni multiple comparisons procedure revealed that the ARND group displayed a significantly higher average connectivity scores ($\bar{x}= 184.9390$, $s=48.6782$) when compared to control (142.4337, $s=30.9048$, $p=0.0018$, $g=1.1964$) and FAS groups (126.4449, $s=10.6688$, $p=0.0000$, $g=1.7653$) (see Figure 5). Additional two-way ANOVAs including sex as a factor revealed no statistically significant difference of sex [$F(1,57)=0.11$, $p=0.7412$, $\eta^2_p=0.0021$] (Appendix 2).

Figure 5 – Mean Overall Connectivity Magnitude Scores.

Mean connectivity magnitude scores and SEM for control, FAS, and ARND groups. *** indicates a p< (0.05/3).

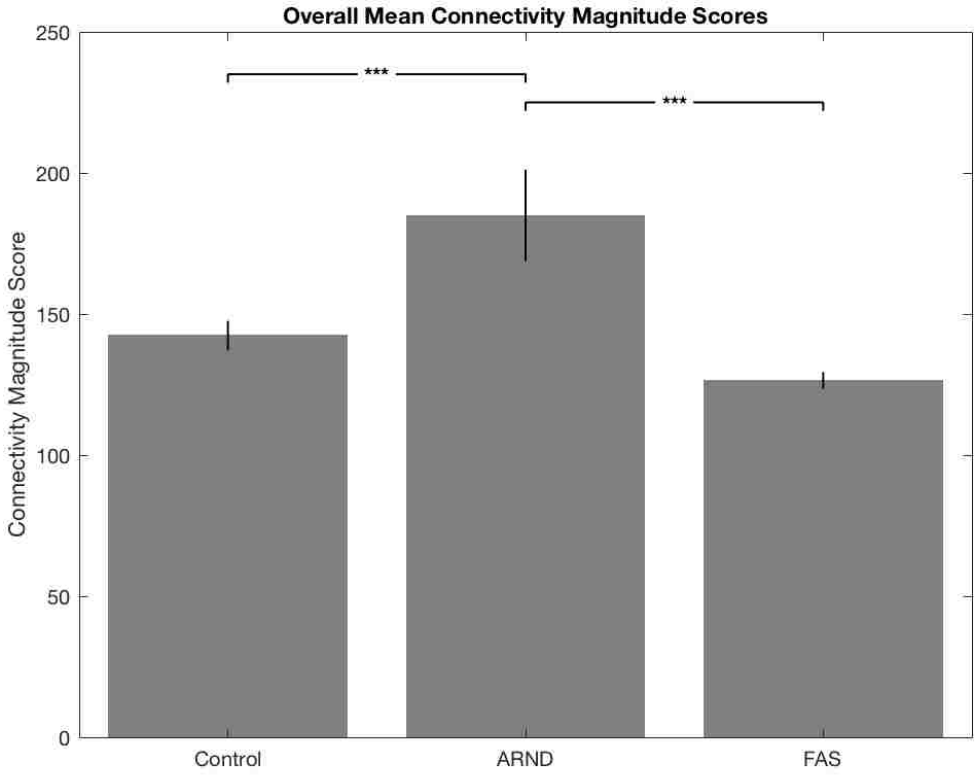

To further examine the contributions of positive versus negative connectivity to the findings displayed in Figure 5, a second set of analyses were performed by separating the positive and negative correlations, squaring, and then comparing across diagnostic groups (control, FAS, and pFAS/ARND combined; Figures 6 and 7). The results of the omnibus test of a one-way ANOVA revealed that at least one group was significantly different in measures of positive magnitude $F(2,57)=8.87$, $p=0.0005$, $\eta^2_p=0.2440$. Post-hoc multiple comparisons utilizing a Bonferroni correction procedure revealed that the ARND

($\bar{x}$= 146.8672, s = 47.3613) group displayed significantly higher positive connectivity magnitude when compared to the control ($\bar{x}$= 103.9063, s=34.048, g=1.1441) and the FAS ($\bar{x}$= 86.3034, s=18.51, g=1.7546) groups. An additional ANOVA including sex as a factor did not reveal a statistically significant difference between sexes [$F(1,57)=0.57$, $p=0.4548$, $\eta^2_p=0.0108$] (Appendix 2).

Figure 6 – Mean Positive Connectivity Magnitude Scores.

Mean positive connectivity magnitude scores and SEM for control, FAS, and ARND groups. *** indicates a $p< (0.05/3)$.

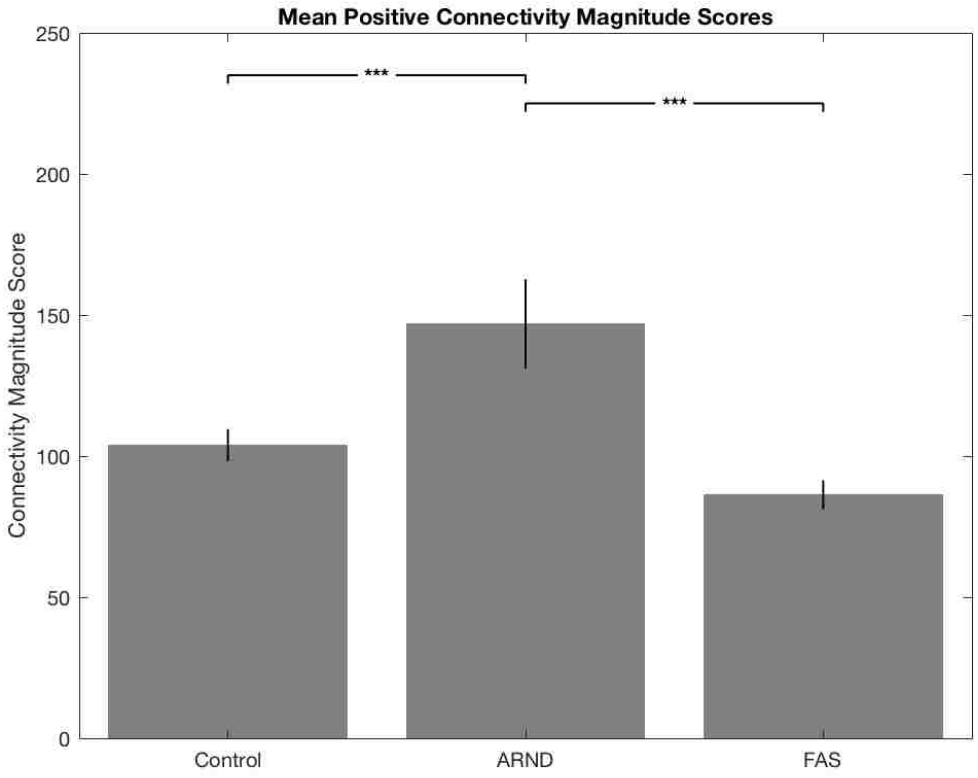

Results of a one-way ANOVA on negative connectivity scores revealed no statistically significant differences when comparing across all three groups [$F(2,57)=0.09$, $p=0.9166$, η^2_p =0,0032]. Similarly, an additional ANOVA including sex as a factor did not reveal a statistically significant difference between sexes [$F(1,57)=1.31$, $p=0.2568$, η^2_p =0.0247] (Appendix 2).

Figure 7 – Mean Negative Connectivity Magnitude Scores.

Mean negative connectivity magnitude scores and SEM for control, FAS, and ARND groups.

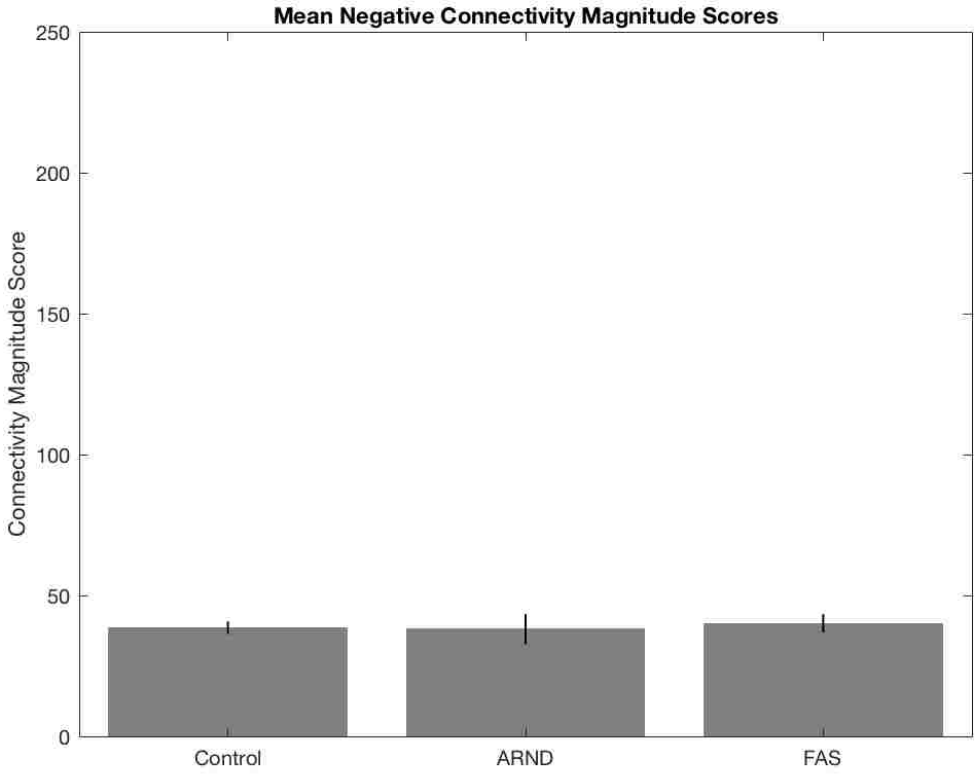

Collectively, these results suggest that the higher ARND connectivity magnitude scores differences in the overall comparison (Figure 5) are driven by higher mean positive connectivity in the ARND group. Further examinations of the sources of contributions to positive connectivity were localized to two couplings in sensory-motor (C33-C17), visual (C60-C43), and default mode (C10-C36) regions. However, comparisons of these couplings were not statistically significant (see figure 12). Scatterplots displaying the relationships between connectivity magnitude scores and neuropsychological assessments are displayed in Appendices 3 and 4.

Functional Network Connectivity

Figure 8 represents the overall connectivity matrix showing the average of all the possible pairwise correlations between retained components for all participants. A total of 903 pairwise correlations were calculated to examine functional connectivity. Strong, positive within-network connectivity was observed for auditory, sensory-motor, and visual groupings. Strong positive within-network connectivity was also observed for DMN components. However, DMN components typically displayed negative connectivity with non-DMN components. Negative correlations were also observed between subcortical and cerebellar, visual, and sensory-motor components.

Figure 8 – Mean r-Value Matrices for All Possible Component Couplings.

Mean r-values from the entire sample. Color bar scale indicates the direction of the connectivity measure (negative correlations in blue, positive in red). Labels indicate network grouping auditory (AUD) sensory-motor (SEN), visual, (VIS), cerebellum (CBLM), default mode network (DMN), fronto-parietal (FR-PR), and subcortical (SBCRT).

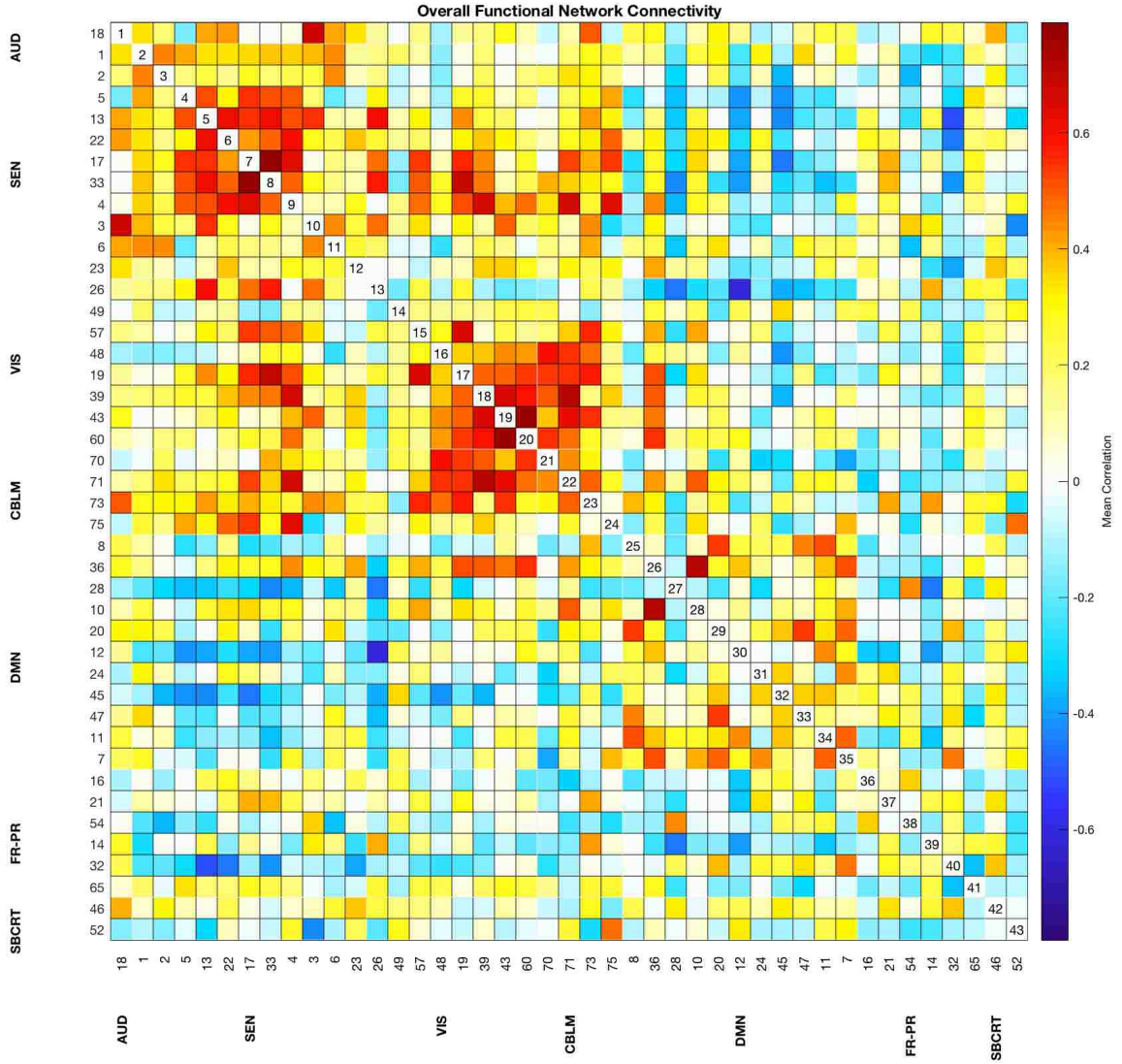

Figures 9-11 represent the connectivity matrix for all possible pairwise correlations between retained components for control, ARND, and FAS groups. As with the overall connectivity matrix the general pattern of connectivity is reproduced across all three diagnostic groups. The data displayed in Figures 9-11 form the basis of subsequent analysis including ANOVAs and t-tests to be described in subsequent sections. Appendix 5 displays the FNC matrices for males and female.

Figure 9 – Mean r-Value Matrices for All Control Component Couplings. Mean r-values from controls. Color bar scale indicates the direction and magnitude of correlation values, negative correlations in blue, positive in red. Labels indicate network grouping auditory (AUD) sensory-motor (SEN), visual, (VIS), cerebellum (CBLM), default mode network (DMN), fronto-parietal (FR-PR), and subcortical (SBCRT).

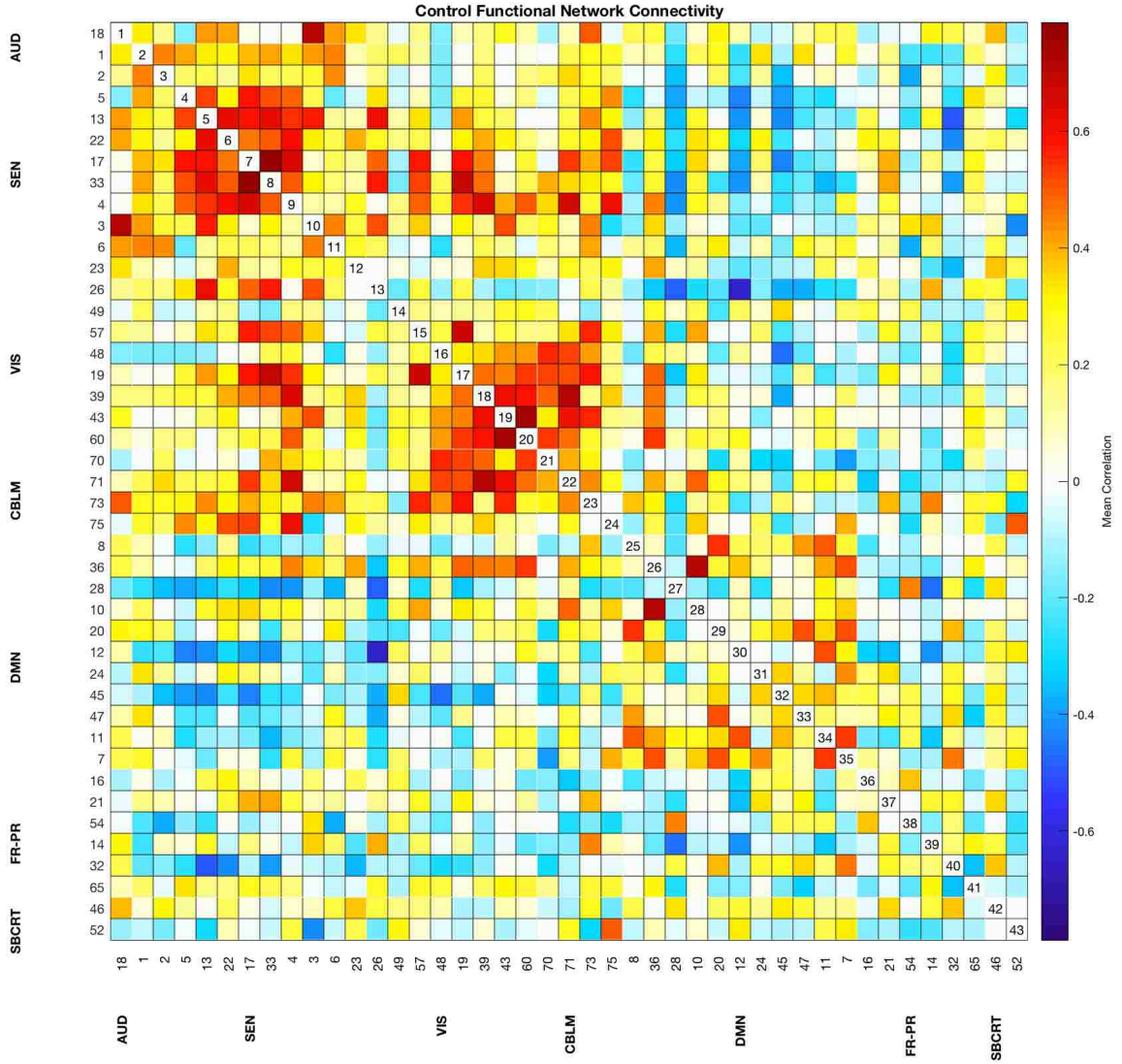

Figure 10 – Mean r-Value Matrices for All pFAS/ARND Component Couplings. Mean r-values from the pFAS/ARND group. Color bar scale indicates the direction of the connectivity measure (negative correlations in blue, positive in red). Labels indicate network grouping auditory (AUD) sensory-motor (SEN), visual, (VIS), cerebellum (CBLM), default mode network (DMN), fronto-parietal (FR-PR), and subcortical (SBCRT).

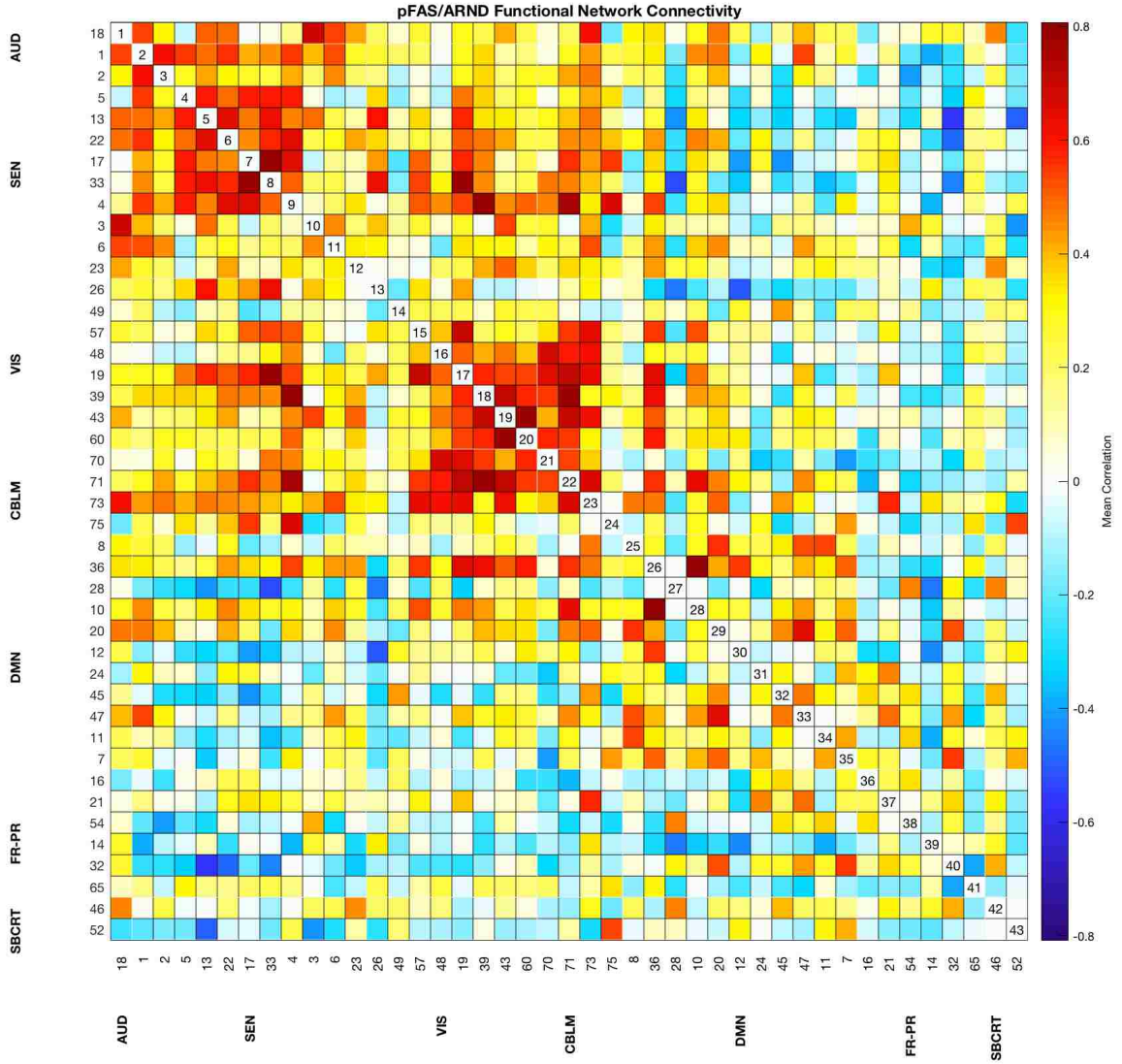

Figure 11 – Mean r-Value Matrices for All FAS Component Couplings.

Mean r-values from the FAS participants. Color bar scale indicates the direction of the connectivity measure (negative correlations in blue, positive in red). Labels indicate network grouping auditory (AUD) sensory-motor (SEN), visual, (VIS), cerebellum (CBLM), default mode network (DMN), fronto-parietal (FR-PR), and subcortical (SBCRT).

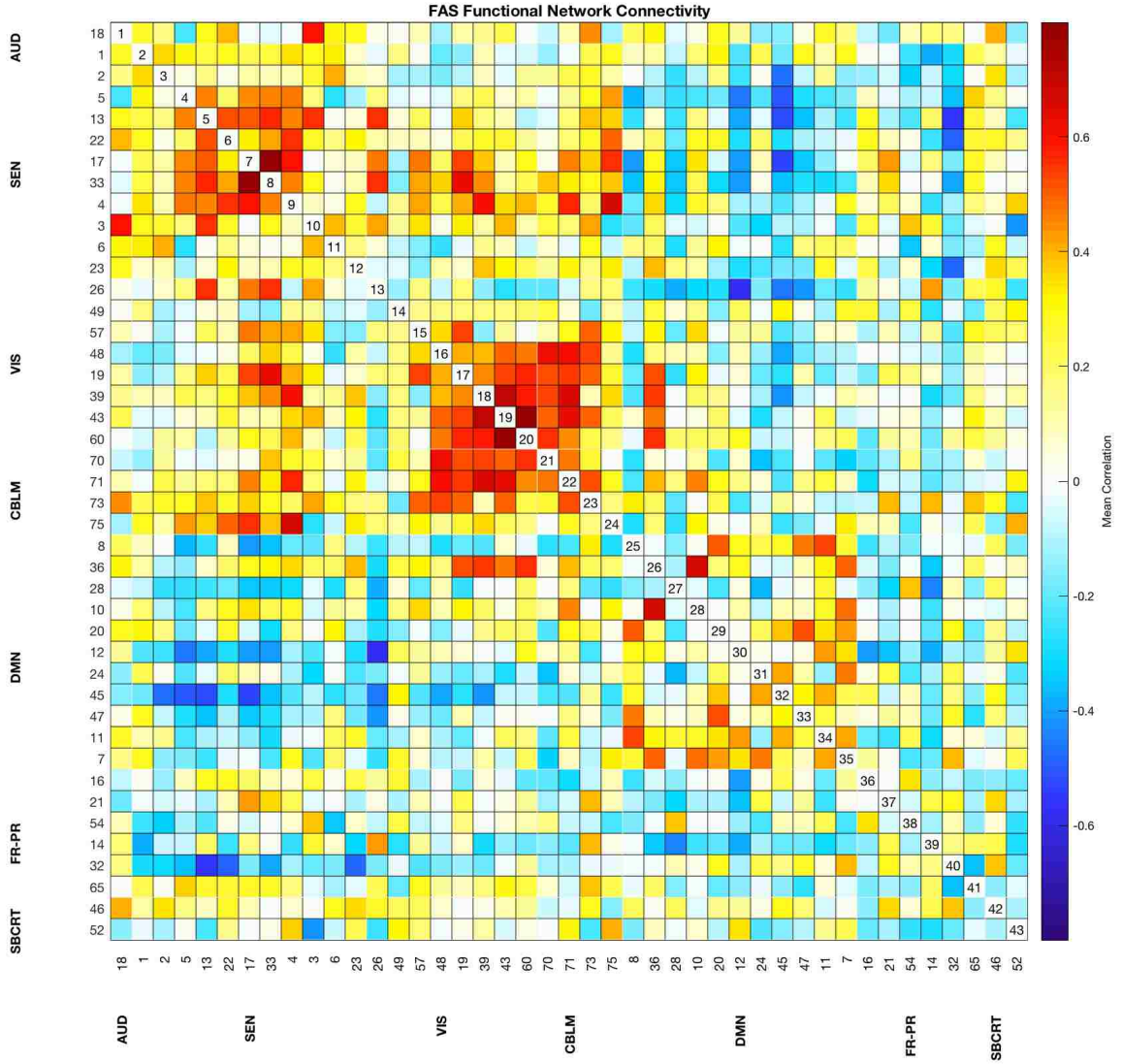

ANOVA Results

Figures 12A-12C display p-value matrices derived from a 2x2 (ANOVA) conducted on the pairwise component connectivity values for all retained participants utilizing prenatal condition (control, FAS, or pFAS/ARND) and sex (male or female) as main factors. Each matrix displays a total of 903 separate analyses where darker cells indicate lower p-values and lighter cells indicate higher p-values. Cells marked with a yellow dot, indicate the analysis was statistically significant at the $p<0.05$ threshold. Cells marked with a red dot indicate the analysis was statistically significant at a corrected threshold, either Bonferroni or the FDR (Storey procedure implemented in Matlab) (Storey, 2002) corrected significance level. However, due to the large number of multiple comparisons, no single analysis met either of the corrected threshold significance levels. The order of results described will begin with the main effect of diagnosis, then sex, and finish with the interaction. While it is customary to describe the interaction effects to contextualize the main effects, here, the interactions are described last because most the main effects observed do not overlap with those of the interactions suggesting the effects of diagnosis are not typically associated with changes across levels of sex.

ANOVAs: Main Effect of Prenatal Condition

Of the 903 possible comparisons along the prenatal condition factor, 111 couplings survived the uncorrected $p < 0.05$ threshold. These couplings were found in auditory (AUD), sensory-motor (SEN), visual (VIS), cerebellar (CBLM),

default mode (DMN,) fronto-parietal (FR-PR), and sub-cortical (SBCRT) groupings. Due to the richness of the results, only the component couplings with the highest frequency of statistical significance will be reported.

Pronounced patterns of effects were observed among couplings with component 47 (superior medial gyrus, grouped into DMN components). In total, C47 exhibited the largest amount of significant effects corresponding to approximately 18% of the observed effects that met the $p<0.05$ significance threshold. Furthermore, many of these effects were between C47 and components in auditory, sensory-motor, and visual components.

Component 19 (bilateral occipital gyrus, grouped into visual components) exhibited 12 significant effects corresponding to approximately 11% of the observed effects that met the $p<0.05$ significance threshold. Couplings between C19 and components of sensory-motor networks were the most frequently observed including C1 (right postcentral gyrus, sensory-motor), C2 (left post central gyrus, sensory-motor), and C5 (midline bilateral supplementary motor area, sensory-motor), C13 (bilateral parietal lobule, sensory-motor), and C22 (bilateral para central lobule, sensory-motor).

Component 10 (bilateral precuneus, DMN) also exhibited 12 significant corresponding to ~11% of the observed effects that met $p<0.05$ statistical significance. Of the total C10 effects, 25% involved components grouped into sensory-motor networks such as C1 (right postcentral gyrus), C2 (left post central gyrus), and C5 (midline bilateral supplementary motor area).

This pattern of results, however, failed to reach corrected significance levels utilizing a stringent Bonferroni and a less conservative FDR correction procedure. Despite this limitation, these findings provide clues for future regionally targeted analyses involving structures associated with sensory, motor, and default mode networks that may overcome the limitation of the vast amount of statistical comparisons.

ANOVAs: Main Effect of Sex

Of the 903 possible comparisons along the sex factor, 73 survived the uncorrected $p < 0.05$ threshold and demonstrated a reduced number of tests reaching statistical threshold when compared to the prenatal condition factor. These effects were found several components grouped in auditor, sensory-motor, visual, cerebellar, default mode, fronto-parietal, and subcortical networks. As with the ANOVAs on prenatal condition, only a small number of patterns will be described in the remainder of this section.

One pronounced pattern of effects involves component 49 (right middle temporal gyrus, visual) as it was implicated in 13, approximately 18%, of the 73 statistical effects observed. Couplings between C49 and sensory-motor and visual components were most abundant. Of interest are couplings with sensory motor components such as C5 (bilateral supplementary motor area), C13 (bilateral superior parietal lobule), C22 (bilateral paracentral lobule), and C17 (left superior parietal lobule) as these were also related to frequently observed effects with components 18 and 45.

An additional pattern of results involves statistically significant ($p<0.05$) differences between component 18 (bilateral superior temporal gyrus) and sensory-motor components. A total of 11 effects corresponding to approximately 15% of the total number of significant effects were observed. Couplings between C18 involved several sensory motor components what were also implicated with C49 (described above). These couplings included C5 (bilateral supplementary motor area), C13 (bilateral superior parietal lobule), C22 (bilateral paracentral lobule), and C17 (left superior parietal lobule) painting an emerging theme that sensory-motor networks not only differ across sex, but also across prenatal condition.

Component 45 (bilateral middle and superior temporal gyrus) demonstrated 11 statistically significant ($p<0.05$) effects corresponding to an additional 15% of statistical effects observed. C45 was implicated in couplings such as C2 (left post-central gyrus) C5 (bilateral supplementary motor area), C13 (bilateral superior parietal lobule), and C22 (bilateral paracentral lobule), and C17 (left superior parietal lobule) which were also involved in the pattern of results for C49 and C18. The remaining couplings involved visual and cerebellar components.

Component 57 (bilateral middle and inferior temporal gyrus) was also associated with a frequent amount of effects, 11 corresponding to 15% of total effects, that met the $p<0.05$ threshold. Many of these effects were found in couplings with sensory motor and default mode networks, that shared couplings

with C5 and C22. However, as with the results with the comparisons across condition, these results do not survive Bonferroni nor FDR correction procedures.

ANOVAs: Interaction

Of the 903 possible comparisons to investigate an interaction between sex and diagnostic label, 47 survived the uncorrected $p < 0.05$ threshold. While these effects were observed in all network groupings, their frequency was reduced compared to the main effects of diagnosis and sex.

Component 46 (bilateral basal ganglia) was most frequently associated with a statistically significant effect resulting in 9 (~19%) effects. Couplings with C46 most frequently included sensory-motor components including C13 (bilateral superior parietal lobule), C6(bilateral post central gyrus), and C23 (bilateral supplementary motor area). C46 was also associated with visual component 43 (bilateral lingual gyrus) and cerebellar component 75 (bilateral cerebellum) which were also observed in additional component couplings.

Component 11 (bilateral posterior cingulate gyrus) was associated with 8 (approximately 17%) of the effects. Couplings between C11 and visual, and DMN components were most frequently observed.

Components 20 (bilateral superior frontal gyrus and anterior cingulate gyrus) and 75 (bilateral cerebellum) were both associated with 7 (~15%) observed effects for the interaction. Statistically significant couplings with C20 were most frequently observed in sensory-motor and visual groupings and with

C75. Statistically significant, at the $p<0.05$ level, couplings with C75 were most frequently observed in the sensory-motor grouping.

ANOVA: Summary

The results of the ANOVA main effect of diagnosis suggest that components associated with the default mode network such as the superior medial gyrus and visual networks such as the occipital gyrus exhibited the most pronounced effects. Although none of these effects survived Bonferroni nor FDR correction procedures, these findings provide clues for future regionally targeted analyses. The results of the ANOVA main effect of sex suggest that the right middle temporal gyrus exhibited the greatest number of differences when comparing across sex and may serve as a target for investigating the sex-dependent effects of prenatal alcohol exposure. The majority of the ANOVA interaction effects were mostly localized to components of the bilateral basal ganglia suggesting an interaction between sex and diagnostic label for this region. However, it is important to note that the basal ganglia components are susceptible to artifactual features due to their proximity to the first, and lateral ventricles which provides motivation for careful interpretation of the results in these components.

Figure 12 – ANOVA p-value Matrices.

Main effect of diagnosis (A), sex (B), and interaction (C). Color bar scale indicates magnitude of p-value (darker cells indicate smaller p-values). Cells marked by a yellow circle indicate uncorrected statistical significance at $p<0.05$. No cells survived Bonferroni or false discovery rate (FDR) corrected thresholds.

A) Main effect of Diagnosis

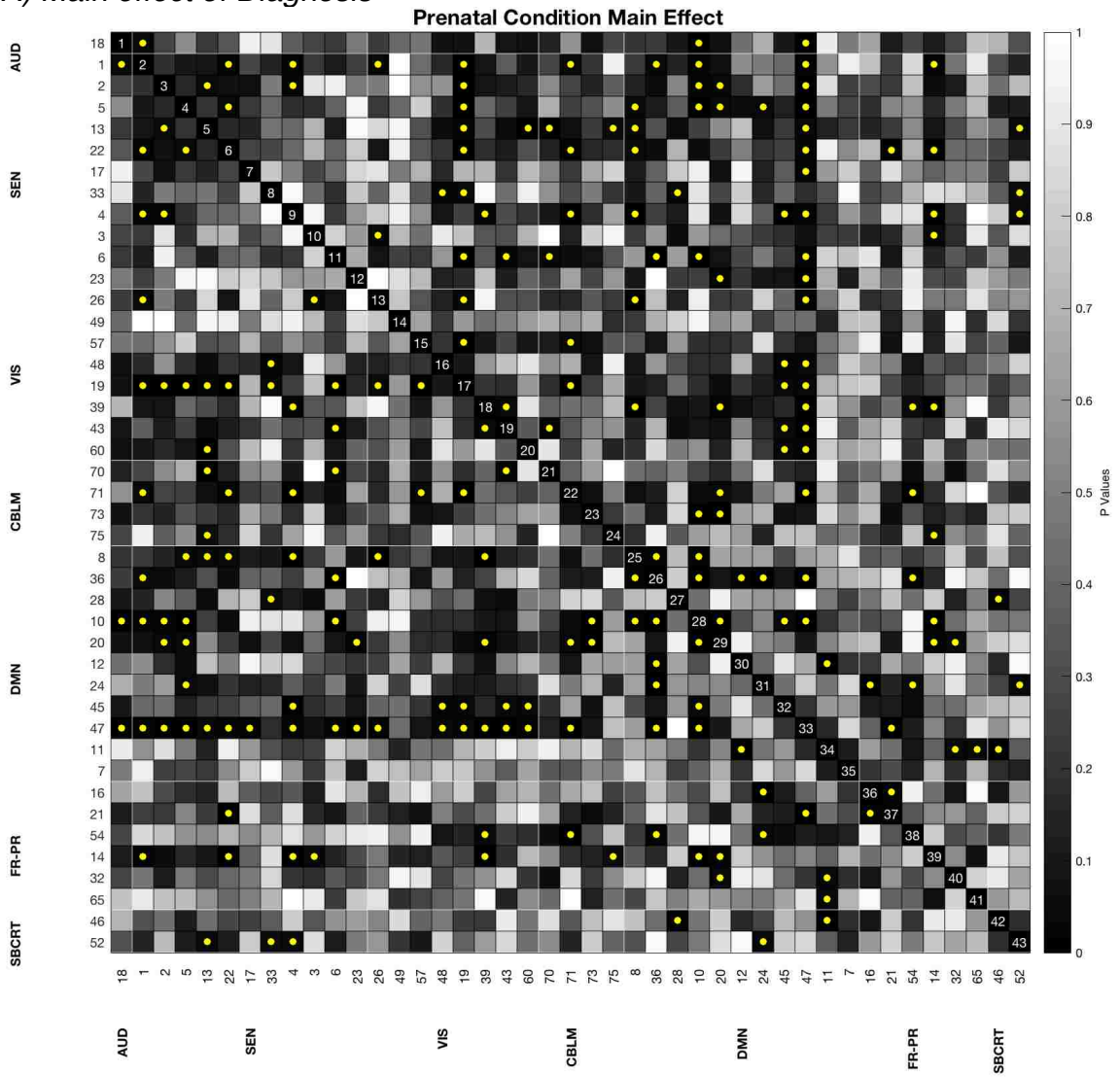

B) Main effect of Sex - Cells marked by a yellow circle indicate uncorrected statistical significance at $p<0.05$. No cells survived Bonferroni or false discovery rate (FDR) corrected thresholds.

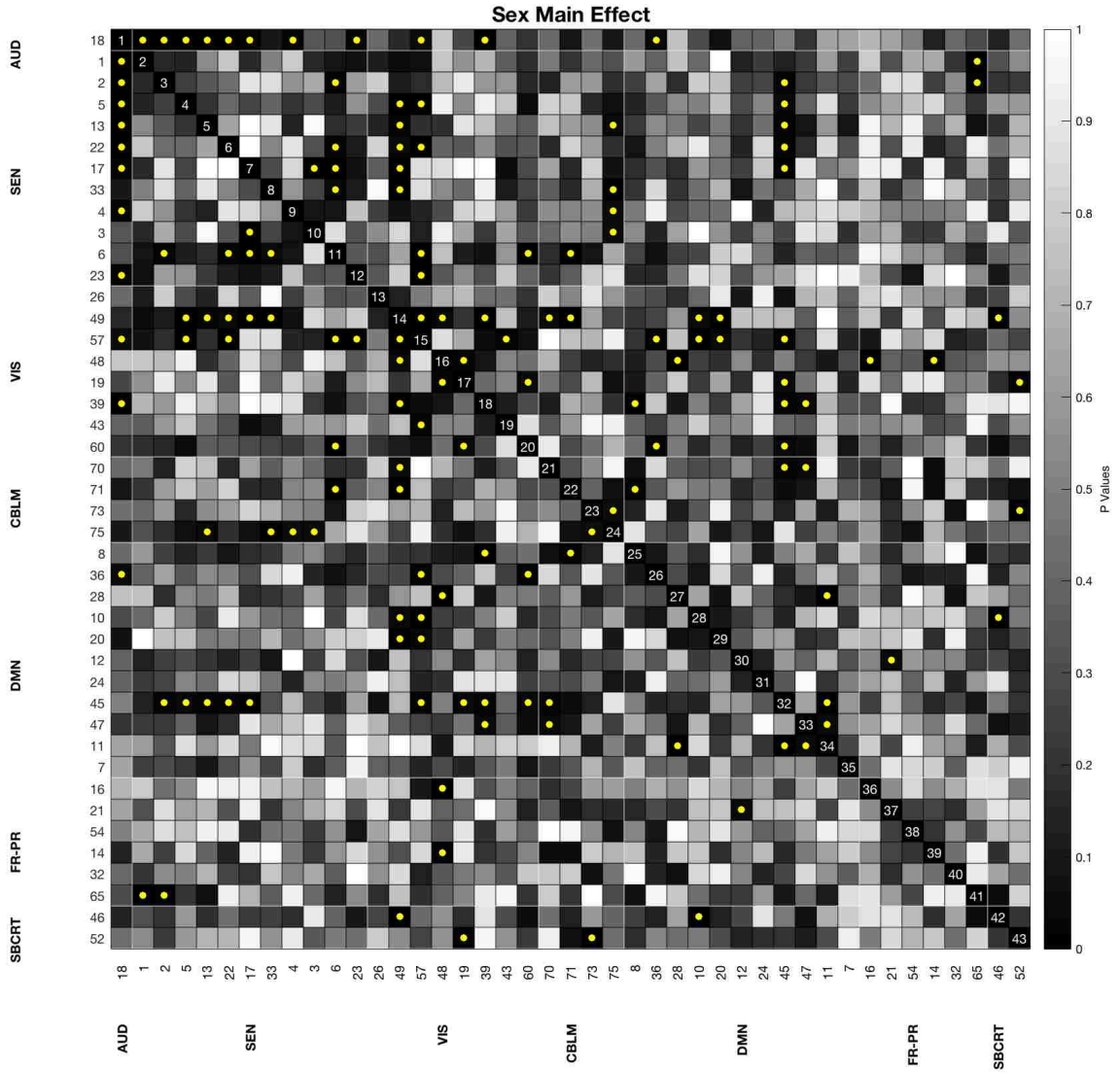

C) Cells marked by a yellow circle indicate uncorrected statistical significance at p<0.05. No cells survived Bonferroni or false discovery rate (FDR) corrected thresholds.

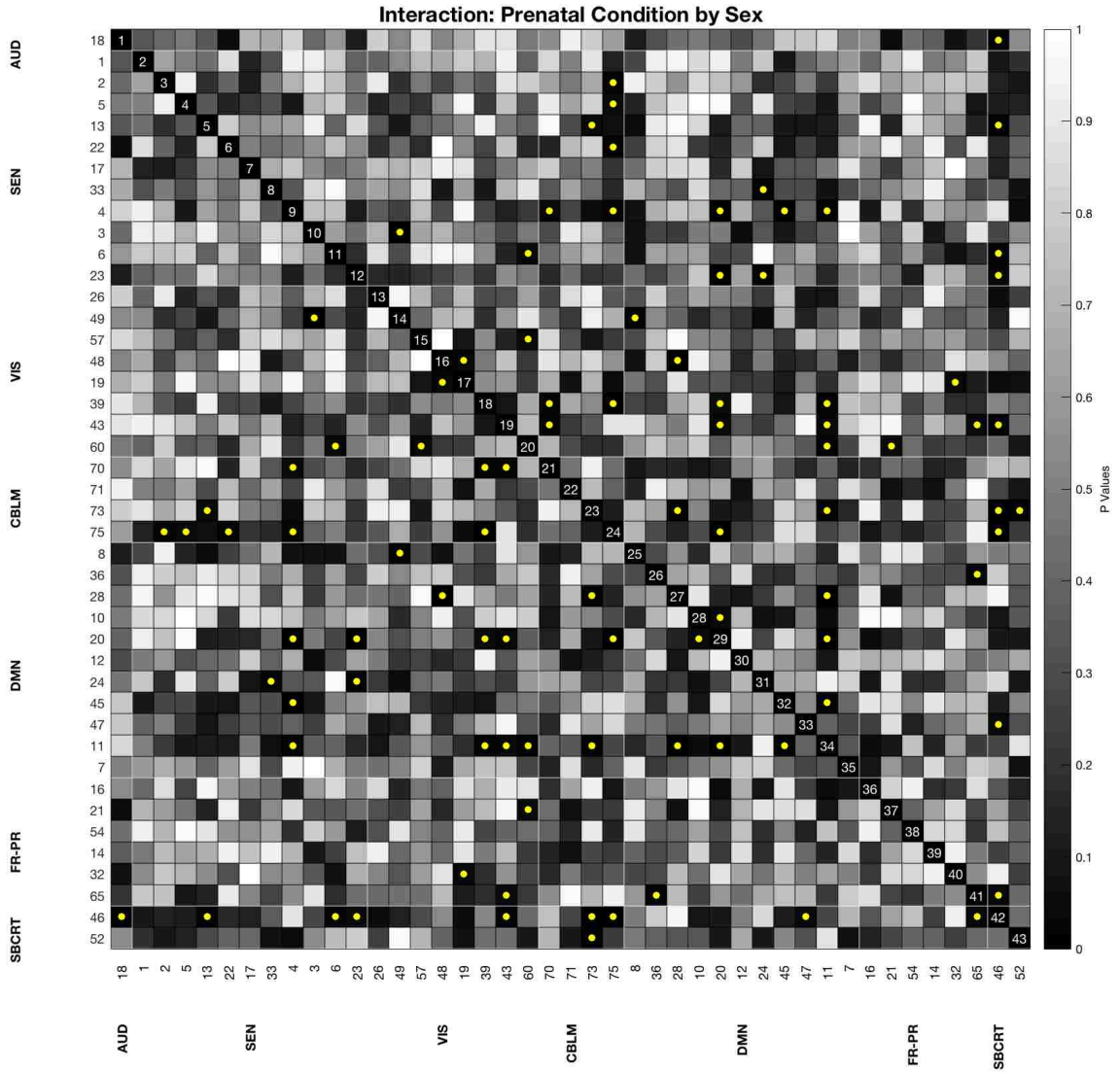

FNC T-test Results

Figures 13-21 display the results of separate two-sample t-tests conducted to evaluate the differences of FNC measures between groups, Controls-FAS (Figure 13), ARND-controls (Figure 16), and ARND-FAS (Figure 21). Each of these figures displays the magnitude of a t-value from the corresponding t-test between the average connectivity measures for each possible pairwise combination of components. In these figures, blue cells reflect negative t-values and red cells reflect positive t-values. Each cell may also be marked with a solid white circle to indicate the results of a statistically significant t-test at the $p<=0.05$ level. No result of these comparisons survived Bonferroni correction and as result, only the $p<=0.05$ effects are displayed.

Accompanying each FNC t-test figure are two separate figures that display the absolute value of the magnitude of the effect size (in Hedges' g which is similar to the more well-known Cohen's d) for each corresponding two sample t-test (Cohen, 1992; Larry, 1981). Cells marked in blue reflect lower effect sizes while cells marked in red reflect higher effect sizes. Each cell may be accompanied by a solid green or magenta circle which indicate effect size of greater than 0.8 or effect sizes greater than or equal to 0.5, but less than 0.79 respectively. There are two effect size matrices for each t-test figure. The first matrix displays all effects that met the 0.5 (magenta) or 0.8 (green) levels. The second matrix displays only the effects that met the 0.8 (green) levels to enhance

the visual contrast of the results and highlight the strongest effects, regardless of the p-value resulting from the corresponding two-sample t-test.

The first set of figures (Figures 13-15) describe the results and effect sizes of two-sample tests conducted between controls and FAS participants. In Figure 13, red cells indicate that controls exhibited stronger connectivity, while blue cells indicate that FAS participants exhibited stronger connectivity. In the second set of figures (Figures 16-18), the results display the results of two-sample t-tests and corresponding effect sizes between ARND and Control participants. In Figure 16, red cells indicate that ARND participants displayed stronger connectivity, while blue cells indicate that controls. In the final set of figures (Figures 19-21), the results displayed compare ARND and FAS participants with red cells in Figure 19 indicating stronger connectivity in ARND participants while blue cells indicating stronger connectivity in FAS participants.

FNC T-test Results: Controls-FAS

A total of 903 two-sample t-tests were conducted to examine the difference in connectivity for each possible component coupling between control and FAS participants. The following is a description of the components that were most frequently observed as having statistically significant effects at the $p < 0.05$ level and are displayed in Figure 13. Individual cells in Figure 13 display the magnitude of the t-value resulting from a two-sample test (controls minus FAS) with red cells indicating strong positive t-values and blue cells indicating strong negative t-values. Cells marked with a white circle indicate the t-statistic met the

$p<0.05$ significance level. To complement the t-value matrices, additional effect size matrices displays the Hedges' g value calculated for each corresponding t-test. All effect sizes (Hedges' g) were converted to an absolute value to simplify visualization and localization of effects. Cells filled in dark blue indicate a small effect size, while cells filled with red indicate a strong effect size. Cells marked with a magenta circle indicate an effect size between 0.5 and 0.79 while cells marked with a green circle indicate an effect size larger than 0.8. To simplify the interpretation of the data, a select number of strong effect sizes will be discussed following descriptions of the outcomes of the two-sample t-tests.

The results of the two-sample t-test comparing connectivity between controls and FAS resulted in a total of 46 unique significant effects at the $p<0.05$. Of the total significant effects, components 1 (right postcentral gyrus) and 14 (left inferior parietal lobule) were the most frequent. C1 was associated with 7 effects, corresponding to approximately 15% of the total significant effects. Of these 7, all but 1, were in the positive direction. Positive t-values were observed in sensory-motor, cerebellar, and fronto-parietal couplings. A single negative t-value was observed in the coupling between C1 and a C28 (bilateral anterior cingulate cortex grouped into the DMN). Couplings between C1 and C26 (right inferior parietal lobule and supra marginal gyrus), C1 and C71 (right cerebellum), and C1-C14 exhibited effect sizes greater than or equal to 0.8 and suggesting strong differences in connectivity between sensory-motor and visual, sensory-motor and

cerebellar, and sensory-motor and fronto-parietal components with control participants displaying stronger connectivity in these couplings.

C14 (left inferior parietal lobule) was also associated with 7 effects, corresponding to an additional 15% of the total observed effects. All statistically significant effects were associated with a positive t-value indicating stronger connectivity in the controls when compared to the FAS participants. Positive values were observed in couplings between C14 and sensory-motor, visual, and DMN components. C14 couplings were also associated with two effect sizes greater than or equal to 0.8. While one was mentioned above, (C1-C14), the remaining effect was observed in the connectivity between C14 and C39 which describes the connectivity between components localized to the inferior parietal lobule (C14) and bilateral cuneus (C39).

Figure 14 displays the corresponding strong effect sizes for the above analyses. Of importance, are components localized to fronto-parietal regions. Components 21 (bilateral superior frontal gyrus), 54 (bilateral insular cortex), 14 (left inferior parietal lobule), and 32 (left inferior frontal gyrus) exhibited effect sizes greater than or equal to 0.8, indicating the connectivity between these regions may be of interest in future studies to examine their susceptibility to the effects of prenatal alcohol exposure. While Figure 14 displays the strongest effect sizes, Figure 15 displays the strong and medium effect sizes and is included here for a more thorough visualization of the data.

Figure 13 – Two-sample t-test values (Control-FAS).

T-test value matrix indicating t-values from a two-sample t-test between controls and FAS participants. Cells marked with a white circle indicate the t-value is statistically significant at the p<=0.05 level.

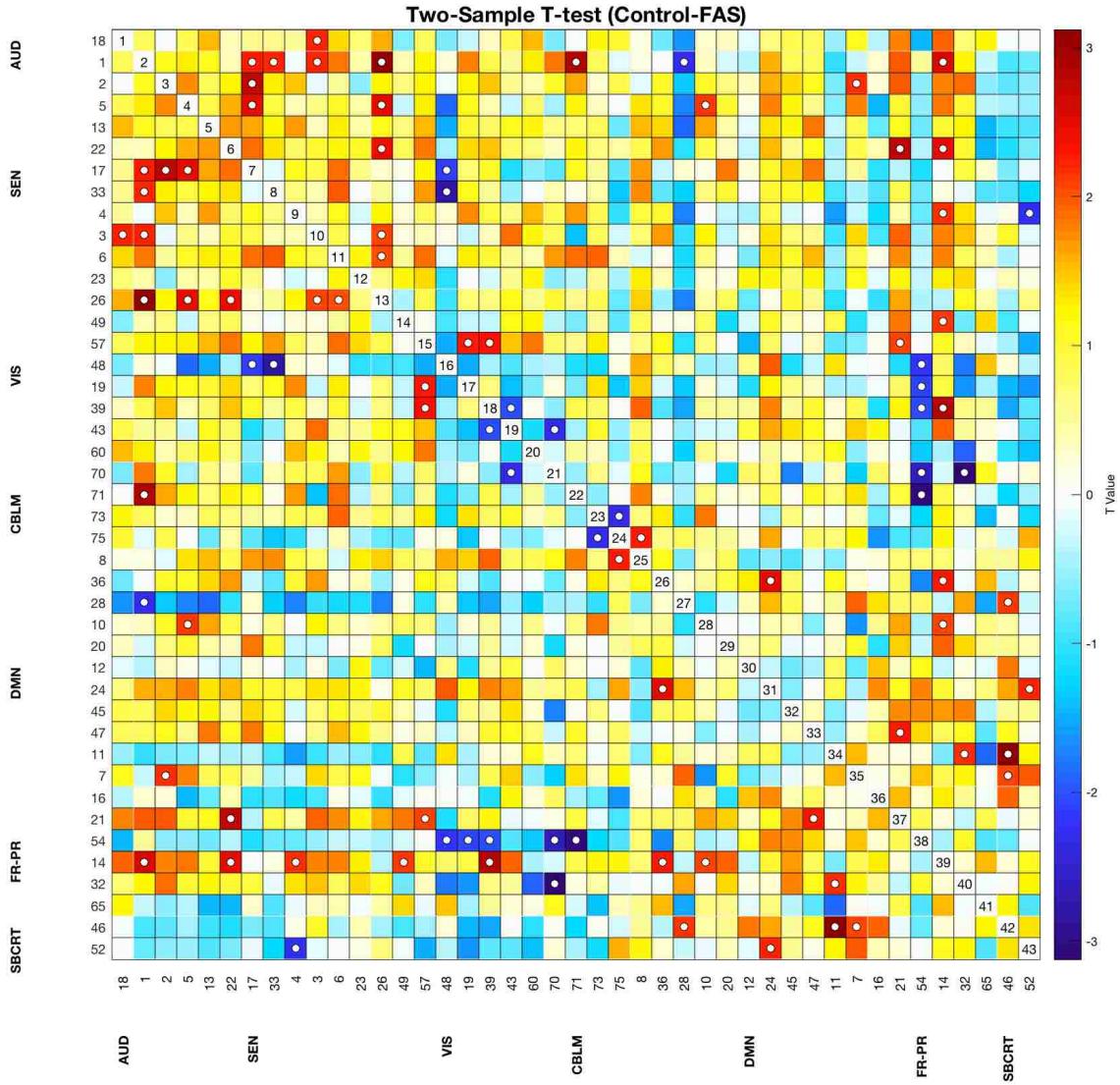

Figure 14 – Two-sample t-test effect size matrix (Control-FAS).

Absolute value of Hedges' g is shown with cells marked with a magenta circle indicating effect size >=0.5<0.80; cells marked with a green circle indicate effect size >= 0.8.

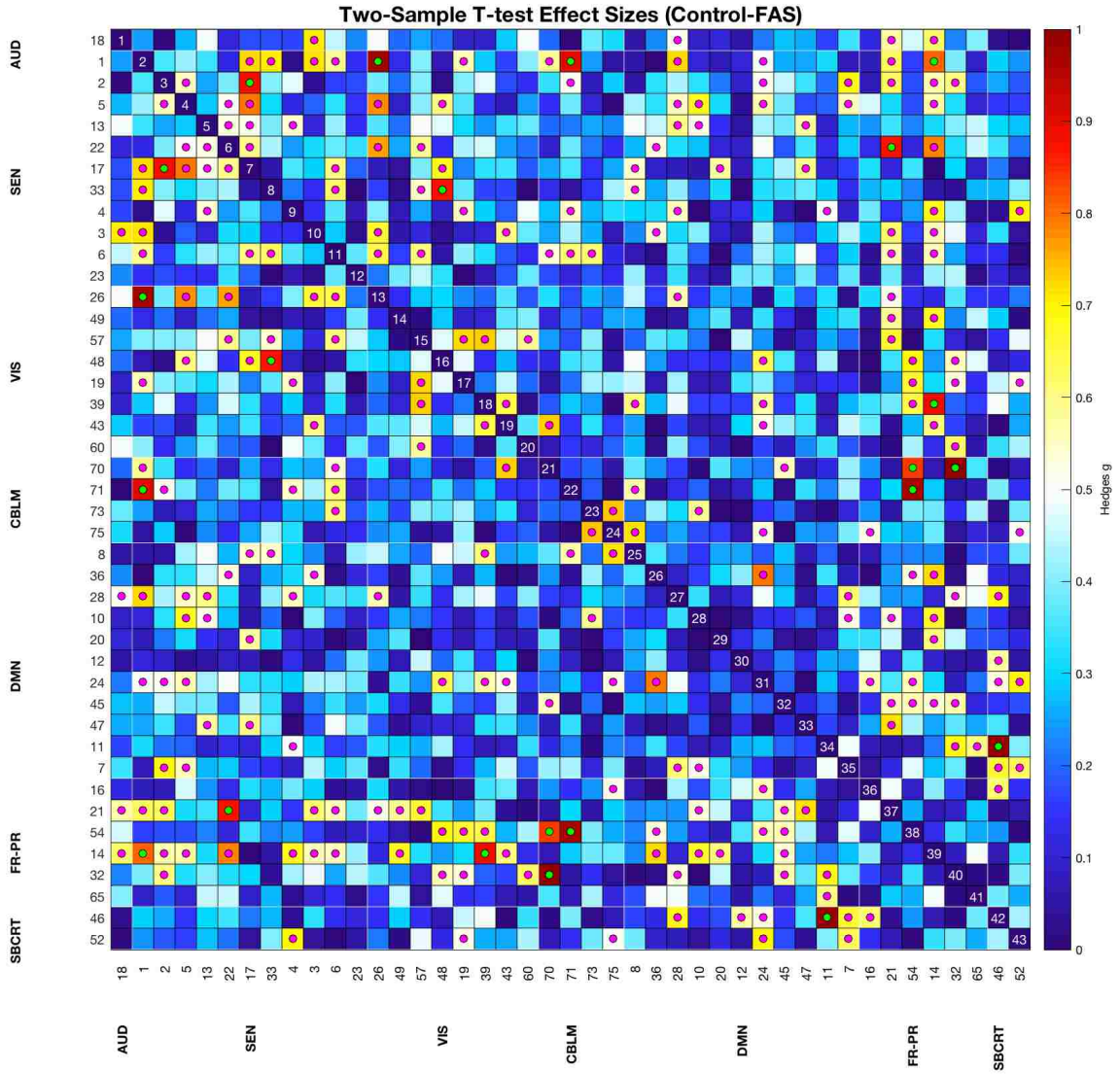

Figure 15 – Two-sample t-test effect size matrix (Control-FAS).

Absolute value of Hedges' g is shown only for cells above the g=0.8 threshold.

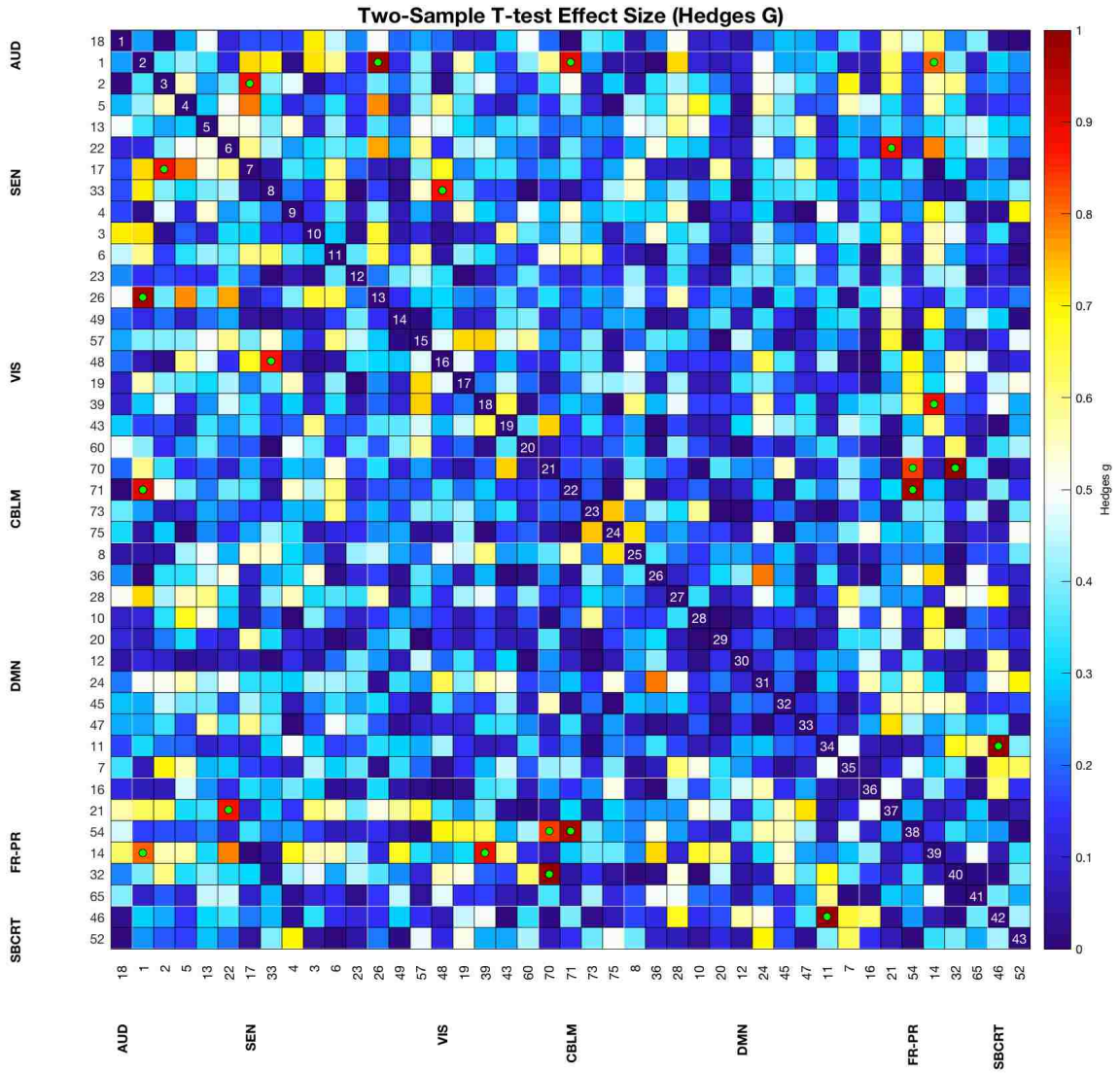

FNC T-tests: ARND-Control

The results of two-sample t-test comparing connectivity between the ARND group and controls are shown Figure 16 and resulted in a total of 106 unique significant effects at the $p<0.05$. The corresponding results of effect size calculations for each t-test are shown in Figure 17 which displays effect sizes that fall in between 0.5 and 0.79 and those that are equal to or above 0.8. Figure 18 displays only those effects greater than or equal to 0.8 to highlight the strongest effect sizes observed.

Of the total significant effects, components 47 (superior medial gyrus), 20 (bilateral superior frontal gyrus, anterior cingulate cortex), 10 (bilateral precuneus), and 19 (bilateral occipital gyrus) were the most frequent. C47 was associated with 20 effects in numerous couplings localized to auditory, sensory-motor, visual, and default mode components. C47 effects corresponded to approximately 19% of the total significant effects of the comparisons between ARND and controls. Of these 20, all were in the positive direction suggesting stronger mean connectivity in ARND participants when compared to controls. Of the 20 t-test effects in C47, 15 of those displayed effect sizes of greater than 0.8. These effect sizes were frequently localized to couplings between C47 and auditory, visual, and cerebellar components.

Component 20 (bilateral superior frontal gyrus, anterior cingulate cortex) was associated with 15 t-test effects, corresponding to approximately 14% of the total observed effects between ARND and controls. Fourteen of the statistically

significant effects were associated with a positive t-value generally indicating stronger connectivity in the ARND group when compared to the control participants. Positive t values were observed in couplings between C20 and auditory, sensory-motor, visual, cerebellar, and DMN components. C20 couplings were also associated with 11 effect sizes greater than or equal to 0.8. The single negative t-value observed in couplings with C20 was localized to C14 (left inferior parietal lobule) and yielded a strong effect size (g>=0.8) indicating less connectivity in the ARND group for these two components.

The remaining components most frequently observed with statistically significant t-values were C10 (bilateral precuneus) and C19 (bilateral occipital gyrus). For C10, a total of 13 t-test effects were observed corresponding to approximately 12% of the total effects. Of the 13 effects observed in C10, all were positive except for one. Positive t-values were exhibited in auditory, sensory motor, visual, cerebellar, and default mode groupings. The single negative t-value was observed in C14 (left inferior parietal lobule). Of the 13 t-test effects, 9 were associated with a g>=0.08 effect size. These strong effect sizes were observed in auditory, sensory-motor, visual, cerebellar, default mode, and fronto-parietal components.

While not frequently associated with statistically significant effects, it is of interest to note that component 14 (left inferior parietal lobule) was generally associated with negative t-values suggesting weakened connectivity in between in C14 of the ARND participants. Similarly, a pattern of results with component

75 (bilateral cerebellum) generally exhibiting negative t-values suggesting weakened connectivity in the ARND group for cerebellar couplings. These findings contrast the general observed pattern of heightened connectivity in components localized to default mode and visual networks.

To summarize the major pattern of effects, higher connectivity in the ARND group was found in components C47 (superior medial gyrus), C20 (bilateral superior frontal gyrus/anterior cingulate cortex, and C10 (bilateral precuneus) –all default mode network components. Higher connectivity in C19 (bilateral occipital gyrus), a visual component accompanied this pattern. Lowered connectivity was also observed in several couplings involving C14 (left inferior parietal lobule-inferior frontal gyrus) in the ARND group when compared to controls. Thus, the ARND group displayed higher connectivity in components associated with default and visual functions compared to controls while displaying lowered connectivity in fronto-parietal regions.

Figure 16 – Two-sample t-test values (ARND-Control).

T-test value matrix indicating t-values from a two-sample t-test between ARND and control participants. Cells marked with a white circle indicate the t-value is statistically significant at the p<=0.05 level.

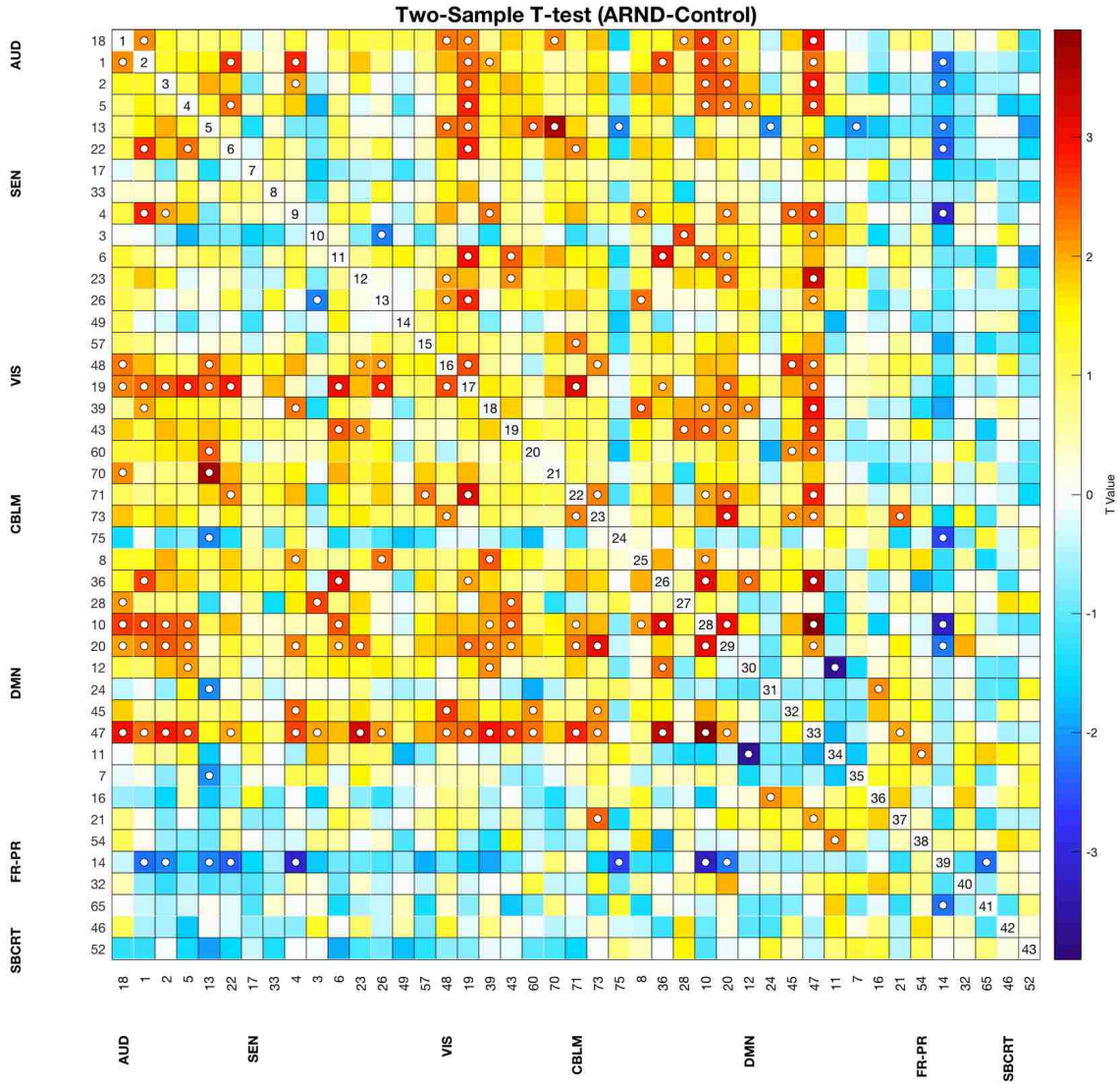

Figure 17 – Two-sample t-test effect size matrix (ARND-Control).

Absolute value of Hedges' g is shown with cells marked with a magenta circle indicating effect size >=0.5<0.80; cells marked with a green circle indicate effect size >= 0.8.

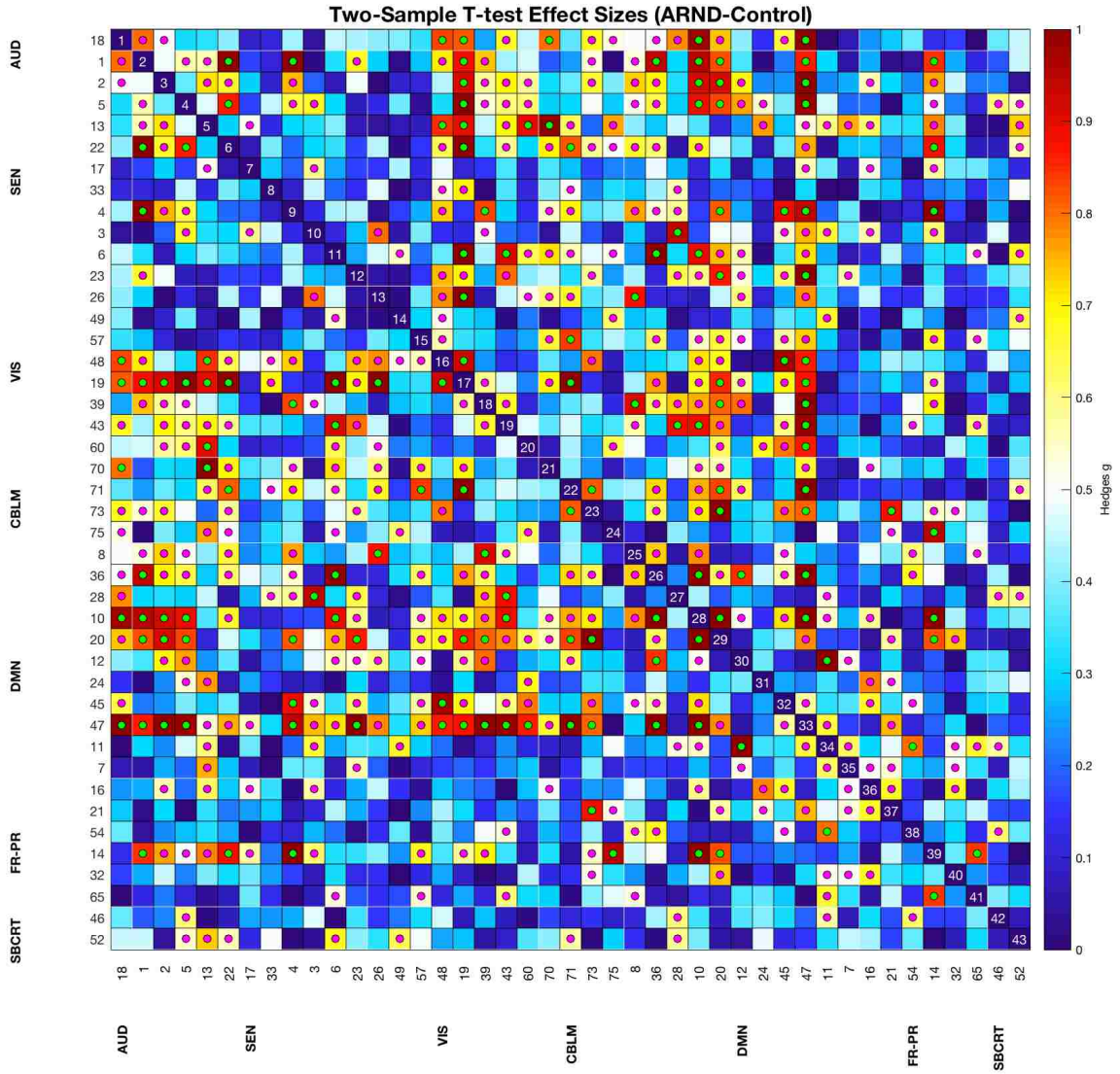

Figure 18 – Two-sample t-test effect size matrix (ARND-Control).

Absolute value of Hedges' g is shown with cells marked with a green circle indicate effect size g>= 0.8.

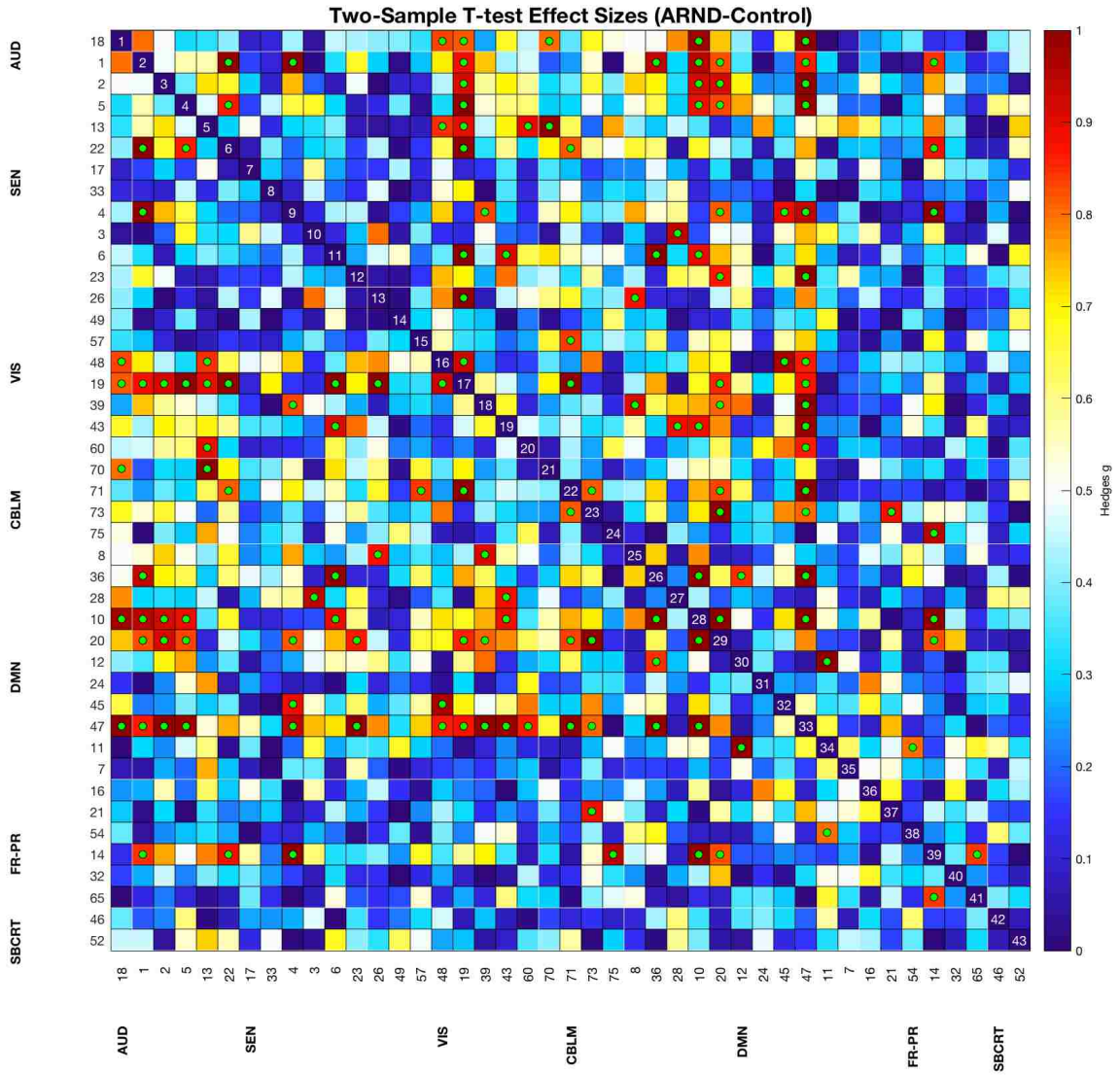

FNC T-tests: ARND-FAS

The results of two-sample t-test comparing connectivity between the ARND and FAS groups resulted in a total of 158 unique significant effects at the $p<0.05$. Of the total significant effects, components 47 (superior medial gyrus) and 1 (right post central gyrus) were the most frequent.

C47 was associated with 23 effects in numerous couplings with auditory, sensory-motor, visual, cerebellar, default mode, and fronto-parietal components. C47 effects corresponded to approximately 15% of the total significant effects of the comparisons between ARND and FAS groups. Of these 23, all were in the positive direction suggesting stronger mean connectivity in ARND participants when compared to FAS. Of the 23 t-test effects in C47, all were associated with effect sizes of $g>=0.8$.

C1 was associated 17 effects in several couplings with auditory, sensory-motor, visual, cerebellar, and default mode components. The significant couplings associated with C1 comprised approximately 11% of the total effects reaching the $p<=0.05$ threshold. These significant effects resulted from positive t-values suggesting stronger connectivity in ARND when compared to FAS for these specific components. Follow-up calculations of effects sizes indicated these effects were associated with a Hedge's g of >= 0.08.

Component 6 (bilateral post-central gyrus) in the sensory-motor group was associated with 15 effects, corresponding to about 9% of the total. Each of these effects was observed in the positive direction and exhibited a corresponding

strong (g>=0.08) effect size, suggesting stronger connectivity in the ARND group compared to the FAS group.

Component 36 (bilateral precuneus, posterior cingulate cortex) grouped into the DMN was associated with 15 effects, corresponding to an additional 9% of the total. Each of these effects was in the positive direction and was linked to a strong effect size suggesting stronger connectivity in the ARND group when compared to FAS.

In summary, higher connectivity in couplings linked to C47 (superior medial gyrus) in the DMN were observed in the ARND group when compared to FAS. In addition, higher connectivity in couplings linked to components C1 (right postcentral gyrus) and C6 (bilateral post-central gyrus) in the sensory-motor grouping were also observed in the ARND group when compared to FAS. Although these effects did not survive multiple comparisons procedures, the results here provide evidence of the regionally targeted effects of prenatal alcohol on functional connectivity that are implicated default mode and motor networks can be further explored and related to the functional deficits characteristic of individuals with FASD in future studies.

Figure 19 – Two-sample t-test values (ARND-FAS).

T-test value matrix indicating t-values from a two-sample t-test between ARND and FAS participants. Cells marked with a white circle indicate the t-value is statistically significant at the p<=0.05 level.

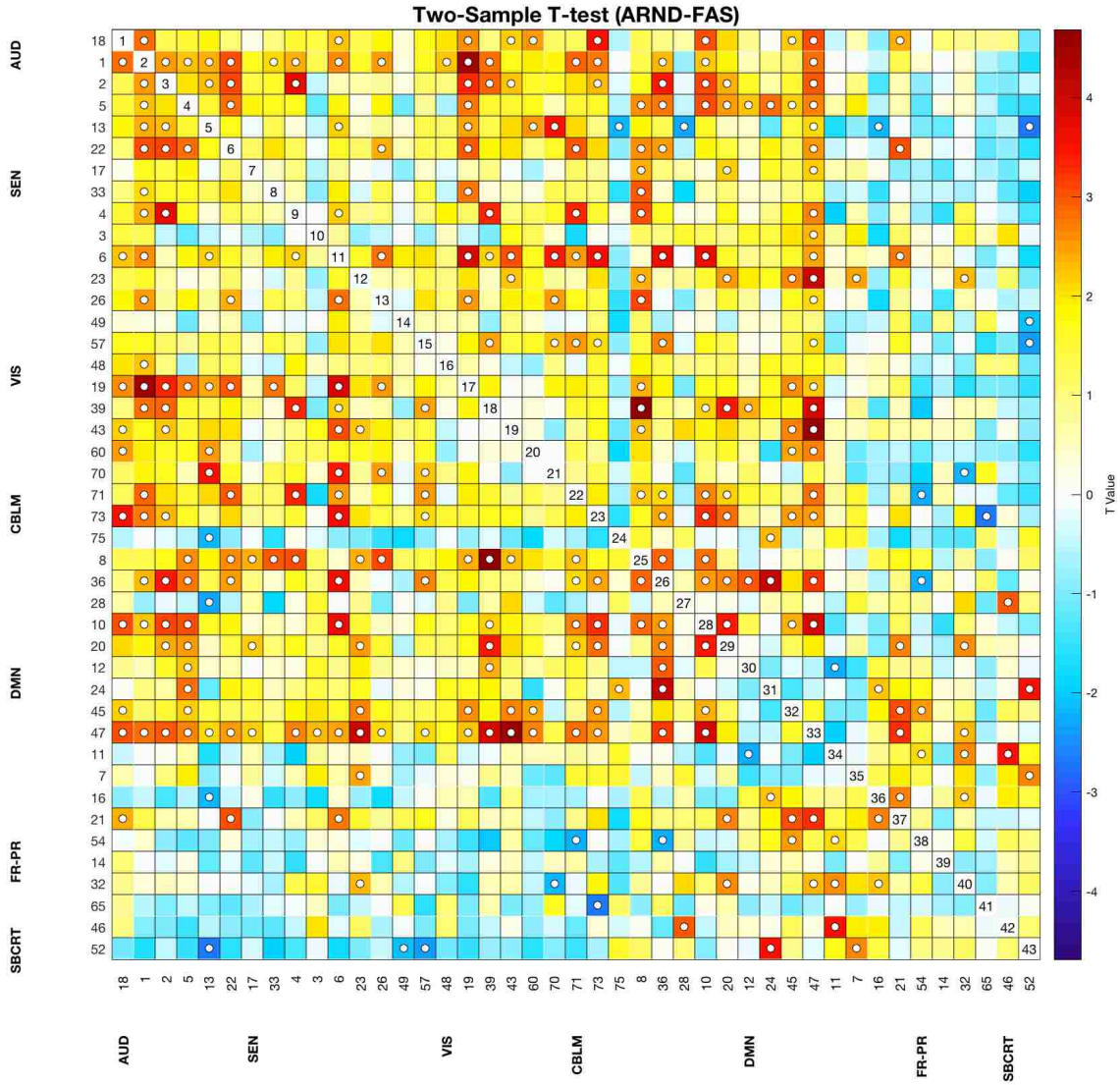

Figure 20 – Two-sample t-test effect size matrix (ARND-FAS).

Absolute value of Hedges' g is shown with cells marked with a magenta circle indicating effect size >=0.5<0.80; cells marked with a green circle indicate effect size >= 0.8.

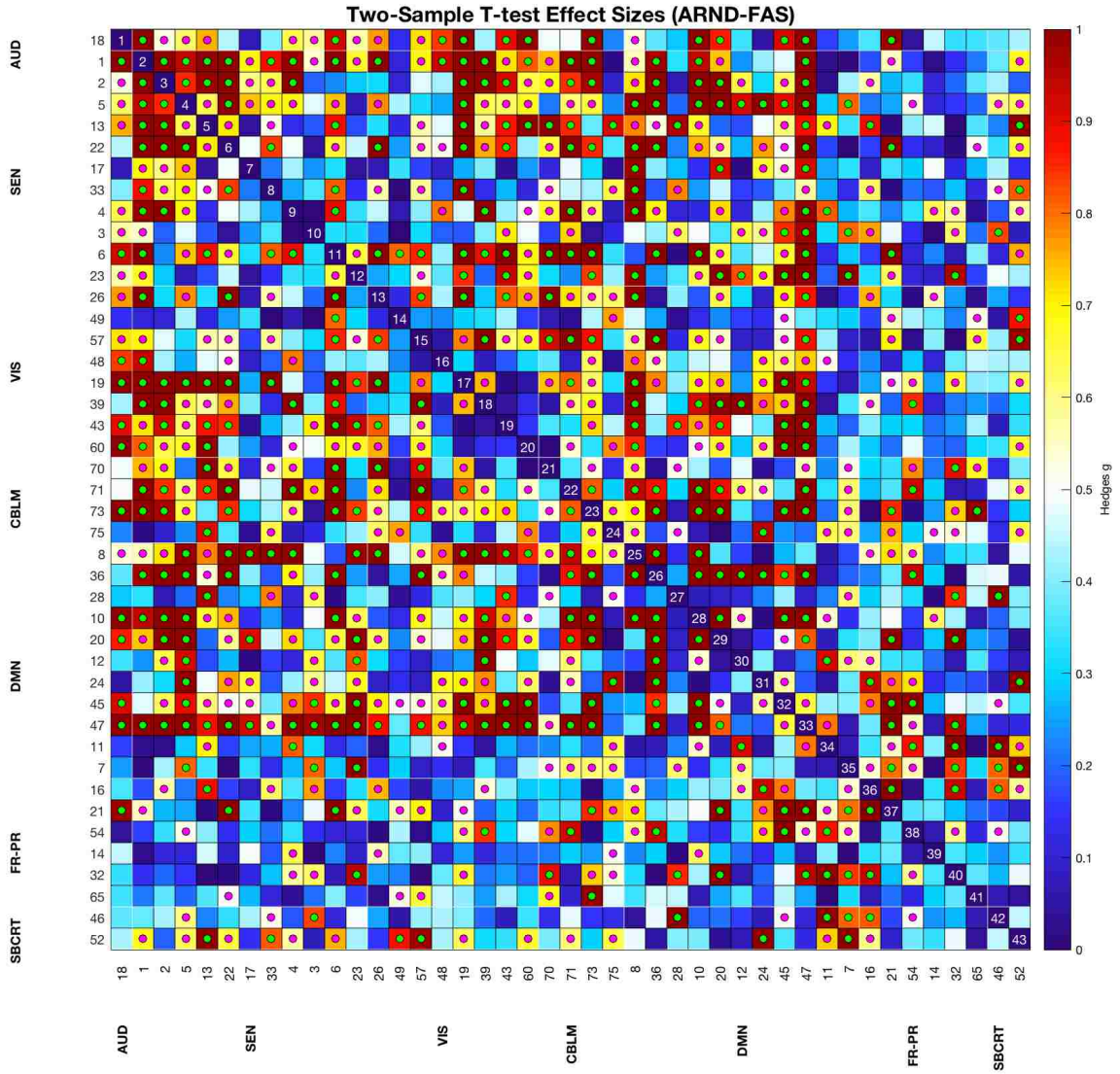

Figure 21 – Two-sample t-test effect size matrix (ARND-FAS).

Absolute value of Hedges' g is shown with cells marked with a magenta circle indicating effect size >=0.5<0.80; cells marked with a green circle indicate effect size >= 0.8.

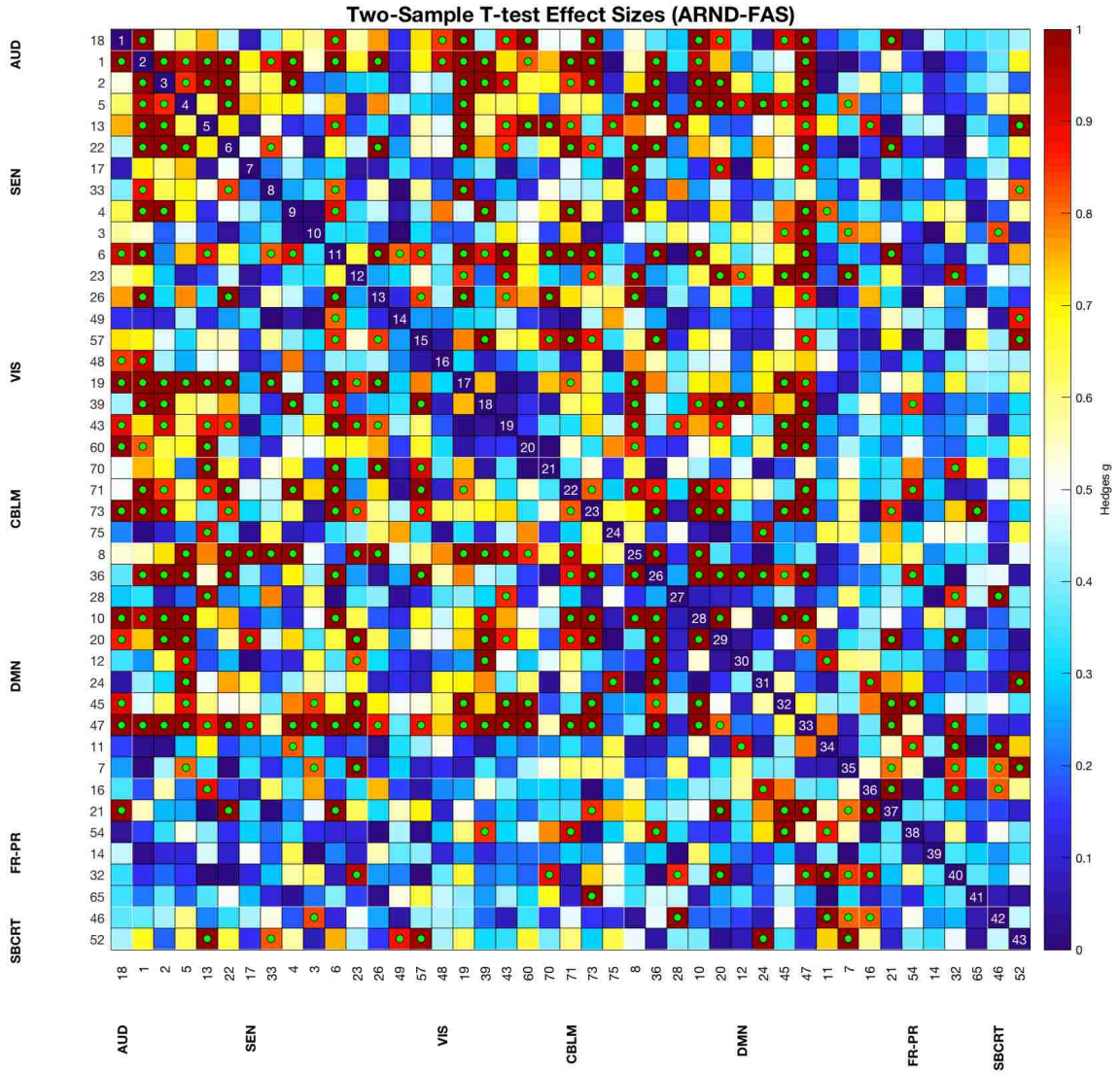

FNC Domain-Specific ANOVAs

The following section discusses explorations on the differences in connectivity between groups with individual component connectivity averaged into network domains. Figure 22 displays the results of ANOVAs conducted on network domain pair mean connectivity utilizing condition and sex as main factors. Because only one component was localized into the auditory network, calculation of within-network connectivity was not possible. Thus, comparisons for auditory-to-auditory mean connectivity were marked with a hashtag (#) to indicate that no analysis was performed.

For comparisons across the main effect of condition (Figure 22A), three significant results at the $p<0.05$ threshold were observed in VIS-to-AUD, DMN-to-SEN, and DMN-to-FR-PR connectivity. However, none of these effects surpassed Bonferroni nor FDR correction thresholds.

For comparisons across the main effect of sex (Figure 22B), two significant results at the $p<0.05$ threshold were observed in SEN-to-AUD, and CBLM-to-AUD connectivity. However, as with the main effect of condition, none of these effects survived Bonferroni nor FDR multiple comparisons procedures.

The ANOVA interaction between condition and sex resulted in one effect at the $p<0.05$ threshold observed in the SBCRT-to-SEN connectivity.

Figure 22 – ANOVA on domain specific networks.

Main effect of condition (A), sex (B), and interaction (C). Color bar scale indicates magnitude of p-value (darker cells indicate smaller p-values). Cells marked by a yellow circle indicate uncorrected statistical significance at $p<0.05$. No cells survived Bonferroni or false discovery rate (FDR) corrected thresholds. # indicates no comparison was made due to only one component grouped into the auditory network.

A)

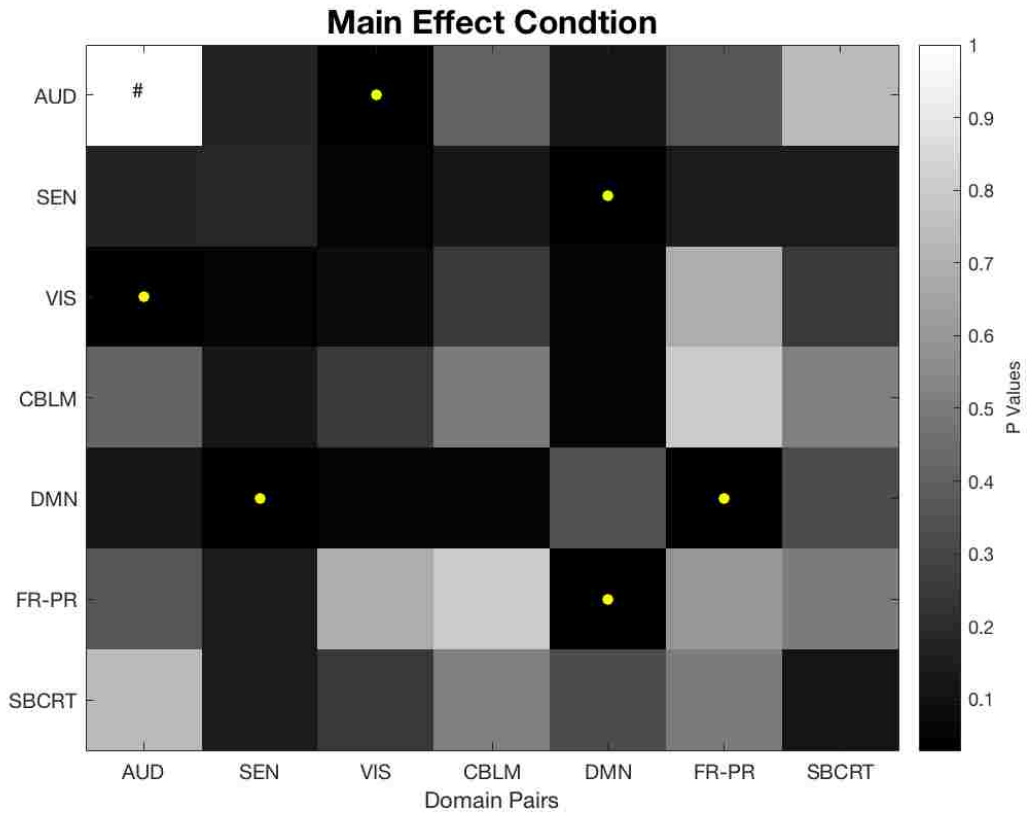

B)

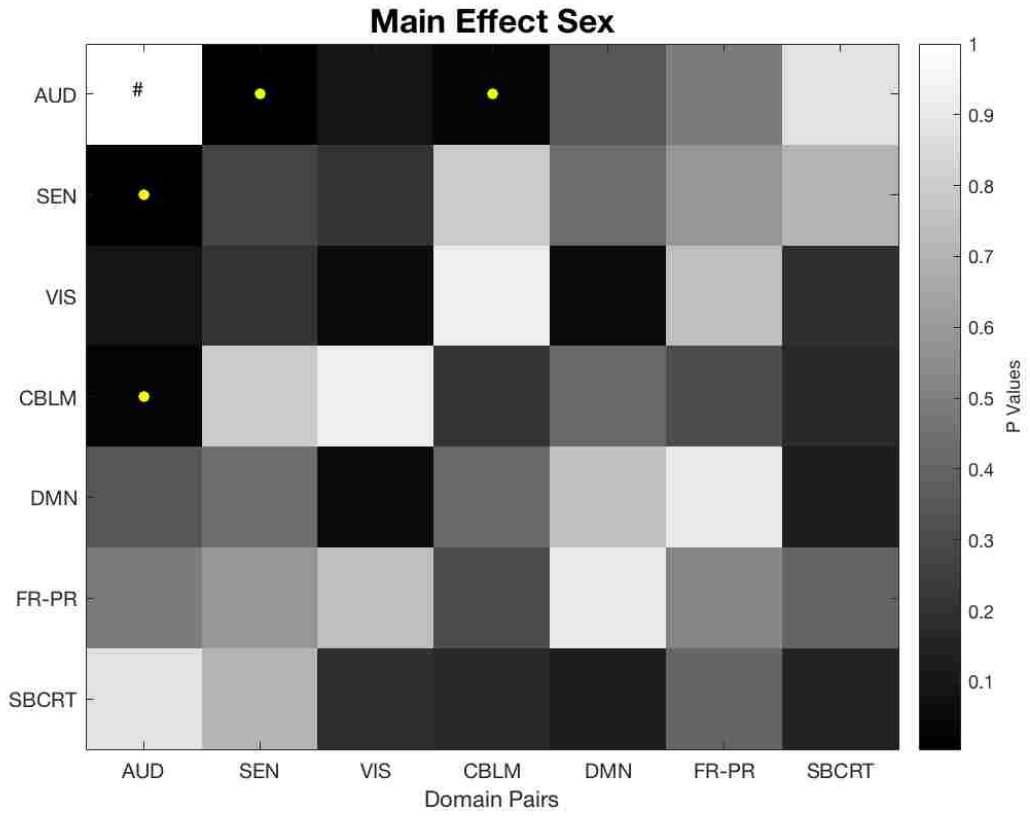
Main Effect Sex
AUD
SEN
VIS
CBLM
DMN
FR-PR
SBCRT
#
AUD
SEN
VIS
CBLM
DMN
FR-PR
SBCRT
Domain Pairs
P Values
1
0.9
0.8
0.7
0.6
0.5
0.4
0.3
0.2
0.1

C)

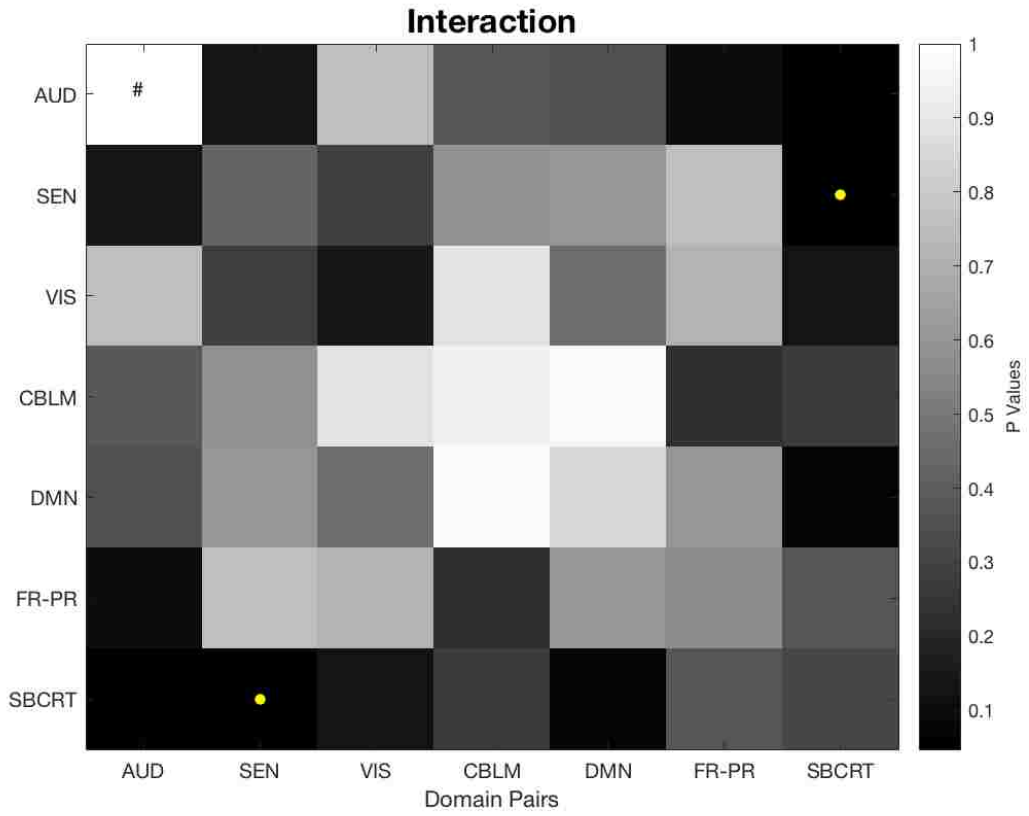
Interaction
AUD
SEN
VIS
CBLM
DMN
FR-PR
SBCRT
#
AUD
SEN
VIS
CBLM
DMN
FR-PR
SBCRT
Domain Pairs
P Values
1
0.9
0.8
0.7
0.6
0.5
0.4
0.3
0.2
0.1

FNC Domain Specific T-Test Comparisons

Control-FAS

The results of two-sample t-tests comparing domain specific average connectivity between the Control and FAS groups indicate 1 significant effect at the $p<0.05$—localized to connectivity between FR-PR and default mode networks and indicating higher connectivity in control participants. The effect size for this result was >= 0.8. Additional effects that did not meet the statistical significance, but displayed moderate effect sizes nonetheless were localized to FR-PR to SEN couplings and DMN to SBCRT couplings.

Figure 23 – Domain specific T-test comparisons Controls-FAS.

T-test and effect size value matrix indicating t-values from a two-sample t-test between control and FAS participants and the corresponding effect size. Cells marked with a white circle indicate the t-value is statistically significant at the p<=0.05. Cells marked in green indicate g>0.08, magenta g=0.5-0.79.

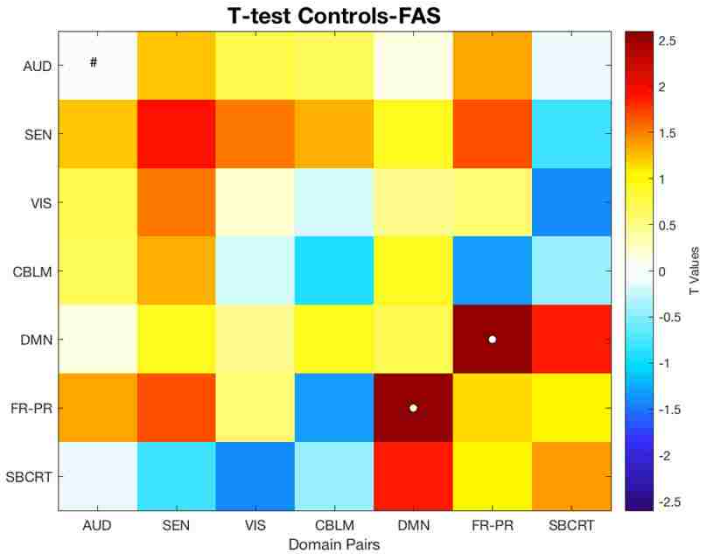

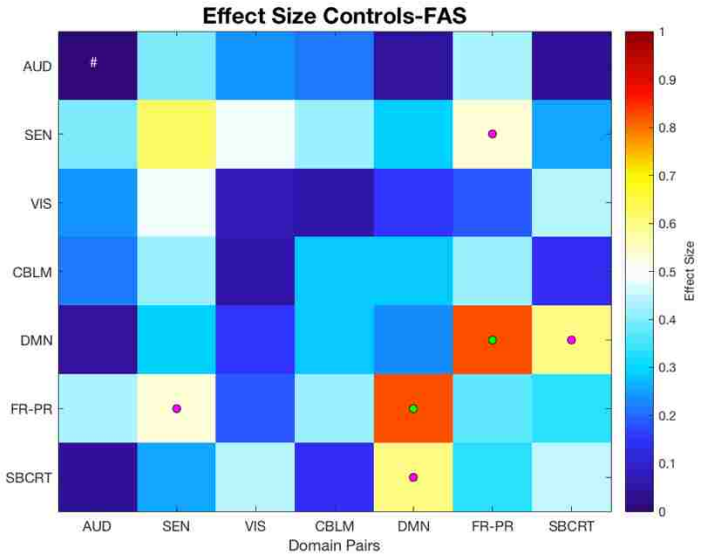

Control-ARND

The results of two-sample t-tests comparing the domain specific average connectivity between networks in control and ARND participants revealed a total of 4 significant effects at the $p<0.05$ level. The majority of these significant effects (three of the four) were localized to DMN couplings to sensory-motor, visual, and cerebellar networks. The remaining significant effect was localized to visual and auditory network connectivity. All four significant effects indicated higher connectivity for these couplings in ARND participants. Effect size calculations for the significant t-test values were all in the $g=.05$-$.79$ range, except for VIS-to-AUD connectivity which demonstrated an effect size of $g> 0.8$.

Figure 24 – Domain specific T-test comparisons Controls-ARND.

T-test and effect size value matrix indicating t-values from a two-sample t-test between control and ARND participants and the corresponding effect size. Cells marked with a white circle indicate the t-value is statistically significant at the p<=0.05. Cells marked in magenta indicate g>0.08 green indicate g=0.5-0.79.

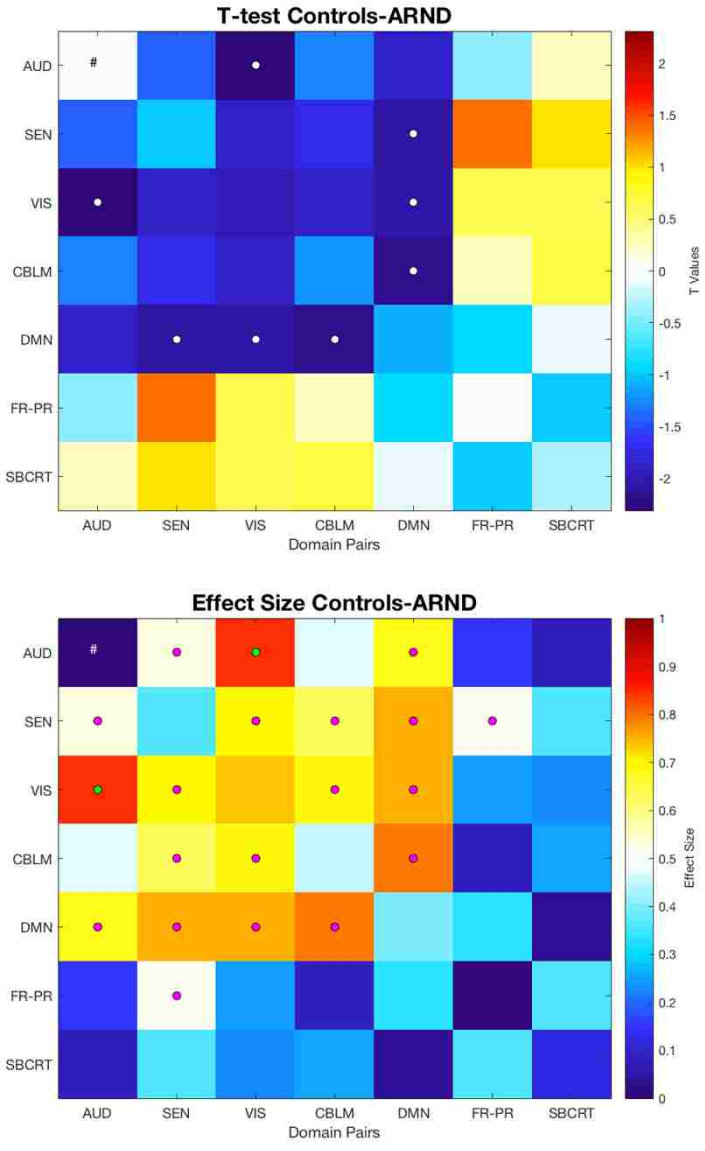

ARND-FAS

The results of two-sample t-tests comparing domain specific average connectivity between components revealed a total of 7 effects. Of the 7 effects, 3 were localized to network connectivity associated with the DMN including-SEN, VIS, and CBLM networks. T-tests revealed higher connectivity in ARND participants when compared to FAS. Higher connectivity in ARND participants was also seen in AUD-SEN, AUD-VIS, and SEN-CBLM networks. Finally, FRPR-DMN connectivity was also higher in ARND participants when compared to FAS.

Summary

Comparisons of functional network connectivity within and between component network domains did not result in any statistical differences that met multiple comparisons thresholds. Despite these observations, statistical comparisons of functional network connectivity across groups yielded reoccurring patterns of results. Controls displayed higher FR-PR-DMN connectivity than FAS. ARND participants displayed higher connectivity in DMN-SEN, DMN-VIS, and DMN-CBLM connectivity when compared to controls. When comparing ARND to FAS, this pattern is repeated with the additional finding that ARND participants exhibited higher connectivity in VIS-AUD, VIS-SEN, and SEN-AUD components. The pattern of these results suggest that components related to the default mode, sensory, and motor networks may be of further interest for discriminating healthy controls from alcohol exposed participants and provide preliminary

evidence as to the source of regions that may display hyperconnectivity as a result of prenatal alcohol exposure.

Figure 25 – Domain specific T-test comparisons ARND-FAS.

T-test and effect size value matrix indicating t-values from a two-sample t-test between ARND and FAS participants and the corresponding effect size. Cells marked with a white circle indicate the t-value is statistically significant at the p<=0.05. Cells marked in magenta indicate g>0.08 green indicate g=0.5-0.79.

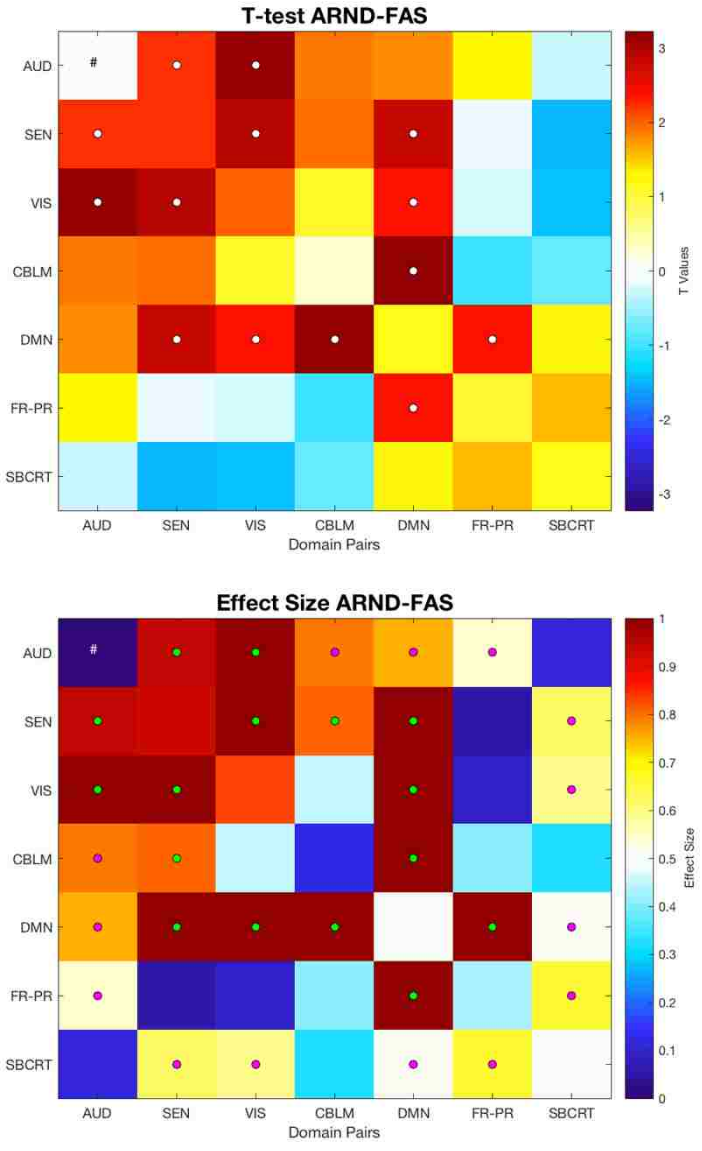

FNC-Behavior Correlations

The following analyses explored the relationship between measures of functional network connectivity and cognitive processes as measured by the WASI-II subtests (Wechsler, 1999). For all participants with available neuropsychological data, all pairwise connectivity measures were correlated with overall and subtest scores. Figures 22A-22C display the results of separate sets of Pearson correlation coefficients between measures of connectivity and measures of overall IQ (22A), Vocabulary subtest scores (22B), and Matrix Reasoning subtest scores. In these figures, blue cells reflect negative correlations while red cells indicate positive correlations. In addition to the direction and intensity of each r value, some cells are marked with a solid white circle to indicate that the r-value is statistically significantly different than 0 at the $p<0.05$ level.

WASI-II Overall IQ Correlations

A general trend of positive correlations between measures of sensory-motor component connectivity and IQ estimates was observed. In total, 62 correlations met statistical significance at the $p<0.05$ level and the majority of these effects are associated with Components 1, 13, 48, and 28.

Component 1 (right postcentral gyrus, SEN) was associated the highest amount of significant correlations totaling 9 and representing approximately 15% of the observed effects. Of the 9 correlations, all but one was in the positive direction. The majority of positive connectivity was within sensory motor

components including C13 (bilateral superior parietal lobule), C17 (left superior parietal lobule, SEN) and C33 (right superior parietal lobule, SEN) suggesting that connectivity between the right post central gyrus and superior parietal regions are positively correlated with overall IQ scores. The connectivity between C14 (Left inferior parietal lobule, and inferior frontal gyrus) and C1 was also positively correlated with measures of overall IQ and demonstrated the strongest correlation of all significant effects. A negative correlation between IQ and the connectivity between component 28 (bilateral anterior cingulate cortex DMN) and Component 1 was also observed and of interest as C28 was frequently implicated in the observed pattern of results indicating a common theme.

For C13, all significant correlations were in the positive direction indicating positive associations between connectivity and overall IQ. Positive correlations were observed in auditory and sensory networks and mirrored the pattern of effects observed in C1 and C17 and C33. Thus, the connectivity between C1 to C13 and C17 to C13, which predominantly represent parietal lobe and motor component connectivity, are positively correlated with overall IQ.

Component 48 (bilateral calcarine gyrus, VIS) had 8 total correlations which contributed to 13% of the total significant effects. All significant effects involving C48 were in the negative direction. The general pattern of results consisted of negative connectivity with sensory components such as C5 (bilateral supplementary motor area), C17, and C33. Thus, while IQ was positively associated with C1 and C13 connectivity, it is negatively correlated with visual

component connectivity. Overall IQ was also negatively associated with connectivity between C48 and fronto-parietal components such as C21(bilateral superior frontal gyrus), C54 (bilateral insular cortex) and C32 (left inferior frontal gyrus).

Component 28 (bilateral anterior cingulate cortex in the DMN) had 7 total significant correlations corresponding to about 11% of the effects. All of the significant correlations between IQ and connectivity with C28 were in the negative direction. Connectivity between C28 and visual components that include C26 (right inferior parietal lobule, and supra marginal gyrus), C57 (bilateral middle and inferior temporal gyrus), C19 (bilateral occipital gyrus), and C39 (bilateral cuneus) were all negatively associated with overall IQ scores.

In sum, overall IQ measures were generally positively correlated with connectivity among sensory-motor components while negatively associated with connectivity involving select visual and default mode components. Notable patterns of results implicated C1, C13, C48, and C28. Frequent positive associations between IQ and connectivity between parietal and motor components was observed while frequent negative associations between IQ and connectivity implicated with visual and default mode components.

WASI-II Vocabulary Correlations

A general trend of negative correlations between measures of default mode component connectivity and vocabulary subtest scores were observed. In

total, 48 correlations met statistical significance at the $p<0.05$ level. Most of these effects were associated with Components 28, 48, and 11.

Component 28 (bilateral anterior cingulate cortex, DMN) was associated with 9 total significant correlations representing nearly 19% of the total number of effects. All of these significant correlations, connectivity with C28 occurred in the negative direction and included negative relationships with C26 (right inferior parietal lobule, and supra marginal gyrus), C57 (bilateral middle and inferior temporal gyrus), C19 (bilateral occipital gyrus), and C39 (bilateral cuneus). As observed in overall IQ-FNC correlations, C28 connectivity is negatively correlated with measures of vocabulary scores.

Component 48 (bilateral calcarine sulcus, VIS) was associated with 8 significant correlations with vocabulary scores comprising nearly 17% of the observed total of effects. All significant correlations associated with C48 were in the negative direction and were pronounced in components that were localized in the fronto-parietal grouping such as C21 (bilateral superior frontal gyrus), C54 (bilateral insular cortex), and C32(left inferior frontal gyrus).

Component 11(bilateral posterior cingulate cortex, DMN) was associated with 6 significant correlations comprising 12.5% of the effects. Most significant correlations were negatively associated with connectivity in sensory-motor couplings. Only one significant positive correlation was observed in the connectivity between C12 (bilateral precuneus in the DMN) and C11.

An additional observation that merits mention is the connectivity between C14 (left inferior parietal lobule, and inferior frontal gyrus) and C1 (right post central gyrus). While these components were not typically associated with frequent significant correlations with behavioral measures, they displayed the strongest positive correlation perhaps indicating an important for role for brain connectivity and the language functions interrogated by the WASI-II.

Collectively the results for vocabulary-connectivity correlations indicate a general pattern of negative relationships that are especially pronounced in visual default mode, and sensory-motor components.

WASI-II Matrix Reasoning Correlations

For correlations between connectivity and matrix reasoning subtest scores, the general pattern of results indicates negative subtest score associations with connectivity in visual and sensory motor couplings, sub-cortical and visual couplings, and fronto parietal and visual couplings. A total of 28 total significant correlations at the $p<0.05$ level were observed. The most frequent effects were associated with connectivity involving components 2 (left post-central gyrus, SEN) and 48 (bilateral calcarine sulcus, VIS).

Component 2 was associated with 7 significant correlations representing 25% of the observed effects. All of these significant correlations were in the positive direction suggesting predominantly positive relationships between motor component connectivity and matrix reasoning scores. Positive correlations were most frequently observe in C2 and fronto-parietal component couplings that

included, C16 (right superior frontal gyrus), C21(bilateral superior frontal gyrus), and C54(bilateral insular cortex).

An additional, yet less pronounced pattern of results involved component 48 (bilateral calcarine sulcus, VIS) representing 4 total significant correlations and 14% of the total significant effects. All significant correlations were in the negative direction and included C5 (bilateral supplementary motor area), C33 (right superior parietal lobule), C23 (bilateral supplementary motor area), and C52 (bilateral thalamus).

In sum, the results for Matrix Reasoning-Connectivity correlations suggest contrasting patterns of results whereby matrix reasoning scores are negatively correlated with C48 couplings yet positively correlated with C2 couplings.

FNC-Behavior Correlations Summary

Overall IQ measures were generally positively correlated with sensory-motor component couplings while negatively associated with select visual and default mode component couplings. Frequent and mirrored positive associations were observed in couplings that involved C1 (right postcentral gyrus) and C13 (superior parietal lobule) suggesting a complimentary role of the connectivity between these networks and overall IQ measures. Frequent negative associations were observed in couplings that included C48 (calcarine sulcus), and C28 (anterior cingulate cortex) suggesting an opposite pattern of resting state coordination with IQ measures.

Vocabulary-connectivity correlations indicated a general pattern of negative significant relationships that were especially pronounced in visual default mode, and sensory-motor couplings. Furthermore, significant correlations between FNC and vocabulary measures overlapped with the results in overall IQ. For example, component couplings involving C28 and C48 demonstrate similar magnitude and direction of correlations with behavioral measures that may be due to the positive correlation between measures of IQ and vocabulary subtest scores.

Matrix Reasoning-connectivity correlations suggest a less pronounced pattern of results with a reduction in the number of significant correlations. While positive correlations were observed for sensory-motor and fronto-parietal component couplings, it is interesting to note that negative correlations were observed with C48 couplings. Thus, negative correlations with C48 couplings may be a general observation rather than specific to overall IQ, vocabulary, or matrix subtest scores.

Despite these results, it is important to note that several participants in the FASD groups came from non-native English speaking communities which may partially explain the differences in overall IQ and Vocab scores, but not on matrix reasoning and serves as an important consideration for contextualizing the data.

Figure 26 – FNC-Neuropsychological Measure Correlations.

Correlations between neuropsychological assessment measures and connectivity IQ (22A), Vocab (22B), and Matrix Reasoning (22C). Cells color represents the correlation magnitude with red indicating a positive correlations and dark blue indicating negative correlations. Cells marked with a dark circle indicate the r-value is statistically significant at the p<0.05 level.

A)

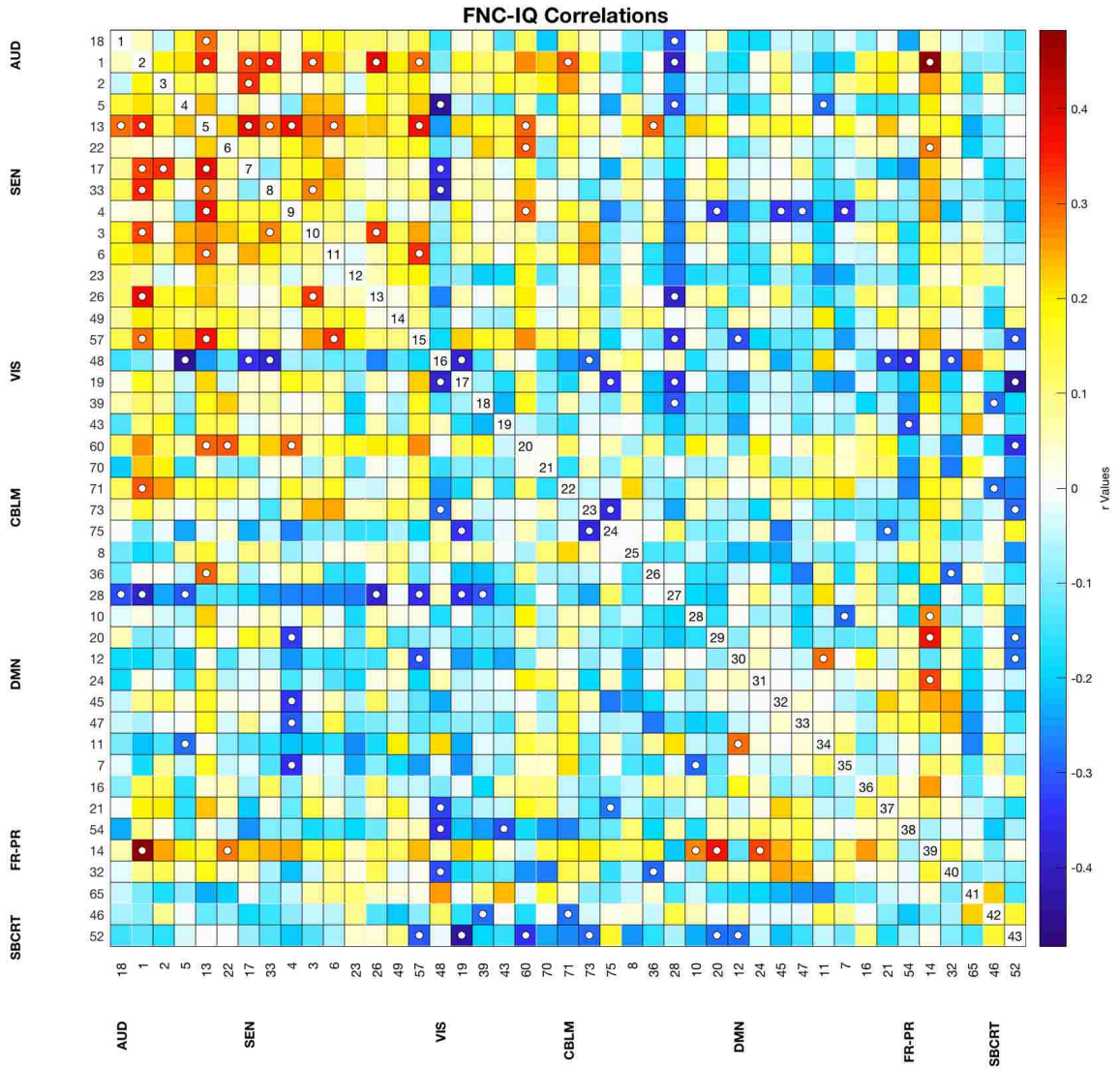

B)

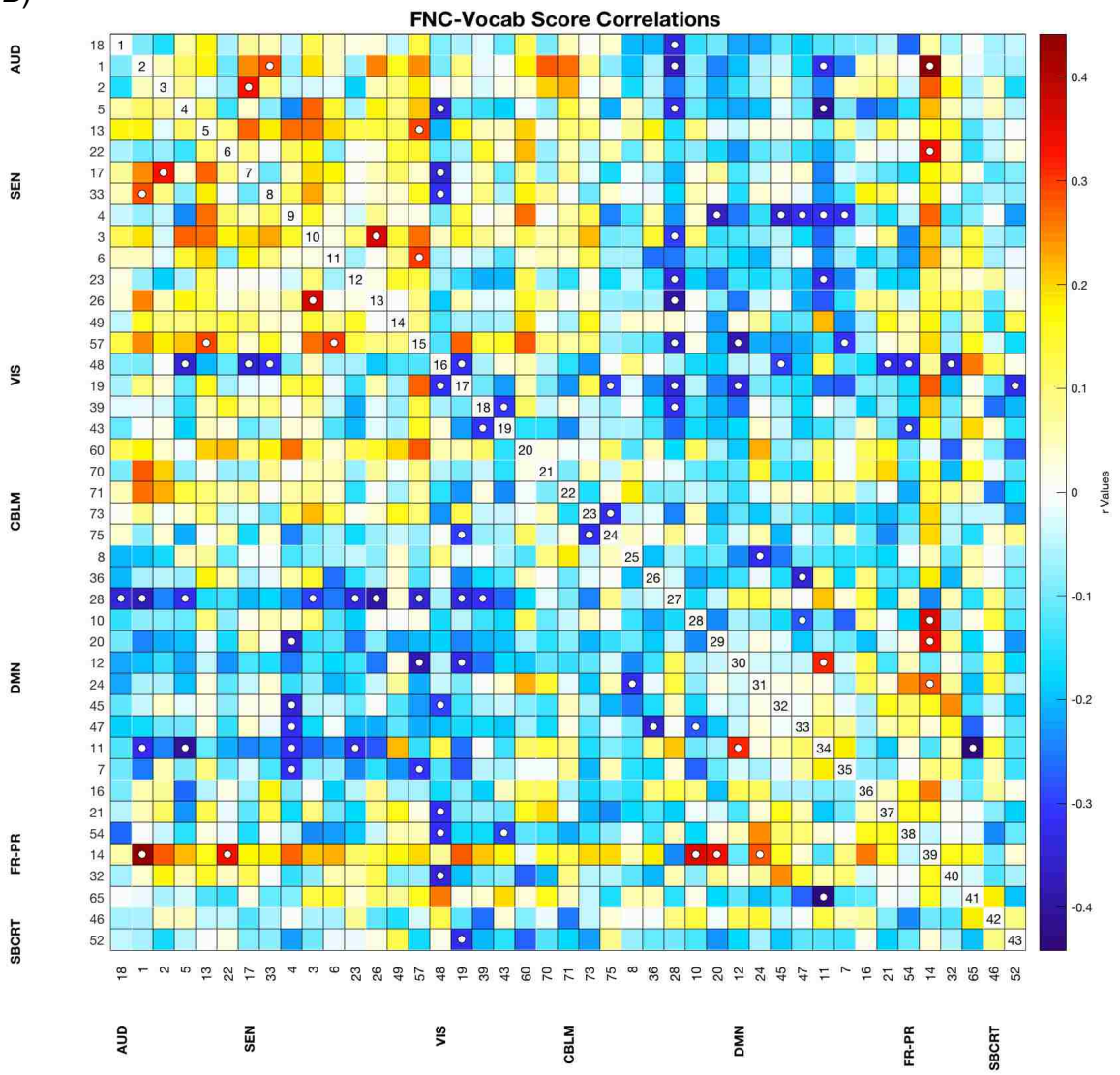
FNC-Vocab Score Correlations
AUD
SEN
VIS
CBLM
DMN
FR-PR
SBCRT
r Values
0.4
0.3
0.2
0.1
0
-0.1
-0.2
-0.3
-0.4

C)

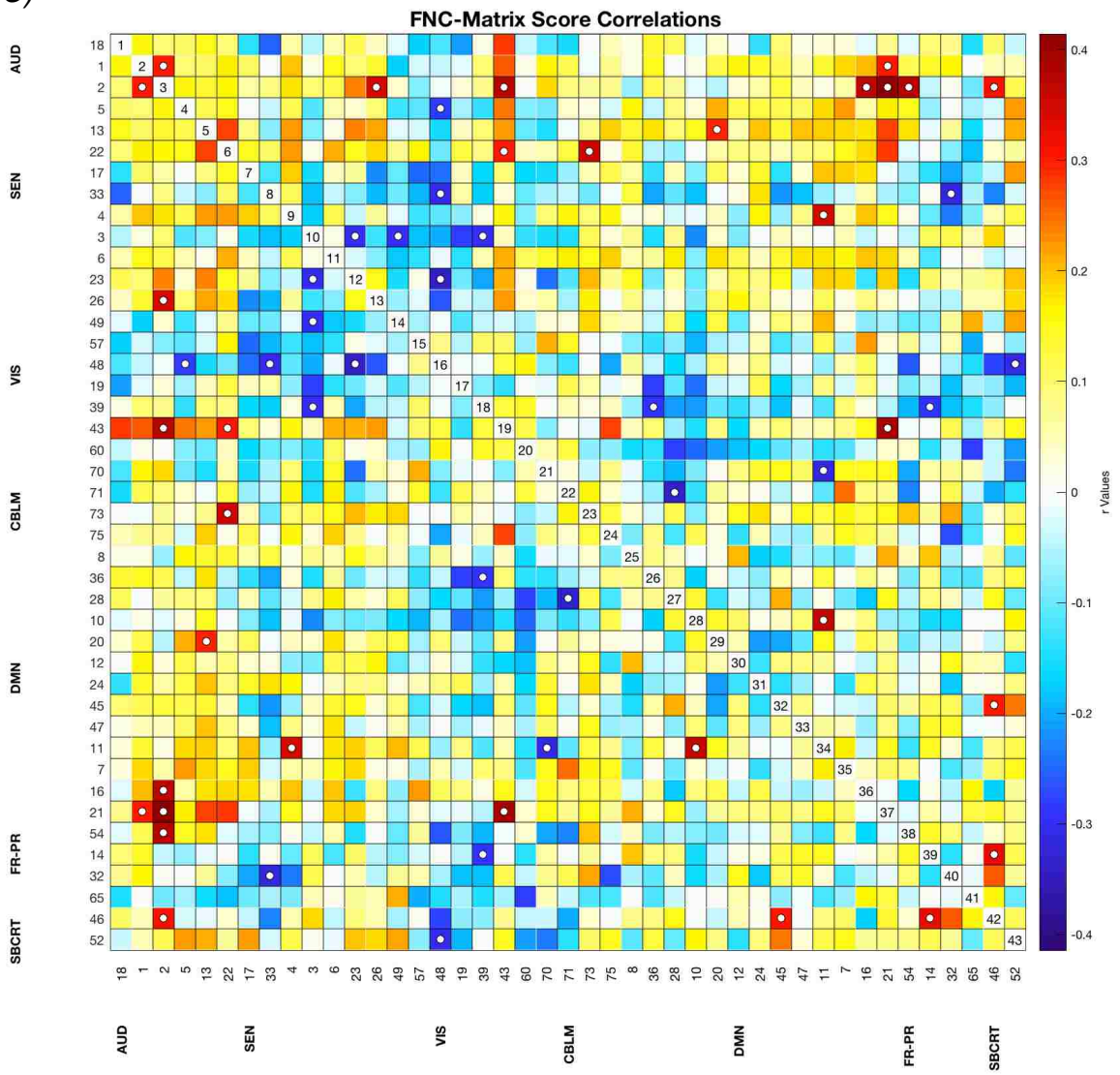
FNC-Matrix Score Correlations
AUD
SEN
VIS
CBLM
DMN
FR-PR
SBCRT
r Values
0.4
0.3
0.2
0.1
0
-0.1
-0.2
-0.3
-0.4

Discussion

The present study was aimed at characterizing the effects of prenatal alcohol exposure on functional network connectivity in a sample of adolescents and young adults by calculating and comparing Pearson product moment correlation coefficients of mean independent component time-courses extracted from resting state fMRI data. A related and secondary aim was to explore relationships between changes in functional network connectivity and behavior as measured by the WASI-II (Wechsler, 1999).

Connectivity Magnitude

Comparisons of connectivity magnitude measures which were derived by squaring and summing each pairwise correlation value yielded one of the most pronounced outcomes of this study. Higher overall connectivity in ARND participants when compared to control and FAS participants was observed. Further inquiry into this finding revealed that higher overall connectivity magnitude in the ARND group was due to higher positive, as opposed to negative, connectivity. Because the extant published literature of functional connectivity in adolescents and young adults with FASD has not explored this measure. While unconventional and broad in its scope, this index captured a trend in connectivity that is abnormal and, to an extent, unique as several studies of this clinical population report reductions in functional connectivity under task and resting-state conditions. Here, the FASD group displayed reductions in overall white matter volume when compared to controls, and highlight the

importance of placing research efforts on functional alongside the plethora of structural brain research conducted in the FASD field to reconcile these incongruent findings. These processes may prove useful for discriminating between the functional network connectivity patterns associated with healthy controls and participants exposed to alcohol prenatally.

ANOVA and T-tests

Comparisons of each pairwise connectivity measure by ANOVA resulted in the main effect of diagnostic condition displaying the highest frequency of differences in couplings. A large portion of these couplings were found default mode (C47, superior medial gyrus) and visual network components (C39, bilateral cuneus). However, it is important to note that none of the highlighted effects survived multiple comparisons procedures which weakens the conclusions from these analyses.

Despite this limitation, T-tests between connectivity measures across conditions for component connectivity were conducted to determine the magnitude and direction of the effects observed in the ANOVA. T-test results suggested higher connectivity in the ARND group for C47(DMN) and C39(VIS) couplings when compared to control and FAS participants. Furthermore, these couplings were associated with effect sizes of $g>=0.08$ providing preliminary evidence for further exploration of default mode and sensory networks in studies of FASD.

ANOVAs conducted on domain specific networks, yielded similar results as those derived from comparisons of all possible pairwise component correlations. The main effect of condition, rather than for sex, or the interaction, resulted in a higher frequently of observed effects and indicate the potential impact of prenatal alcohol exposure on functional network connectivity. Further, as observed in the individual component connectivity comparisons, ARND participants displayed higher domain specific connectivity when compared to control and FAS participants that include couplings between default mode network components and sensory-motor, visual, and cerebellar components. In addition, ARND participants also displayed higher connectivity in the couplings between visual and auditory components. Of these, default mode network components displayed a consistent pattern of differences leading to the possibility that default mode network related regions may be differentially impacted by prenatal alcohol exposure. However, as noted above, these comparisons failed to reach multiple comparison thresholds and more research will be needed to arrive at a definitive conclusion.

General Connectivity Discussion

MRI-based functional connectivity studies in children with FASD are numerous, yet only four studies have been specifically conducted in resting state approaches. Of these four, most utilized either seed- or graph-theory-based analytical approaches. One recently published study utilized gICA to examine resting state functional network connectivity in a sample of young adolescents

(Fan et al., 2017). The results of this report suggested reductions in functional network connectivity in a small number of networks that include aspects of the DMN and networks involved in cognitive salience and attentional functions which can include sensory information processing regions. Furthermore, the authors reported a relationship between the level of prenatal alcohol exposure and measures of connectivity whereby higher levels of prenatal alcohol exposure were associated with reductions in connectivity in the networks of interest.

The results of this study are partially congruent in the sense that DMN components were most frequently associated with displaying effects the met the $p<0.05$ statistical threshold. When observed, these effects demonstrated higher connectivity in controls when compared to FAS participants. However, in ARND participants, the opposite pattern of results was present where higher connectivity was observed when compared to FAS and controls. It is important to note, however, that the samples of the Fan et al., 2017 and the present study share demographically unique characteristics. For example in the study here, participants are recruited from American Indian reservations and often do not speak English as their first language. In contrast, the Fan et al., 2017 study drew from the Cape Coloured sample, a community of mixed ancestry, with a long-standing history of prenatal alcohol use.

Other lines of research in FASD samples have targeted interhemispheric connectivity in brain regions known to communicate through the posterior regions of the corpus callosum– a brain structure known to be damaged by prenatal

alcohol (Wozniak et al., 2011). In the present investigation, the findings of the Wozniak (2011) study are partially supported by the observation of reductions in functional network connectivity of the parietal regions of children diagnosed with FAS. However, the connectivity between parietal components was not restricted to the contralateral area and changes were most often observed with components that lie in an anterior-posterior plane, rather than a medial-lateral one. For example, FAS children displayed lower connectivity, when compared to controls, in couplings with C14 (left inferior parietal lobule- inferior frontal gyrus) that include somatosensory (post-central gyrus) and visual processing (cuneus) regions.

More difficult to reconcile with the present investigation are studies that employ graph theory metrics (Wozniak et al., 2013; Wozniak et al., 2017) as they capture related, but distinct aspects of connectivity. While one study reported higher path length and reduced efficiency in a small sample of children with FASD, a follow up, large, and multi-site sample study revealed only a higher likelihood of abnormal connectivity in children exposed to prenatal alcohol.

Absent from available research reports on FASD are findings that suggest increased functional connectivity among brain regions. In the work presented here, preliminary evidence points to the possibility of increased connectivity in select brain networks that serve default mode, sensory, and motor functions acquired through fMRI. While this finding has not been fully explored upon in the existing human FASD literature, previous work employing an animal model of

moderate prenatal alcohol exposure supports the need to further investigate this phenomenon (Rodriguez, Davies, Calhoun, Savage, & Hamilton, 2016). Briefly, the Rodriguez et. al study applied GICA to resting state fMRI data gathered from adult rats that were exposed to moderate amounts of prenatal alcohol and showed network and sex dependent changes in functional network connectivity. Female rats exposed to moderate prenatal alcohol demonstrated more instances of increased connectivity, especially in couplings between thalamic components and several brain regions that included the hippocampus and parts of the midbrain. Male rats on the other hand displayed increased connectivity in couplings between cortical and cerebellar, midbrain, and hippocampal components. The results set precedence for the possibility of increased connectivity as a result of prenatal alcohol exposure in a preclinical model. Although the present study here was conducted in humans and fMRI data were acquired in a distinctly different developmental period than the rodent study described above, the two share similar themes in suggesting increases in functional network connectivity in select brain regions. Connectivity increases observed in alcohol exposed participants represent an additional, and important perspective for the complete characterization of prenatal alcohol exposure effects.

Increases in functional network connectivity are not unheard of in resting state studies of neurological conditions. One report studied functional connectivity in patients with multiple sclerosis (MS) – a condition marked by the

diffuse degradation of white matter leading to impaired neuronal communication that contributes to deficits in motor and cognitive functions (Hawellek, Hipp, Lewis, Corbetta, & Engel, 2011). When compared to healthy controls, the authors reported increases in functional connectivity of MS patients despite the well-established observation that the condition leads to diffuse disintegration of central white matter.

One interpretation of the results presented here, is that changes in functional network connectivity may be due to disruptions in the normal development of white matter. Prenatal alcohol exposure has been linked to numerous disruptions of white matter that range from changes in density (Sowell et al., 2001) and microstructure (Fan et al., 2016; Wozniak et al., 2006) to complete agenesis of the corpus callosum (Riley et al., 1995) in humans, and a wide range white matter related physiological processes in preclinical models (Wilhelm & Guizzetti, 2015).

The results presented in this investigation may parallel those observed in the Hawellek et al. 2011 study whereby increases in functional network connectivity are associated with disruptions in white matter. Hawellek and others proposed that increases in connectivity may be partially explained by compensatory mechanisms in neuronal plasticity that can be interpreted as increased neuronal efforts. The finding that the ARND group displayed higher overall connectivity magnitude may be explained by a similar conceptual framework. However, this explanation does not account for the observation that

differences in connectivity magnitude were not observed between FAS and healthy controls. Nor does it coincide with the notion with increased effort as both FAS and ARND participants demonstrated comparable performance on measures of matrix reasoning.

An additional interpretation proposed that the coordination of neuronal activity is disrupted which leads to net loss of dynamic brain activity. The loss of the normal ability of neuronal populations to cycle from states that range from excitation to inhibition may then be observed as increased connectivity over the duration of the scan period (Hawellek et al., 2011). Disruption of axonal fibers or myelination processes are two candidate mechanism that may influence the ability of neuronal populations to coordinate activity dynamically and lead to the observation of increased connectivity in the ARND group.

Since the FAS group did not display increases in connectivity, a distinct alteration in brain structure and or function resulting from early developmental exposure to alcohol may result in the diverging pattern of effect of connectivity magnitude. For example, first trimester prenatal alcohol exposure is associated with the facial dysmorphologies required for a diagnosis of FAS (Sulik, Johnston, & Webb, 1981). In contrast, second trimester exposure is more strongly associated with the development of glia including astrocytes and oligodendrocytes with the latter being responsible for myelinating central white matter (Medina, 2011; Wilhelm & Guizzetti, 2015).

Thus, one way differences in connectivity may be reconciled in this and other functional network connectivity studies is that exposure to prenatal alcohol during the first trimester which leads to the facial dysmorphologies associated with FAS may be more strongly related to reductions in functional connectivity by means of reduced development of axonal fibers. In contrast, increases in functional connectivity observed in the ARND participants may be more strongly related to a distinct patter of exposure beyond the time point when the facial features of FAS are developing and impact myelination process that can lead to losses in dynamic brain activity.

FNC Behavior Correlations

Overall IQ and vocabulary subtest measures were positively correlated with sensory-motor component connectivity, a pattern of negative correlations with DMN and visual component couplings was observed. Negatively associated components were distinct from those implicated in the ANOVA and T-tests and notable that behavior FNC correlations were predominantly observed in midline, frontal and posterior brain regions. Matrix Reasoning-connectivity correlations suggested positive correlations for sensory-motor and fronto-parietal component couplings and negative correlations with DMN component couplings.

However, as mentioned above, participants in this sample included individuals from non-native English speaking communities in rural New Mexico. This is an important consideration for contextualizing the differences observed in overall IQ estimates and Vocabulary subtest scores across diagnostic

Limitations and Future Directions

The interpretation of the results presented in this study, require caution as several limitations are present. To begin, sample sizes were small in ARND (n=13 in) and FAS (n=9) groups which will must be ameliorated in follow up studies that can form a more accurate picture of the developmental consequences of alcohol exposure on functional connectivity. It is also important to note that the age range of the sample was wide, spanning from a minimum of 12 years to a maximum of 22. As a result, controlling for the role of maturation processes (synaptic pruning and axonal myelination) are beyond the scope of this investigation. Although attempts were made to circumvent this problem, future investigations may benefit from narrower age ranges to rule out potential confounds. Additional variables that can be taken into consideration in future studies include the participant's handedness, socio-economic, status and whether English was spoken as a first language. Language may be particularly useful for explaining the null effects on differences in matrix reasoning scores across groups, but reductions in vocabulary performance.

While the results of this investigation provide preliminary evidence of differential patterns of connectivity and their relationship to behavior, it is important to note that FNC analyses did not survive multiple comparisons procedures. The advantage of including a large number of components in this study was to explore connectivity in regions that may be traditionally overlooked by studies aiming to study specific brain regions. Future investigations may

benefit from targeting select networks of interest and or increased sample sizes. In this study, white matter volume was estimated from T1 structural images. While this provides a general reference of white matter volume, this type of scan may not be nuanced enough to reveal changes in white matter microstructural connectivity that can be gathered from diffusion weighted imaging.

Finally, although practically difficult to gather, information regarding the amount of alcohol consumed, when it was consumed during pregnancy, and the pattern of consumption may help further clarify the full scope of the teratogenic effects of alcohol in this sample.

Conclusions

Curiously, the results of connectivity magnitude here indicate that overall connectivity may be differentially altered according to alcohol exposure with the ARND group displaying higher connectivity magnitude when compared to control and FAS participants. The characterization of prenatal alcohol on whole brain functional connectivity resulted in distinct patterns of connectivity in multiple brain regions including bilateral and midline structures implicated in the default mode- and visual networks. Although none of the statistical effects of FNC comparisons survived multiple comparisons procedures, the results here provide clues for analyses that may be further explored in future research.

References

Allen, E. A., Erhardt, E. B., Damaraju, E., Gruner, W., Segall, J. M., Silva, R. F., . . . Calhoun, V. D. (2011). A baseline for the multivariate comparison of resting-state networks. *Front Syst Neurosci, 5*, 2. doi:10.3389/fnsys.2011.00002

Astley, S. J., Aylward, E. H., Olson, H. C., Kerns, K., Brooks, A., Coggins, T. E., . . . Richards, T. (2009a). Functional magnetic resonance imaging outcomes from a comprehensive magnetic resonance study of children with fetal alcohol spectrum disorders. *J Neurodev Disord, 1*(1), 61-80. doi:10.1007/s11689-009-9004-0

Astley, S. J., Aylward, E. H., Olson, H. C., Kerns, K., Brooks, A., Coggins, T. E., . . . Richards, T. (2009b). Magnetic resonance imaging outcomes from a comprehensive magnetic resonance study of children with fetal alcohol spectrum disorders. *Alcohol Clin Exp Res, 33*(10), 1671-1689. doi:10.1111/j.1530-0277.2009.01004.x

Autti-Ramo, I., Autti, T., Korkman, M., Kettunen, S., Salonen, O., & Valanne, L. (2002). MRI findings in children with school problems who had been exposed prenatally to alcohol. *Dev Med Child Neurol, 44*(2), 98-106.

Bell, A. J., & Sejnowski, T. J. (1995). An Information Maximization Approach to Blind Separation and Blind Deconvolution. *Neural Computation, 7*(6), 1129-1159. doi:Doi 10.1162/Neco.1995.7.6.1129

Bertrand, J., Floyd, L. L., Weber, M. K., Fetal Alcohol Syndrome Prevention Team, D. o. B. D., Developmental Disabilities, N. C. o. B. D., Developmental Disabilities, C. f. D. C., & Prevention. (2005). Guidelines for identifying and referring persons with fetal alcohol syndrome. *MMWR Recomm Rep, 54*(RR-11), 1-14.

Bockholt, H. J., Scully, M., Courtney, W., Rachakonda, S., Scott, A., Caprihan, A., . . . Calhoun, V. D. (2010). Mining the mind research network: a novel framework for exploring large scale, heterogeneous translational neuroscience research data sources. *Front Neuroinform, 3*, 36. doi:10.3389/neuro.11.036.2009

Bullmore, E., & Sporns, O. (2009). Complex brain networks: graph theoretical analysis of structural and functional systems. *Nat Rev Neurosci, 10*(3), 186-198. doi:10.1038/nrn2575

Coffman, B. A., Kodituwakku, P., Kodituwakku, E. L., Romero, L., Sharadamma, N. M., Stone, D., & Stephen, J. M. (2013). Primary visual response (M100) delays in adolescents with FASD as measured with MEG. *Hum Brain Mapp, 34*(11), 2852-2862. doi:10.1002/hbm.22110

Cohen, J. (1992). A power primer. *Psychol Bull, 112*(1), 155-159.

Connor, P. D., Sampson, P. D., Bookstein, F. L., Barr, H. M., & Streissguth, A. P. (2000). Direct and indirect effects of prenatal alcohol damage on executive function. *Dev Neuropsychol, 18*(3), 331-354. doi:10.1207/S1532694204Connor

Cox, R. W. (1996). AFNI: software for analysis and visualization of functional magnetic resonance neuroimages. *Comput Biomed Res, 29*(3), 162-173.

Donald, K. A., Eastman, E., Howells, F. M., Adnams, C., Riley, E. P., Woods, R. P., . . . Stein, D. J. (2015). Neuroimaging effects of prenatal alcohol exposure on the developing human brain: a magnetic resonance imaging review. *Acta Neuropsychiatr, 27*(5), 251-269. doi:10.1017/neu.2015.12

Dwyer-Lindgren, L., Flaxman, A. D., Ng, M., Hansen, G. M., Murray, C. J. L., & Mokdad, A. H. (2015). Drinking Patterns in US Counties From 2002 to 2012. *American journal of public health, 105*(6), 1120-1127. doi:10.2105/ajph.2014.302313

Etkin, A., Prater, K. E., Schatzberg, A. F., Menon, V., & Greicius, M. D. (2009). Disrupted amygdalar subregion functional connectivity and evidence of a compensatory network in generalized anxiety disorder. *Arch Gen Psychiatry, 66*(12), 1361-1372. doi:10.1001/archgenpsychiatry.2009.104

Fan, J., Jacobson, S. W., Taylor, P. A., Molteno, C. D., Dodge, N. C., Stanton, M. E., . . . Meintjes, E. M. (2016). White matter deficits mediate effects of prenatal alcohol exposure on cognitive development in childhood. *Hum Brain Mapp, 37*(8), 2943-2958. doi:10.1002/hbm.23218

Fan, J., Taylor, P. A., Jacobson, S. W., Molteno, C. D., Gohel, S., Biswal, B. B., . . . Meintjes, E. M. (2017). Localized reductions in resting-state functional connectivity in children with prenatal alcohol exposure. *Hum Brain Mapp, 38*(10), 5217-5233. doi:10.1002/hbm.23726

Frankel, F., Paley, B., Marquardt, R., & O'Connor, M. (2006). Stimulants, neuroleptics, and children's friendship training for children with fetal alcohol spectrum

disorders. *J Child Adolesc Psychopharmacol, 16*(6), 777-789. doi:10.1089/cap.2006.16.777

Friston, K. J., Holmes, A. P., Worsley, K. J., Poline, J. P., Frith, C. D., & Frackowiak, R. S. J. (1994). Statistical parametric maps in functional imaging: A general linear approach. *Human Brain Mapping, 2*(4), 189-210. doi:10.1002/hbm.460020402

Fryer, S. L., Tapert, S. F., Mattson, S. N., Paulus, M. P., Spadoni, A. D., & Riley, E. P. (2007). Prenatal alcohol exposure affects frontal-striatal BOLD response during inhibitory control. *Alcohol Clin Exp Res, 31*(8), 1415-1424. doi:10.1111/j.1530-0277.2007.00443.x

Green, C. R., Mihic, A. M., Nikkel, S. M., Stade, B. C., Rasmussen, C., Munoz, D. P., & Reynolds, J. N. (2009). Executive function deficits in children with fetal alcohol spectrum disorders (FASD) measured using the Cambridge Neuropsychological Tests Automated Battery (CANTAB). *J Child Psychol Psychiatry, 50*(6), 688-697. doi:10.1111/j.1469-7610.2008.01990.x

Greicius, M. D., Flores, B. H., Menon, V., Glover, G. H., Solvason, H. B., Kenna, H., . . . Schatzberg, A. F. (2007). Resting-state functional connectivity in major depression: abnormally increased contributions from subgenual cingulate cortex and thalamus. *Biol Psychiatry, 62*(5), 429-437. doi:10.1016/j.biopsych.2006.09.020

Greicius, M. D., Srivastava, G., Reiss, A. L., & Menon, V. (2004). Default-mode network activity distinguishes Alzheimer's disease from healthy aging: evidence from

functional MRI. *Proc Natl Acad Sci U S A, 101*(13), 4637-4642. doi:10.1073/pnas.0308627101

Hawellek, D. J., Hipp, J. F., Lewis, C. M., Corbetta, M., & Engel, A. K. (2011). Increased functional connectivity indicates the severity of cognitive impairment in multiple sclerosis. *Proc Natl Acad Sci U S A, 108*(47), 19066-19071. doi:10.1073/pnas.1110024108

He, B. J., Snyder, A. Z., Vincent, J. L., Epstein, A., Shulman, G. L., & Corbetta, M. (2007). Breakdown of functional connectivity in frontoparietal networks underlies behavioral deficits in spatial neglect. *Neuron, 53*(6), 905-918. doi:10.1016/j.neuron.2007.02.013

Hoyme, H. E., May, P. A., Kalberg, W. O., Kodituwakku, P., Gossage, J. P., Trujillo, P. M., . . . Robinson, L. K. (2005). A practical clinical approach to diagnosis of fetal alcohol spectrum disorders: clarification of the 1996 institute of medicine criteria. *Pediatrics, 115*(1), 39-47. doi:10.1542/peds.2004-0259

Hyvärinen, A., Karhunen, J., Oja, E., & NetLibrary Inc. (2001). *Independent component analysis Adaptive and learning systems for signal processing, communications, and control.* (pp. xxi, 481 p.). Retrieved from http://libproxy.unm.edu/login?url=http://www.netLibrary.com/urlapi.asp?action=summary&v=1&bookid=98960

Jones, K. L., & Smith, D. W. (1973). Recognition of the fetal alcohol syndrome in early infancy. *Lancet, 302*(7836), 999-1001.

Jones, K. L., & Smith, D. W. (1975). The fetal alcohol syndrome. *Teratology, 12*(1), 1-10. doi:10.1002/tera.1420120102

Kable, J. A., O'Connor, M. J., Olson, H. C., Paley, B., Mattson, S. N., Anderson, S. M., & Riley, E. P. (2015). Neurobehavioral Disorder Associated with Prenatal Alcohol Exposure (ND-PAE): Proposed DSM-5 Diagnosis. *Child Psychiatry Hum Dev*. doi:10.1007/s10578-015-0566-7

Kodituwakku, P. W. (2007). Defining the behavioral phenotype in children with fetal alcohol spectrum disorders: a review. *Neurosci Biobehav Rev, 31*(2), 192-201. doi:10.1016/j.neubiorev.2006.06.020

Kodituwakku, P. W., Handmaker, N. S., Cutler, S. K., Weathersby, E. K., & Handmaker, S. D. (1995). Specific impairments in self-regulation in children exposed to alcohol prenatally. *Alcohol Clin Exp Res, 19*(6), 1558-1564.

Larry, V. H. (1981). Distribution Theory for Glass's Estimator of Effect size and Related Estimators. *Journal of Educational Statistics, 6*(2), 107-128. doi:10.3102/10769986006002107

Lebel, C., Mattson, S. N., Riley, E. P., Jones, K. L., Adnams, C. M., May, P. A., . . . Sowell, E. R. (2012). A longitudinal study of the long-term consequences of drinking during pregnancy: heavy in utero alcohol exposure disrupts the normal processes of brain development. *J Neurosci, 32*(44), 15243-15251. doi:10.1523/JNEUROSCI.1161-12.2012

Malisza, K. L., Allman, A. A., Shiloff, D., Jakobson, L., Longstaffe, S., & Chudley, A. E. (2005). Evaluation of spatial working memory function in children and adults

with fetal alcohol spectrum disorders: a functional magnetic resonance imaging study. *Pediatr Res, 58*(6), 1150-1157. doi:10.1203/01.pdr.0000185479.92484.a1

Mattson, S. N., & Riley, E. P. (1998). A review of the neurobehavioral deficits in children with fetal alcohol syndrome or prenatal exposure to alcohol. *Alcohol Clin Exp Res, 22*(2), 279-294.

May, P. A., Baete, A., Russo, J., Elliott, A. J., Blankenship, J., Kalberg, W. O., . . . Hoyme, H. E. (2014). Prevalence and characteristics of fetal alcohol spectrum disorders. *Pediatrics, 134*(5), 855-866. doi:10.1542/peds.2013-3319

May, P. A., & Gossage, J. P. (2001). Estimating the prevalence of fetal alcohol syndrome. A summary. *Alcohol Res Health, 25*(3), 159-167.

Medina, A. E. (2011). Fetal alcohol spectrum disorders and abnormal neuronal plasticity. *Neuroscientist, 17*(3), 274-287. doi:10.1177/1073858410383336

Meintjes, E. M., Jacobson, J. L., Molteno, C. D., Gatenby, J. C., Warton, C., Cannistraci, C. J., . . . Jacobson, S. W. (2010). An FMRI study of number processing in children with fetal alcohol syndrome. *Alcohol Clin Exp Res, 34*(8), 1450-1464. doi:10.1111/j.1530-0277.2010.01230.x

Moore, E. M., Migliorini, R., Infante, M. A., & Riley, E. P. (2014). Fetal Alcohol Spectrum Disorders: Recent Neuroimaging Findings. *Curr Dev Disord Rep, 1*(3), 161-172. doi:10.1007/s40474-014-0020-8

O'Brien, J. W., Norman, A. L., Fryer, S. L., Tapert, S. F., Paulus, M. P., Jones, K. L., . . . Mattson, S. N. (2013). Effect of predictive cuing on response inhibition in

children with heavy prenatal alcohol exposure. *Alcohol Clin Exp Res, 37*(4), 644-654. doi:10.1111/acer.12017

Paley, B., & O'Connor, M. J. (2011). Behavioral interventions for children and adolescents with fetal alcohol spectrum disorders. *Alcohol Res Health, 34*(1), 64-75.

Peadon, E., Rhys-Jones, B., Bower, C., & Elliott, E. J. (2009). Systematic review of interventions for children with Fetal Alcohol Spectrum Disorders. *Bmc Pediatrics, 9*. doi:Artn 35

10.1186/1471-2431-9-35

Popova, S., Stade, B., Bekmuradov, D., Lange, S., & Rehm, J. (2011). What do we know about the economic impact of fetal alcohol spectrum disorder? A systematic literature review. *Alcohol Alcohol, 46*(4), 490-497. doi:10.1093/alcalc/agr029

Power, J. D., Barnes, K. A., Snyder, A. Z., Schlaggar, B. L., & Petersen, S. E. (2012). Spurious but systematic correlations in functional connectivity MRI networks arise from subject motion. *Neuroimage, 59*(3), 2142-2154. doi:10.1016/j.neuroimage.2011.10.018

Riley, E. P., Mattson, S. N., Sowell, E. R., Jernigan, T. L., Sobel, D. F., & Jones, K. L. (1995). Abnormalities of the corpus callosum in children prenatally exposed to alcohol. *Alcohol Clin Exp Res, 19*(5), 1198-1202.

Rodriguez, C. I., Davies, S., Calhoun, V., Savage, D. D., & Hamilton, D. A. (2016). Moderate Prenatal Alcohol Exposure Alters Functional Connectivity in the Adult Rat Brain. *Alcohol Clin Exp Res, 40*(10), 2134-2146. doi:10.1111/acer.13175

Santhanam, P., Coles, C. D., Li, Z., Li, L., Lynch, M. E., & Hu, X. (2011). Default mode network dysfunction in adults with prenatal alcohol exposure. *Psychiatry Res, 194*(3), 354-362. doi:10.1016/j.pscychresns.2011.05.004

Segall, J. M., Turner, J. A., van Erp, T. G., White, T., Bockholt, H. J., Gollub, R. L., . . . Calhoun, V. D. (2009). Voxel-based morphometric multisite collaborative study on schizophrenia. *Schizophr Bull, 35*(1), 82-95. doi:10.1093/schbul/sbn150

Snyder, A. Z., & Raichle, M. E. (2012). A brief history of the resting state: the Washington University perspective. *Neuroimage, 62*(2), 902-910. doi:10.1016/j.neuroimage.2012.01.044

Sokol, R. J., Delaney-Black, V., & Nordstrom, B. (2003). Fetal alcohol spectrum disorder. *JAMA, 290*(22), 2996-2999. doi:10.1001/jama.290.22.2996

Sowell, E. R., Lu, L. H., O'Hare, E. D., McCourt, S. T., Mattson, S. N., O'Connor, M. J., & Bookheimer, S. Y. (2007). Functional magnetic resonance imaging of verbal learning in children with heavy prenatal alcohol exposure. *Neuroreport, 18*(7), 635-639. doi:10.1097/WNR.0b013e3280bad8dc

Sowell, E. R., Thompson, P. M., Mattson, S. N., Tessner, K. D., Jernigan, T. L., Riley, E. P., & Toga, A. W. (2001). Voxel-based morphometric analyses of the brain in children and adolescents prenatally exposed to alcohol. *Neuroreport, 12*(3), 515-523.

Stephen, J. M., Coffman, B. A., Stone, D. B., & Kodituwakku, P. (2013). Differences in MEG gamma oscillatory power during performance of a prosaccade task in

adolescents with FASD. *Front Hum Neurosci, 7*, 900. doi:10.3389/fnhum.2013.00900

Stone, J. V. (2004). *Independent component analysis : a tutorial introduction*. Cambridge, Mass.: MIT Press.

Storey, J. D. (2002). A direct approach to false discovery rates. *Journal of the Royal Statistical Society Series B-Statistical Methodology, 64*, 479-498. doi:Unsp 1369-7412/02/64479

Doi 10.1111/1467-9868.00346

Stratton, K. R., Institute of, M., National Institute on Alcohol, A., Alcoholism, Howe, C. J., & Battaglia, F. (1996). *Fetal Alcohol Syndrome : Diagnosis, Epidemiology, Prevention, and Treatment*. Washington, D.C.: National Academies Press.

Streissguth, A. P., Bookstein, F. L., Barr, H. M., Sampson, P. D., O'Malley, K., & Young, J. K. (2004). Risk factors for adverse life outcomes in fetal alcohol syndrome and fetal alcohol effects. *Journal of Developmental and Behavioral Pediatrics, 25*(4), 228-238. doi:Doi 10.1097/00004703-200408000-00002

Sulik, K. K., Johnston, M. C., & Webb, M. A. (1981). Fetal alcohol syndrome: embryogenesis in a mouse model. *Science, 214*(4523), 936-938.

Tan, C. H., Denny, C. H., Cheal, N. E., Sniezek, J. E., & Kanny, D. (2015). Alcohol Use and Binge Drinking Among Women of Childbearing Age - United States, 2011-2013. *Mmwr-Morbidity and Mortality Weekly Report, 64*(37), 1042-1046.

Tavor, I., Jones, O. P., Mars, R. B., Smith, S. M., Behrens, T. E., & Jbabdi, S. (2016). Task-free MRI predicts individual differences in brain activity during task performance. *Science, 352*(6282), 216-220. doi:10.1126/science.aad8127

van den Heuvel, M. P., & Hulshoff Pol, H. E. (2010). Exploring the brain network: a review on resting-state fMRI functional connectivity. *Eur Neuropsychopharmacol, 20*(8), 519-534. doi:10.1016/j.euroneuro.2010.03.008

Wechsler, D. (1999). Wechsler Abbreviated Scale of Intelligence. San Antonio, TX: Psychological Corporation.

Wilhelm, C. J., & Guizzetti, M. (2015). Fetal Alcohol Spectrum Disorders: An Overview from the Glia Perspective. *Front Integr Neurosci, 9*, 65. doi:10.3389/fnint.2015.00065

Williams, J. F., Smith, V. C., & Committee On Substance, A. (2015). Fetal Alcohol Spectrum Disorders. *Pediatrics*. doi:10.1542/peds.2015-3113

Wozniak, J. R., Fuglestad, A. J., Eckerle, J. K., Fink, B. A., Hoecker, H. L., Boys, C. J., . . . Georgieff, M. K. (2015). Choline supplementation in children with fetal alcohol spectrum disorders: a randomized, double-blind, placebo-controlled trial. *Am J Clin Nutr, 102*(5), 1113-1125. doi:10.3945/ajcn.114.099168

Wozniak, J. R., Mueller, B. A., Bell, C. J., Muetzel, R. L., Hoecker, H. L., Boys, C. J., & Lim, K. O. (2013). Global functional connectivity abnormalities in children with fetal alcohol spectrum disorders. *Alcohol Clin Exp Res, 37*(5), 748-756. doi:10.1111/acer.12024

Wozniak, J. R., Mueller, B. A., Chang, P. N., Muetzel, R. L., Caros, L., & Lim, K. O. (2006). Diffusion tensor imaging in children with fetal alcohol spectrum disorders. *Alcohol Clin Exp Res, 30*(10), 1799-1806. doi:10.1111/j.1530-0277.2006.00213.x

Wozniak, J. R., Mueller, B. A., Mattson, S. N., Coles, C. D., Kable, J. A., Jones, K. L., . . . Cifasd. (2017). Functional connectivity abnormalities and associated cognitive deficits in fetal alcohol Spectrum disorders (FASD). *Brain Imaging and Behavior, 11*(5), 1432-1445. doi:10.1007/s11682-016-9624-4

Wozniak, J. R., Mueller, B. A., Muetzel, R. L., Bell, C. J., Hoecker, H. L., Nelson, M. L., . . . Lim, K. O. (2011). Inter-hemispheric functional connectivity disruption in children with prenatal alcohol exposure. *Alcohol Clin Exp Res, 35*(5), 849-861. doi:10.1111/j.1530-0277.2010.01415.x

Wozniak, J. R., & Muetzel, R. L. (2011). What does diffusion tensor imaging reveal about the brain and cognition in fetal alcohol spectrum disorders? *Neuropsychol Rev, 21*(2), 133-147. doi:10.1007/s11065-011-9162-1

Wozniak, J. R., Muetzel, R. L., Mueller, B. A., McGee, C. L., Freerks, M. A., Ward, E. E., . . . Lim, K. O. (2009). Microstructural corpus callosum anomalies in children with prenatal alcohol exposure: an extension of previous diffusion tensor imaging findings. *Alcohol Clin Exp Res, 33*(10), 1825-1835. doi:10.1111/j.1530-0277.2009.01021.x

Appendix

Appendix 1 – WASI-II by Sex and Condition

Neuropsychological measurements displayed by sex and condition for overall IQ (A), vocabulary subtest score (B), and matrix reasoning subtest score (C). Control males (ControlM), control females (ControlF), ARND males (ARNDM), ARND females (ARNDF), FAS males (FASM), and FAS females (FASF).

A)

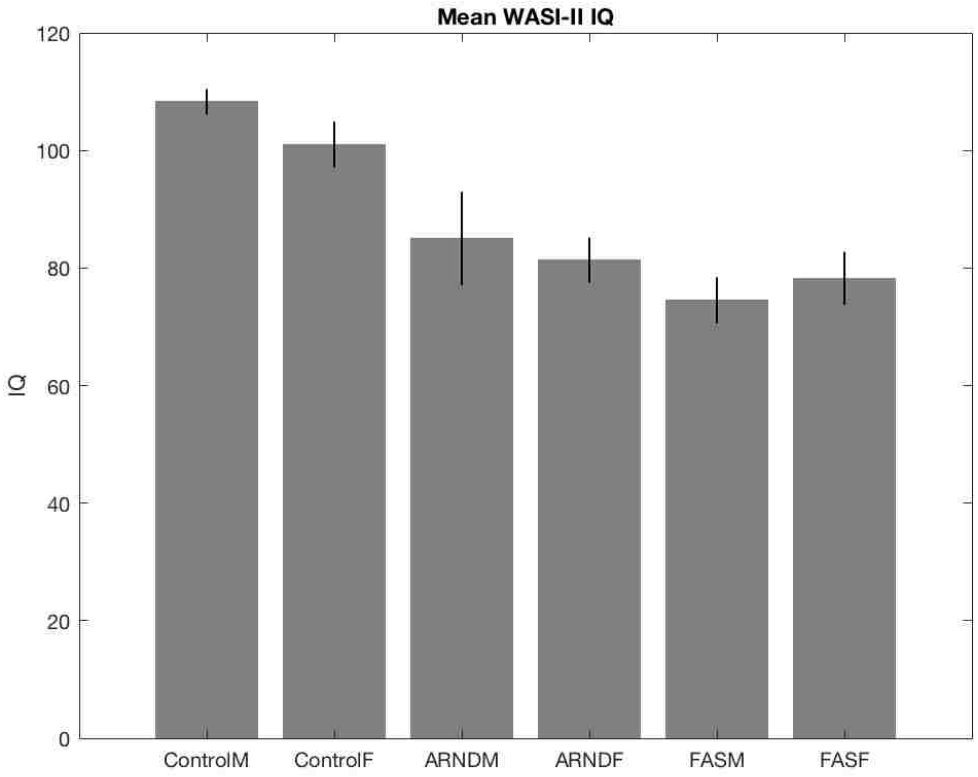

B)

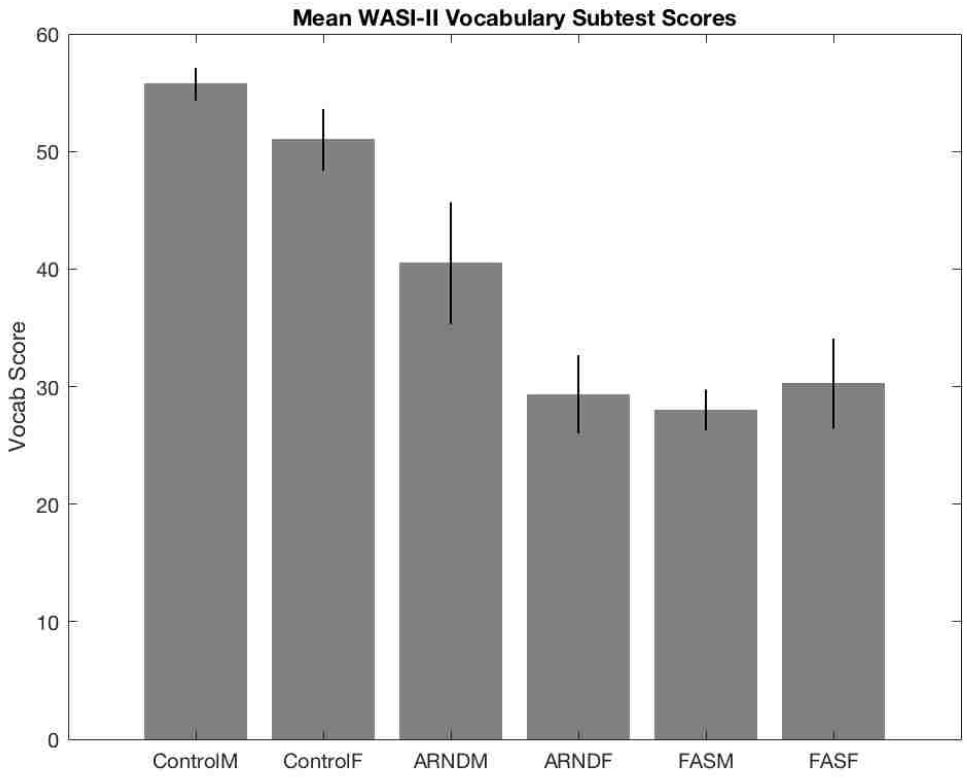
Mean WASI-II Vocabulary Subtest Scores
Vocab Score
60
50
40
30
20
10
0
ControlM
ControlF
ARNDM
ARNDF
FASM
FASF

C)

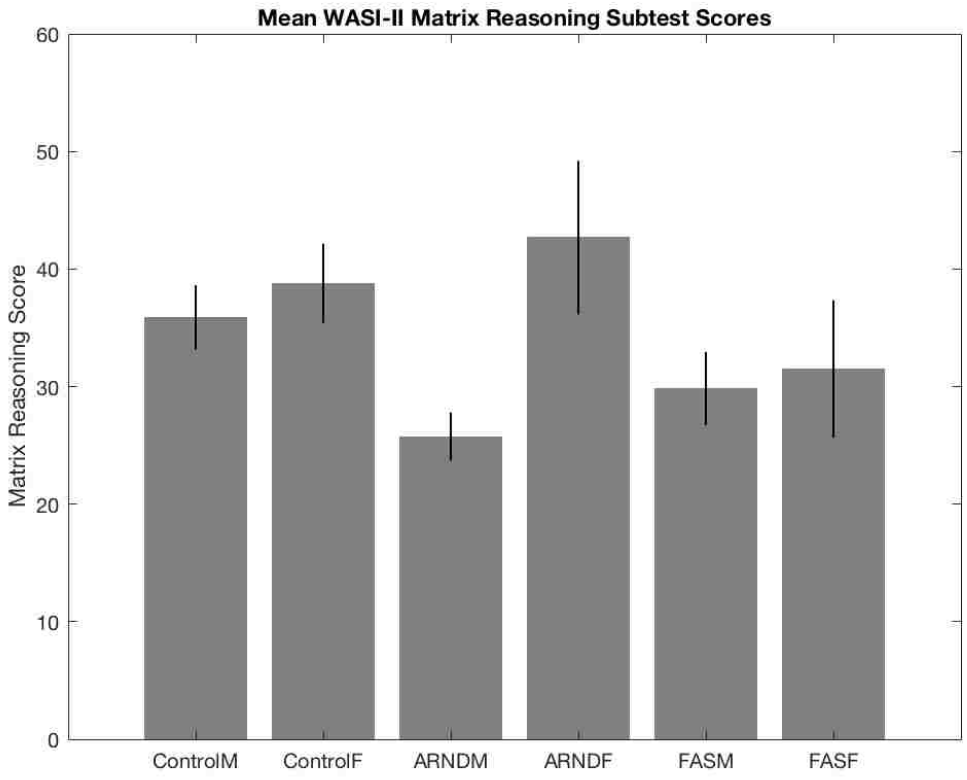
Mean WASI-II Matrix Reasoning Subtest Scores
Matrix Reasoning Score
60
50
40
30
20
10
0
ControlM
ControlF
ARNDM
ARNDF
FASM
FASF

Appendix 2 Mean Connectivity Magnitude Scores by Sex and Condition

Mean connectivity magnitude scores displayed by sex and condition for overall connectivity (A), positive connectivity (B), and negative connectivity (C). Control males (ControlM), control females (ControlF), ARND males (ARNDM), ARND females (ARNDF), FAS males (FASM), and FAS females (FASF).

A)

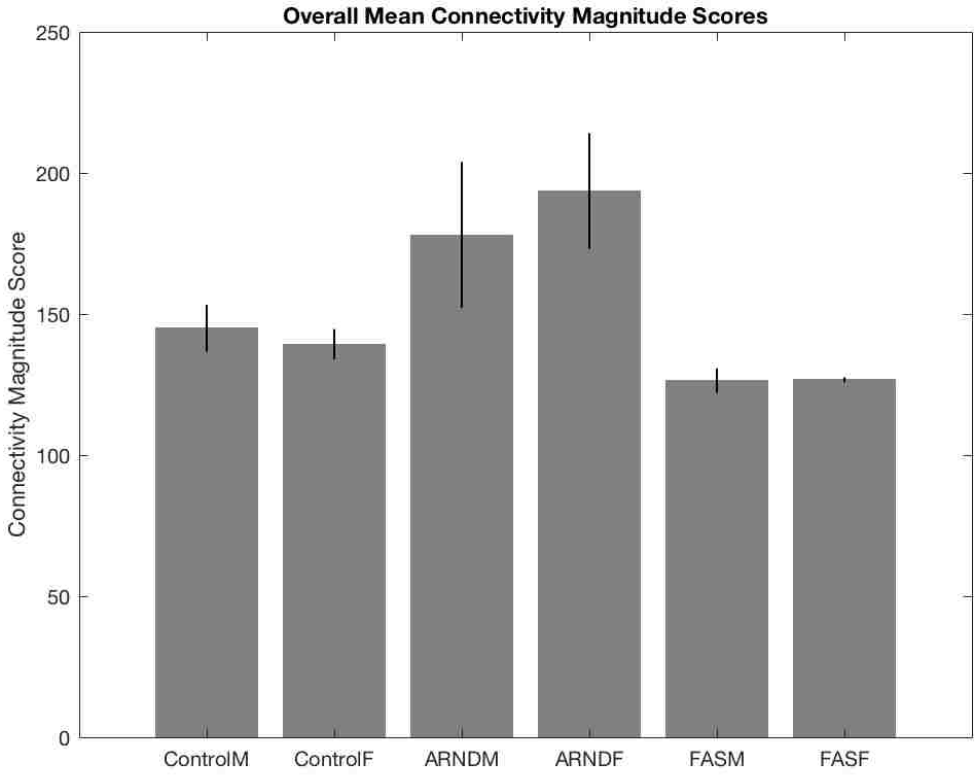

B)

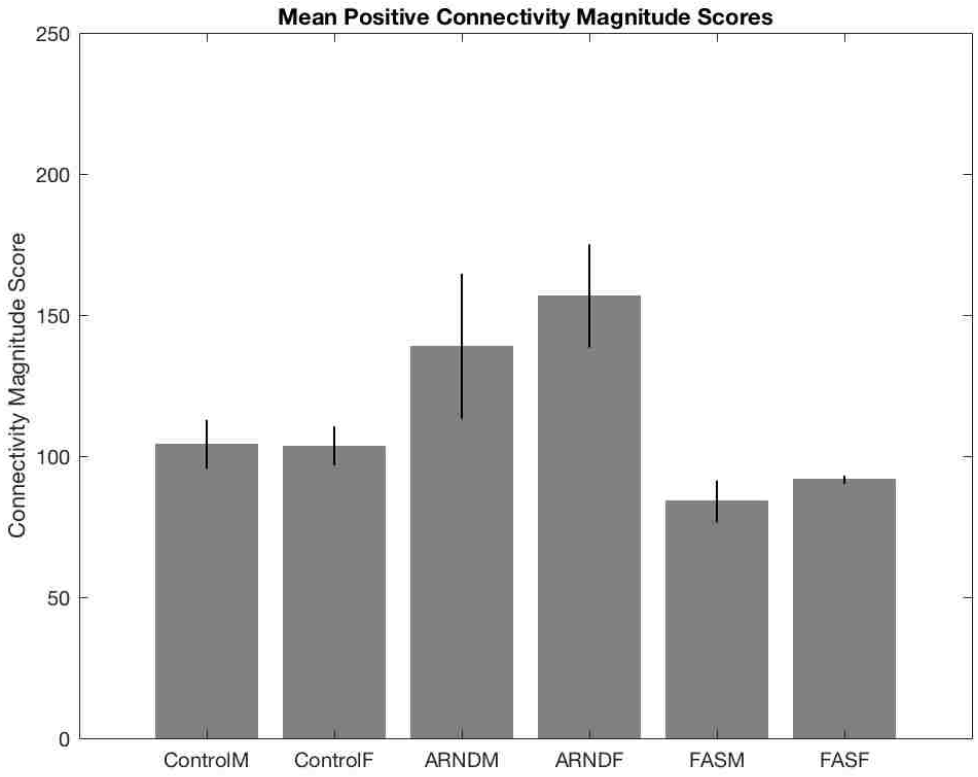
Mean Positive Connectivity Magnitude Scores
Connectivity Magnitude Score
250
200
150
100
50
0
ControlM
ControlF
ARNDM
ARNDF
FASM
FASF

C)

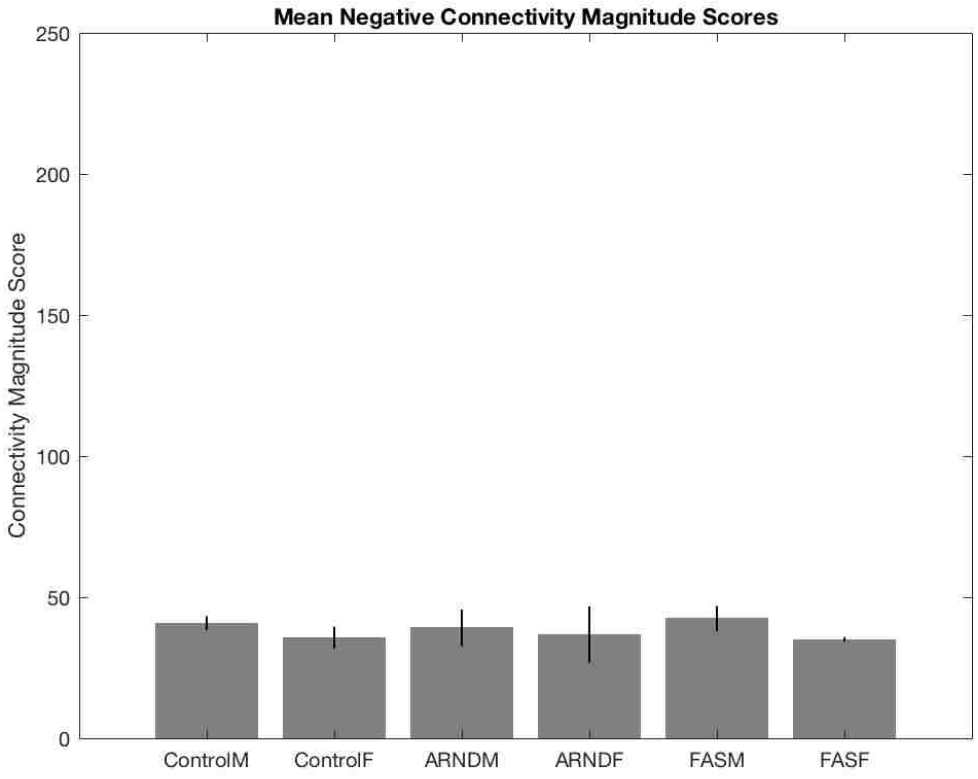
Mean Negative Connectivity Magnitude Scores
Connectivity Magnitude Score
250
200
150
100
50
0
ControlM
ControlF
ARNDM
ARNDF
FASM
FASF

Appendix 3 – Connectivity Magnitude and Neuropsychological Measurement Scatter Plots for Females.

Overall mean connectivity magnitude scores plotted by sex and condition for overall IQ estimate (A), Vocabulary subtest scores, (B), and Matrix Reasoning subtest scores (C).

A)

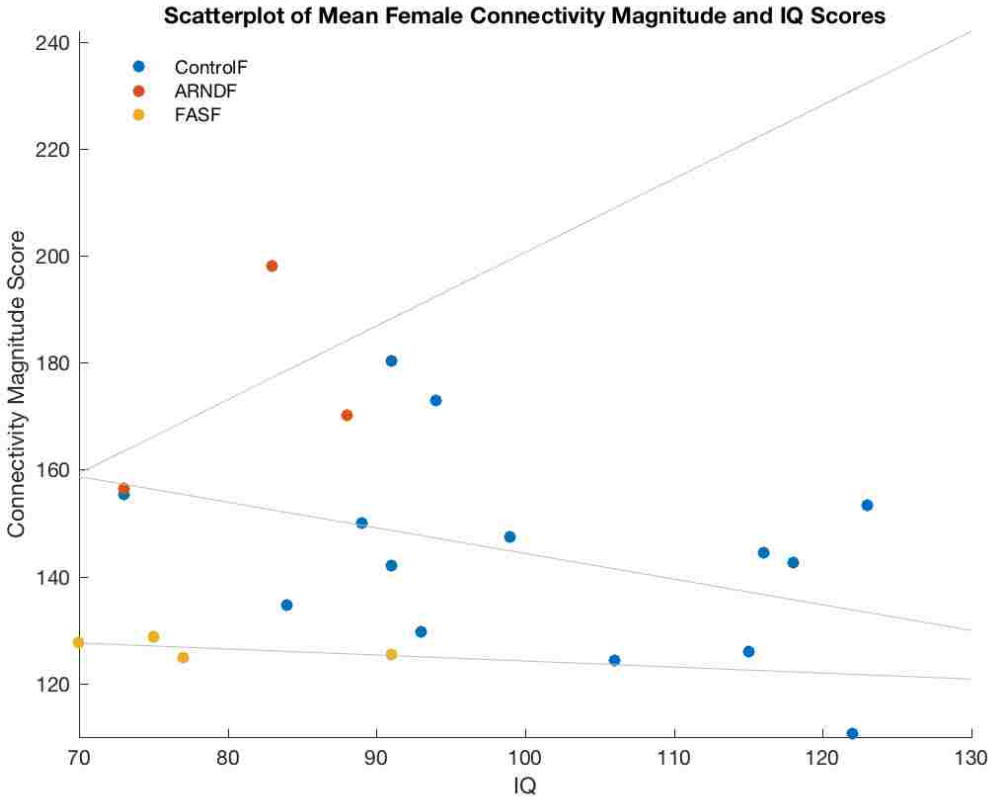

B)

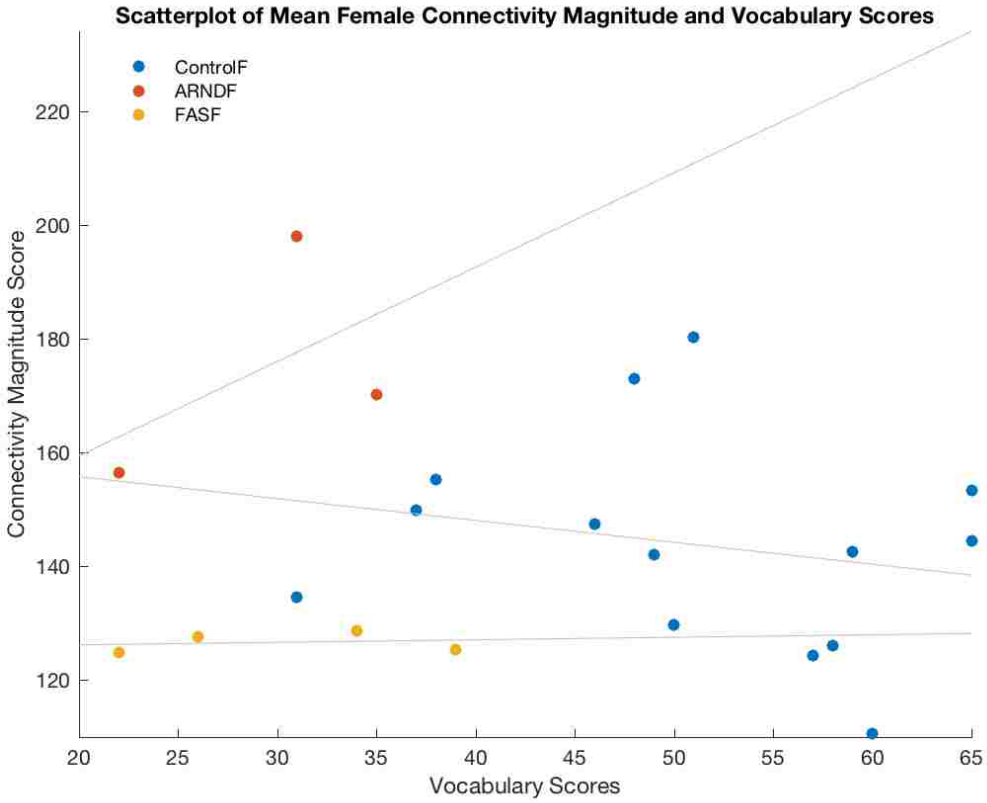
Scatterplot of Mean Female Connectivity Magnitude and Vocabulary Scores
ControlF
ARNDF
FASF
Connectivity Magnitude Score
220
200
180
160
140
120
20
25
30
35
40
45
50
55
60
65
Vocabulary Scores

C)

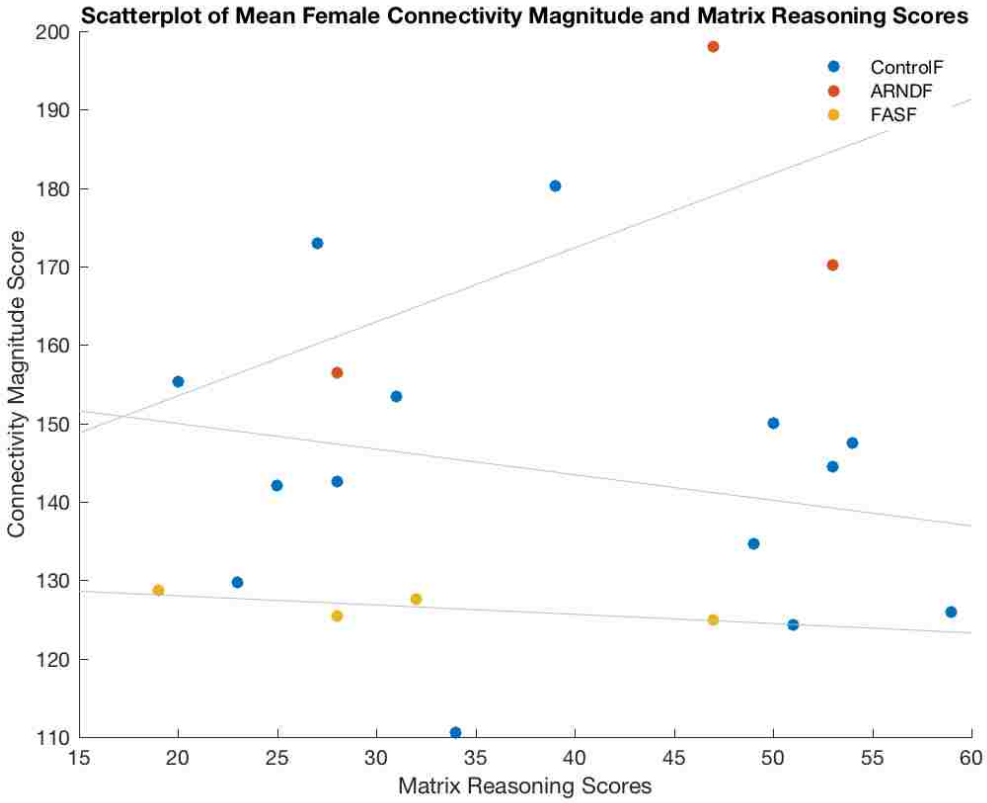
Scatterplot of Mean Female Connectivity Magnitude and Matrix Reasoning Scores
ControlF
ARNDF
FASF
Connectivity Magnitude Score
Matrix Reasoning Scores
200
190
180
170
160
150
140
130
120
110
15
20
25
30
35
40
45
50
55
60

D)

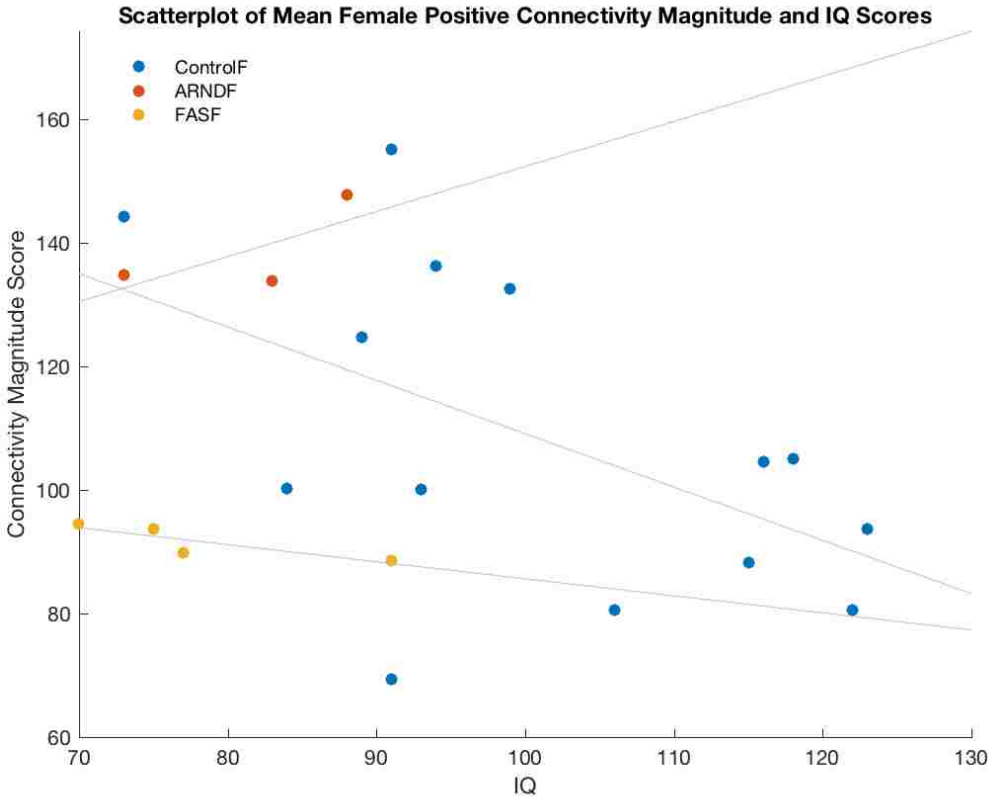
Scatterplot of Mean Female Positive Connectivity Magnitude and IQ Scores
ControlF
ARNDF
FASF
Connectivity Magnitude Score
160
140
120
100
80
60
70
80
90
100
110
120
130
IQ

E)

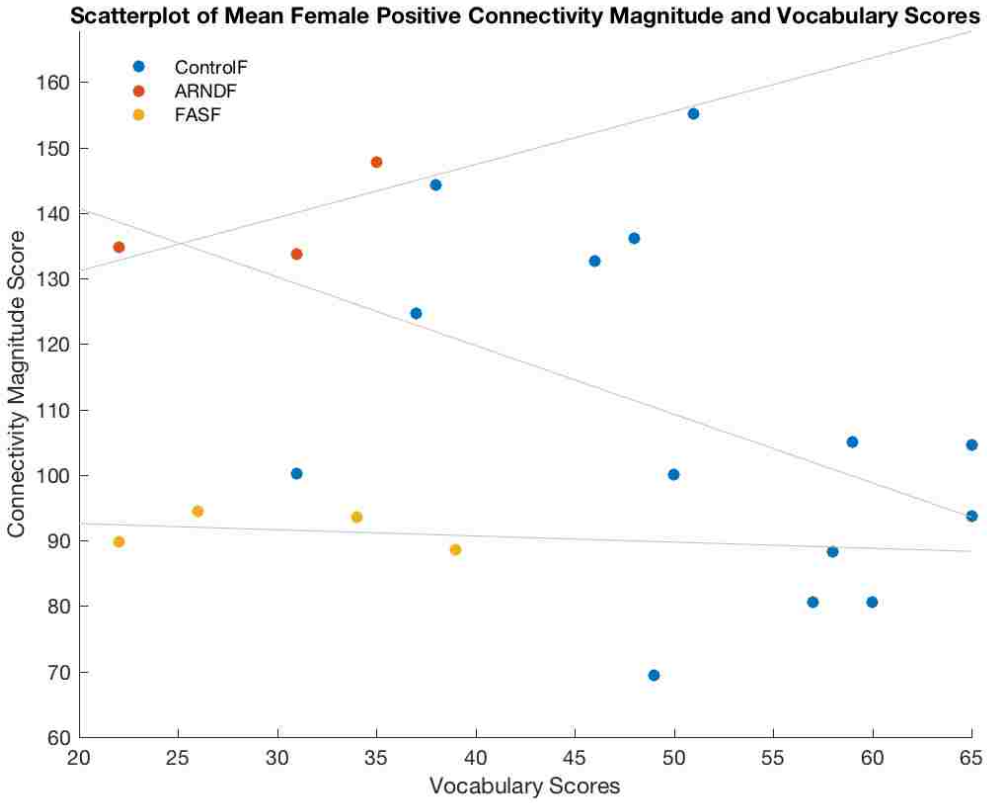
Scatterplot of Mean Female Positive Connectivity Magnitude and Vocabulary Scores
ControlF
ARNDF
FASF
Connectivity Magnitude Score
Vocabulary Scores
160
150
140
130
120
110
100
90
80
70
60
20
25
30
35
40
45
50
55
60
65

F)

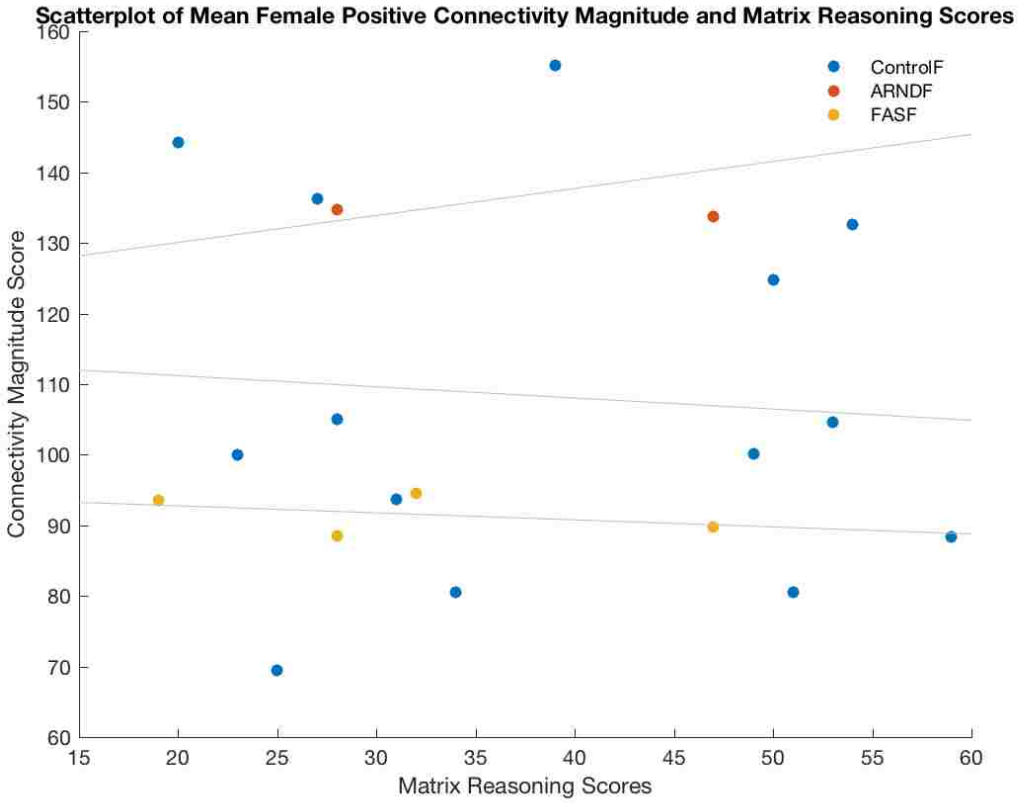
Scatterplot of Mean Female Positive Connectivity Magnitude and Matrix Reasoning Scores
ControlF
ARNDF
FASF
Connectivity Magnitude Score
Matrix Reasoning Scores
160
150
140
130
120
110
100
90
80
70
60
15
20
25
30
35
40
45
50
55
60

G)

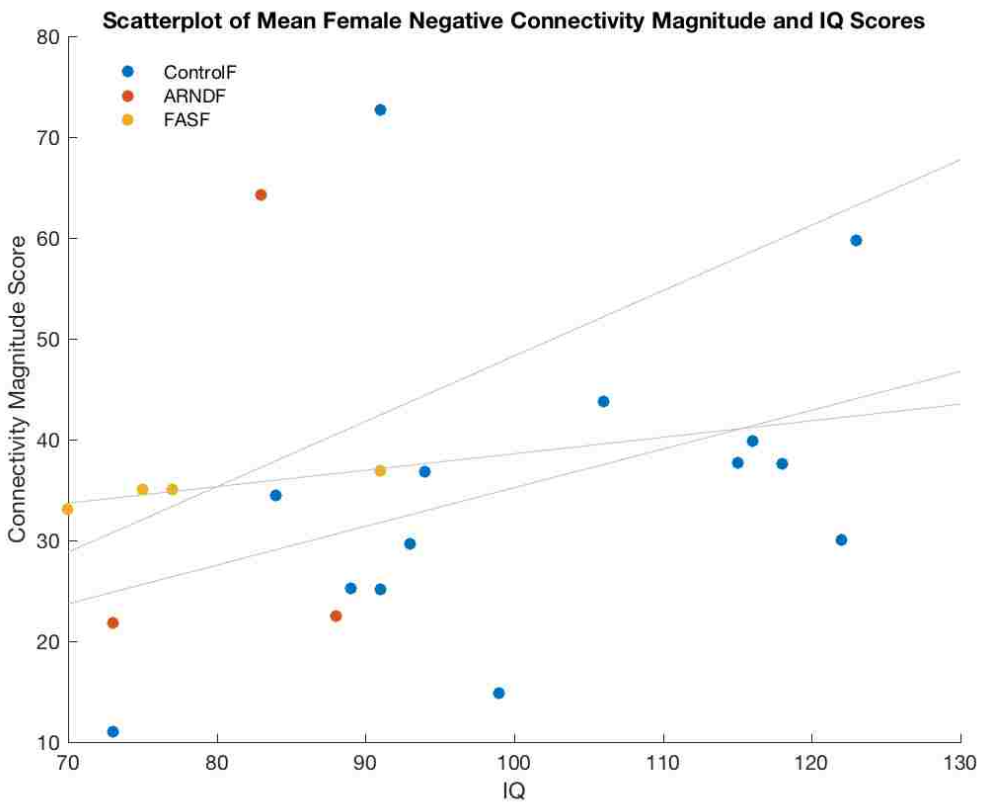
Scatterplot of Mean Female Negative Connectivity Magnitude and IQ Scores
ControlF
ARNDF
FASF
Connectivity Magnitude Score
IQ
80
70
60
50
40
30
20
10
70
80
90
100
110
120
130

H)

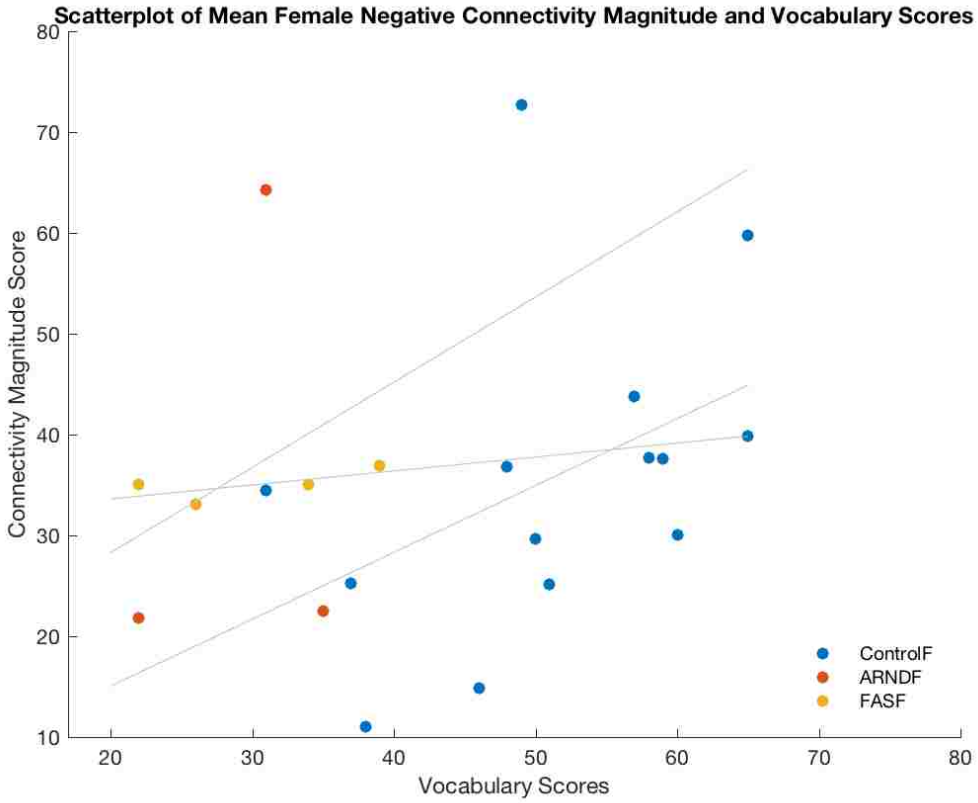
Scatterplot of Mean Female Negative Connectivity Magnitude and Vocabulary Scores
Connectivity Magnitude Score
Vocabulary Scores
80
70
60
50
40
30
20
10
20
30
40
50
60
70
80
ControlF
ARNDF
FASF

I)

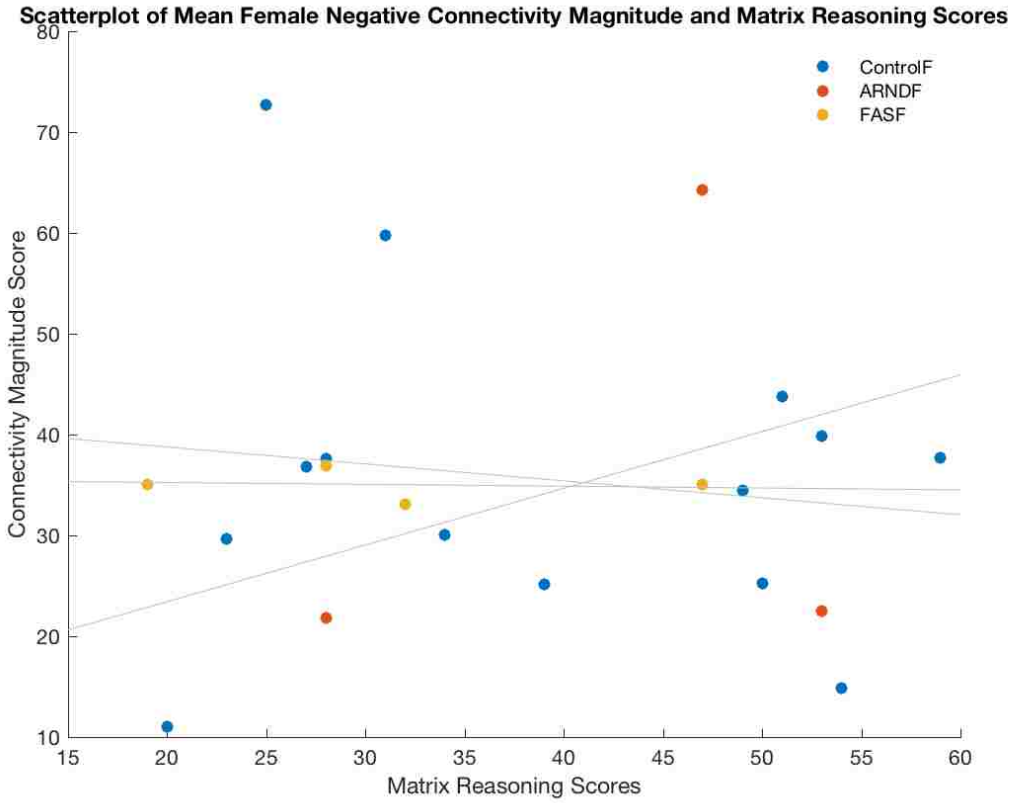
Scatterplot of Mean Female Negative Connectivity Magnitude and Matrix Reasoning Scores
ControlF
ARNDF
FASF
Connectivity Magnitude Score
Matrix Reasoning Scores
80
70
60
50
40
30
20
10
15
20
25
30
35
40
45
50
55
60

Appendix 4 - Connectivity Magnitude and Neuropsychological Measurement Scatter Plots for Males.

A)

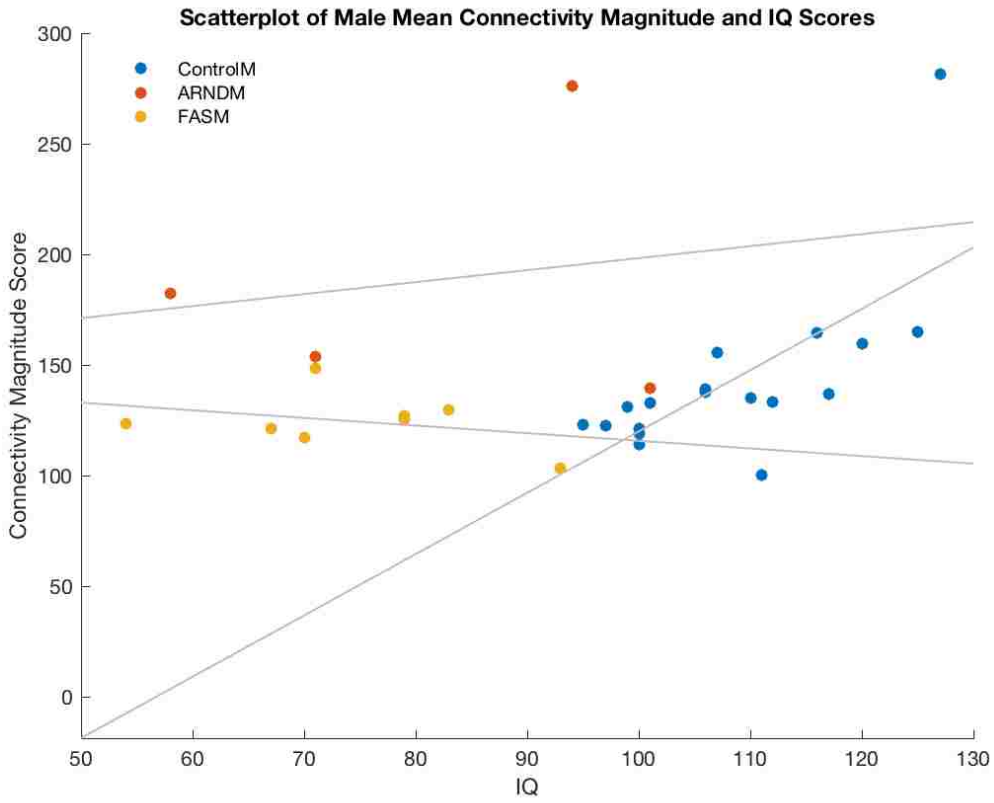

B)

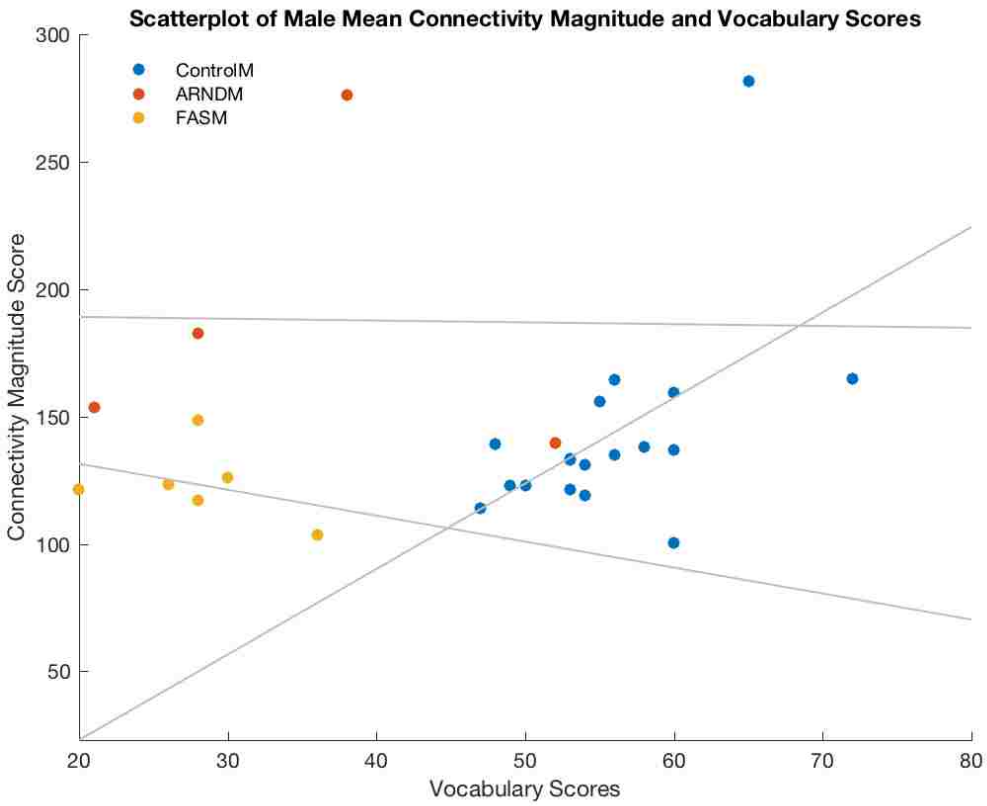
Scatterplot of Male Mean Connectivity Magnitude and Vocabulary Scores
ControlM
ARNDM
FASM
Connectivity Magnitude Score
Vocabulary Scores
300
250
200
150
100
50
20
30
40
50
60
70
80

C)

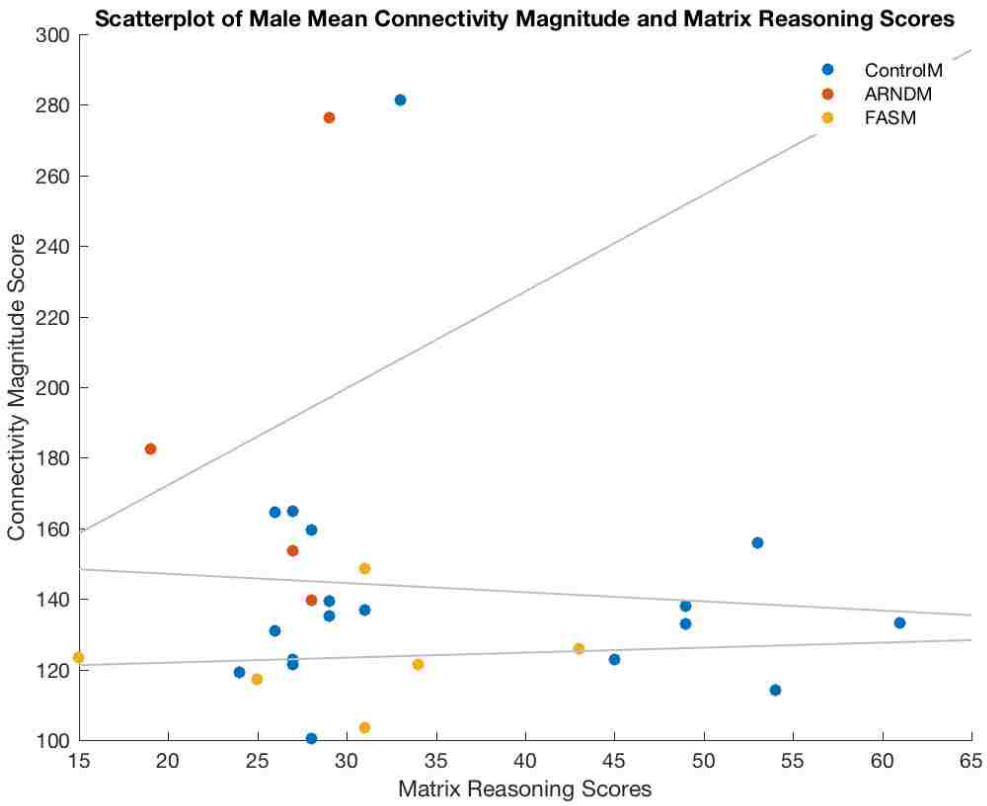
Scatterplot of Male Mean Connectivity Magnitude and Matrix Reasoning Scores
ControlM
ARNDM
FASM
Connectivity Magnitude Score
Matrix Reasoning Scores
300
280
260
240
220
200
180
160
140
120
100
15
20
25
30
35
40
45
50
55
60
65

D)

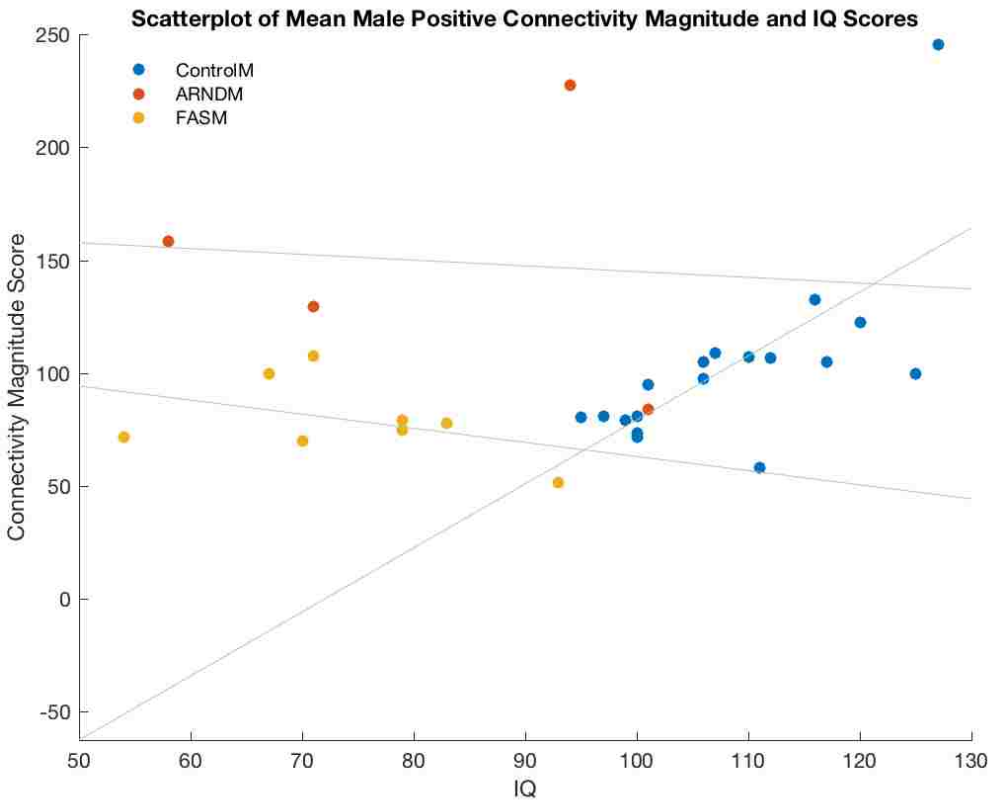
Scatterplot of Mean Male Positive Connectivity Magnitude and IQ Scores
ControlM
ARNDM
FASM
Connectivity Magnitude Score
IQ
250
200
150
100
50
0
-50
50
60
70
80
90
100
110
120
130

E)

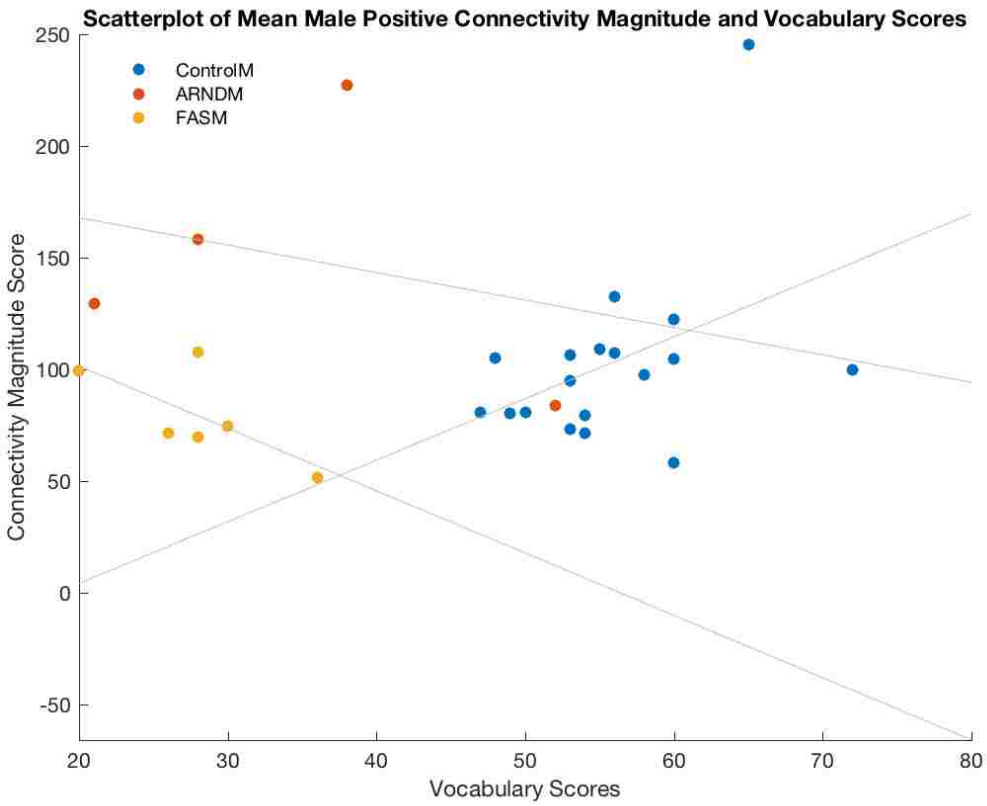
Scatterplot of Mean Male Positive Connectivity Magnitude and Vocabulary Scores
ControlM
ARNDM
FASM
Connectivity Magnitude Score
Vocabulary Scores
250
200
150
100
50
0
-50
20
30
40
50
60
70
80

F)

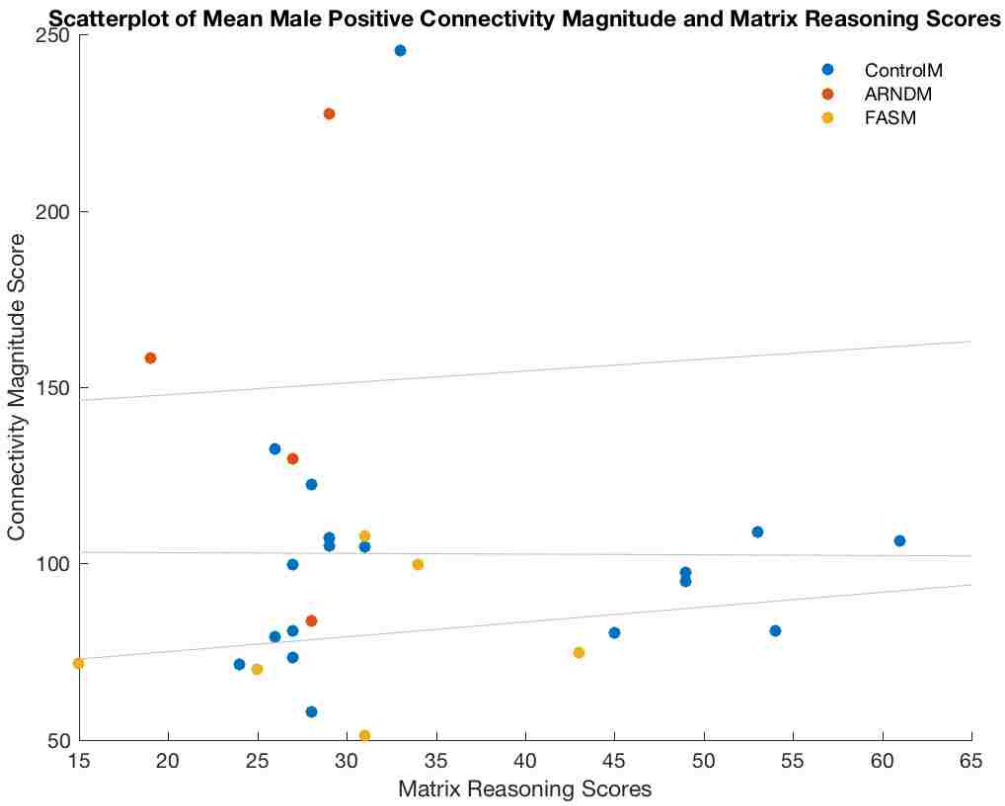
Scatterplot of Mean Male Positive Connectivity Magnitude and Matrix Reasoning Scores
ControlM
ARNDM
FASM
Connectivity Magnitude Score
Matrix Reasoning Scores
250
200
150
100
50
15
20
25
30
35
40
45
50
55
60
65

G)

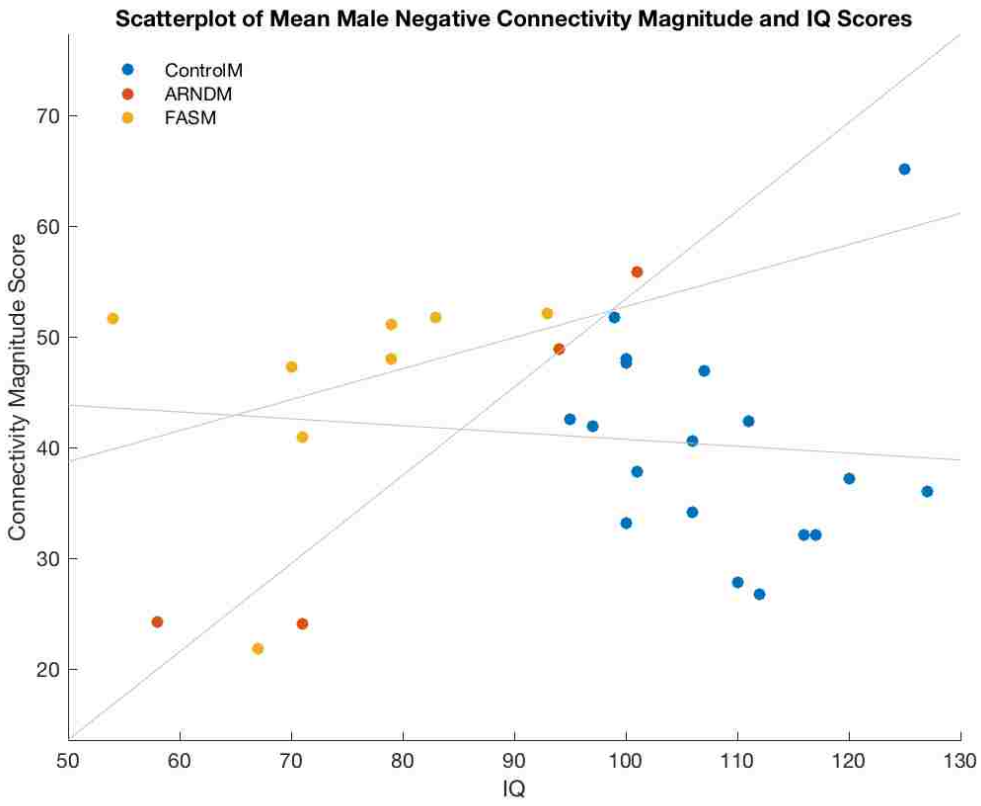
Scatterplot of Mean Male Negative Connectivity Magnitude and IQ Scores
ControlM
ARNDM
FASM
Connectivity Magnitude Score
70
60
50
40
30
20
50
60
70
80
90
100
110
120
130
IQ

H)

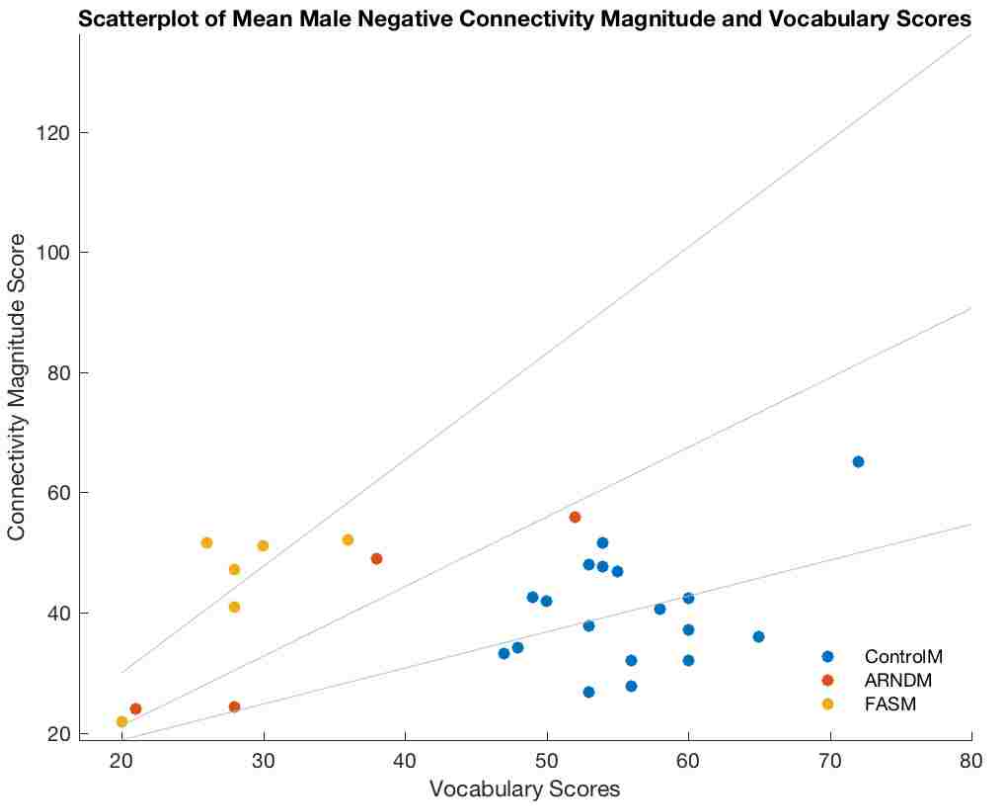
Scatterplot of Mean Male Negative Connectivity Magnitude and Vocabulary Scores
Connectivity Magnitude Score
Vocabulary Scores
120
100
80
60
40
20
20
30
40
50
60
70
80
ControlM
ARNDM
FASM

I)

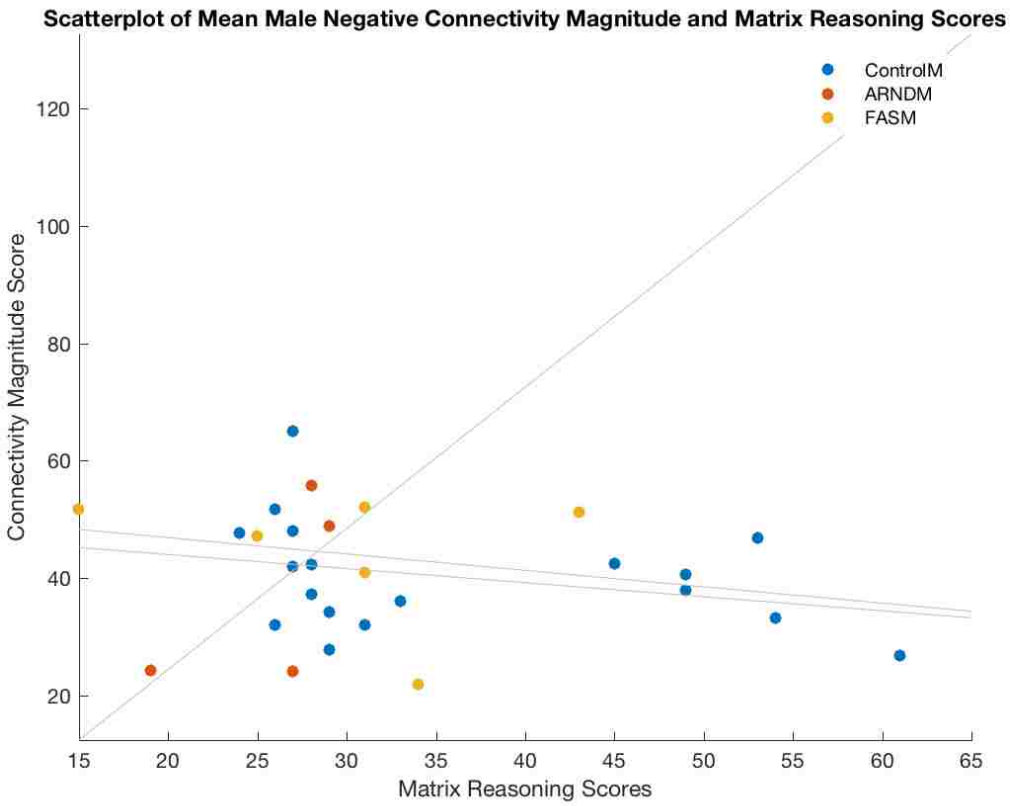
Scatterplot of Mean Male Negative Connectivity Magnitude and Matrix Reasoning Scores
ControlM
ARNDM
FASM
Connectivity Magnitude Score
Matrix Reasoning Scores
120
100
80
60
40
20
15
20
25
30
35
40
45
50
55
60
65

Appendix 5 – FNC by Sex

Mean component time course correlation r-values by sex—males (A) and females (B). Color bar scale indicates the direction of the connectivity measure (negative correlations in blue, positive in red). Labels indicate network grouping auditory (AUD) sensory-motor (SEN), visual, (VIS), cerebellum (CBLM), default mode network (DMN), fronto-parietal (FR-PR), and subcortical (SBCRT).

A)

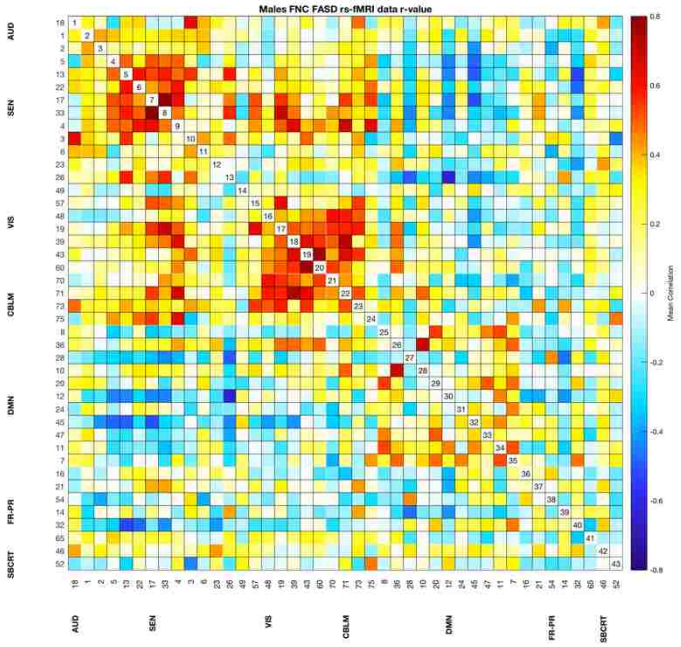

B)

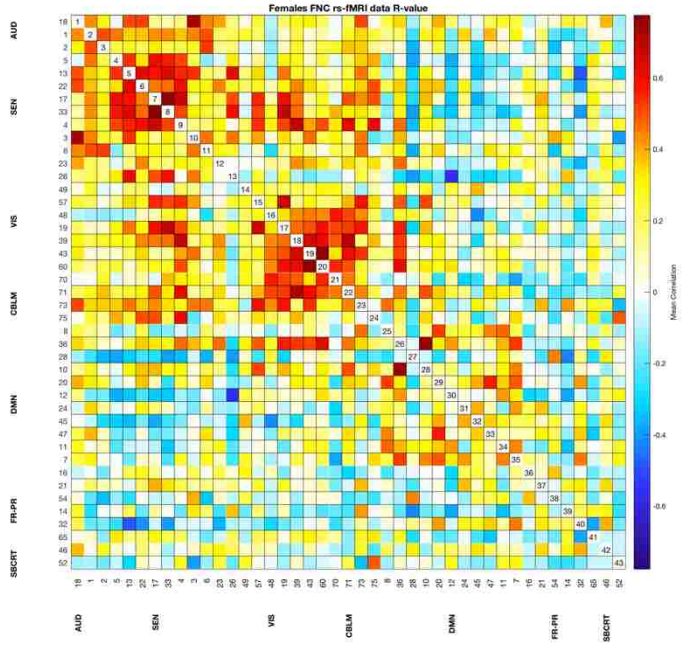
Females FNC rs-fMRI data R-value
AUD
SEN
VIS
CBLM
DMN
FR-PR
SBCRT
Mean Correlation